2013

Metabolic Remodeling and Mitochondrial Dysfunction in Maladaptive Right Ventricular Hypertrophy Secondary to Pulmonary Arterial Hypertension

Jose Gomez-Arroyo
Virginia Commonwealth University

Follow this and additional works at: http://scholarscompass.vcu.edu/etd

Part of the Biochemistry, Biophysics, and Structural Biology Commons

Downloaded from
http://scholarscompass.vcu.edu/etd/3257

Metabolic Remodeling and Mitochondrial Dysfunction in Maladaptive Right

Ventricular Hypertrophy Secondary to Pulmonary Arterial hypertension

Metabolic Remodeling and Mitochondrial Dysfunction in Maladaptive Right

Ventricular Hypertrophy Secondary to Pulmonary Arterial hypertension

A dissertation submitted in partial fulfillment of the requirements for the degree of

Doctor of Philosophy at Virginia Commonwealth University

By

Jose Gomez-Arroyo

Medical Doctor, Monterrey Institute of Technology and Higher Education – "Ignacio

Santos" School of Medicine.

Advisor: **Norbert F. Voelkel**

Professor of Medicine, Pathology and Molecular Biology and Biochemistry

Director, Victoria Johnson Center for Pulmonary Disease Research

At Virginia Commonwealth University.

Virginia Commonwealth University

Richmond, Virginia,

November 2013

Acknowledgments

"De sueños vive el hombre"

Anonymous

(masterfully adapted by José Gómez Moreno, my father)

To my parents, María de Jesús Arroyo Valladares and José G. Gómez Moreno

for their genetic information, infinite love and unconditional support.

To my sister Adriana and my brother Iván,

for inspiring me to become the best role model for them.

To my patients with pulmonary hypertension who survived long enough

to teach me that there are still a million questions to be answered;

To my patients who died too soon and yet had enough time to show me

the significance of true courage and taught me that life, indeed, is only borrowed;

To Paulina, Naomi and all my pediatric patients who taught me

not to be afraid of asking any question,

even when you do not want to hear the answer.

"Only those who will risk going too far

can possibly find out how far one can go."

T.S. Elliot

"One can see the whole world through a small window

if it is just high enough"

Hans Zinser

To Norbert F. Voelkel, my supervisor, life mentor, friend and

occasionally,

even my primary care physician;

for showing me the path of research and always pushing me to walk it

without the fear of failing;

for taking me not only as a student, but as part of his family;

for the countless hours of anecdotes and advices;

for teaching me that in research, as in life, you should always try to have fun.

"La medicina no debe de enfocarse sólo a curar la enfermedad, sino también a entender

los principios básicos que la generan y a prevenir que suceda"

Dr. Julio Sandoval Zárate

To Julio Sandoval Zárate, my mentor and friend,

without whom I would have never considered becoming a physician-scientist;

for nurturing my career, even from the distance;

for believing that one day, together, we could make a difference for our people.

To Gail Christie, my program director,

for believing in me,

always.

(even before I knew what the *trp* operon was)

To Erin Ashley Wall, my friend and honorary committee member,

for tutoring me when everyone else thought I was not worth their time;

for believing in me, even when I would not do it.

"Jose, you must understand that statistically significant does not necessarily mean

clinically relevant."

Dr. Antonio Abbate

To Antonio Abbate, my co-supervisor, committee member, friend and teacher,

for sharing the tough-love and unfiltered honesty that taught me how to enjoy

the bitter and sweet of basic science research.

Table of Contents

List of Figures

List of Tables

List of Abbreviations

α: Alpha

β: Beta

ACADM: Acyl-Coenzyme A dehydrogenase, C-4 to C-12 straight chain

ACADS: Acyl-Coenzyme A dehydrogenase, C-4 to C-8(6) short chain

ACADVL: Acyl-Coenzyme A dehydrogenase, very long chain

ACSL1: Acyl-CoA synthetase long-chain family member 1

ALK-1: Activin receptor-like kinase-1

BMPR2: Bone Morphogenic Type II Receptor

c-Kit: Tyrosine-protein kinase Kit

CD: Cluster of differentiation

CD36: Trombospondin Receptor/Fatty acid translocase

cDNA: complementary DNA

COUP-TF1: Chicken Ovalbumin Upstream Promoter Transcription Factor 1

CPT: Carnitine palmitoyltransferase

CS: Citrate Synthase

CTGF: Connective Tissue Growth Factor

CXCR4: C-X-C chemokine receptor type 4

DNA: Deoxyribonucleic acid

EMS: Eisenmenger Syndrome

ERR: Estrogen-related receptor

ETC: Electron transport chain

FAO: Fatty acid oxidation

GLUT: Solute carrier family 2 (facilitated glucose transporter)

HIV: Human Immunodeficienty Virus

HPAP: Hereditary pulmonary hypertension

IDH1: Isocitrate Dehydrogenase 1

IL: Interleukin

IPAH: Idiopathic Pulmonary Arterial Hypertension

KO: Knock-out

LV: Left ventricle

MCPT: Dehydromonocrotaline

MCT: Monocrotaline

miRNA: Micro RNA

NIH: National Institutes of Health

PAB: Pulmonary Artery Banding

PAEC: Pulmonary arterial endothelial cell

PAH: Pulmonary Arterial Hypertension

PDGF: Platelet Derived Growth Factor

PDHb: Pyruvate dehydrogenase subunit beta

PDK: Pyruvate dehydrogenase kinase

PGC-1: Peroxisome proliferator-activated receptor gamma coactivator-1

PH: Pulmonary Hypertension

POLG2: Polymerase (DNA directed), gamma 2, accessory subunit

POLRMT: Polymerase (RNA) mitochondrial (DNA directed)

PPAR: Peroxisome proliferator activated receptor

PGC-1α: Peroxisome proliferator-activated receptor gamma coactivator 1 alpha

RNA: Ribonucleic acid

RV: Right Ventricle

RV/LV+S: Right ventricular weight/Left ventricular plus septum weight index

RVD: Right Ventricular Dysfunction

RVEF: Right ventricular ejection fraction

RVF: Right Ventricular Failure

SP: Transcription factor Sp1

SScPAH: Scleroderma associated pulmonary arterial hypertension

STAT3: Signal transducer and activator of transcription 3

SU5416: (3*Z*)-3-[(3,5-dimethyl-1*H*-pyrrol-2-yl)methylidene]-1,3-dihydro-2*H*-indol-2-one

SuHx: SU5416/hypoxia

TAPSE: Tricuspid annular plannar systolic excursion

TFAM: Transcription factor A mitochondrial

TGF-β: Transforming growth factor β

TLR-9: toll-like receptor 9

TOP1mt: Topoisomerase (DNA) I, mitochondrial

Tregs: Regulatory T cells

VEGF: Vascular endothelial growth factor

WHO: World Health Organization

WT: Wild Type

Abstract

Right ventricular dysfunction is the most frequent cause of death in patients with pulmonary arterial hypertension. Although abnormal energy substrate use has been implicated in the development of chronic left heart failure, data describing such metabolic remodeling in failing right ventricular tissue remain incomplete. In the present dissertation we sought to characterize metabolic gene expression changes and mitochondrial dysfunction in functional and dysfunctional RV hypertrophy.

Two different rat models of RV hypertrophy were studied. The model of right ventricular failure (SU5416/hypoxia) exhibited a significantly decreased gene expression of peroxisome proliferator-activated receptor- coactivator-1α, peroxisome proliferator-activated receptor-α and estrogen-related receptor-α. The expression of multiple peroxisome proliferator-activated receptor- coactivator-1α target genes required for fatty acid oxidation was similarly decreased. Decreased peroxisome proliferator-activated receptor- coactivator-1α expression was also associated with a net loss of mitochondrial protein and oxidative capacity. Reduced mitochondrial number was associated with a downregulation of transcription factor A, mitochondrial, and other genes required for mitochondrial biogenesis. Electron microscopy demonstrated that, in right ventricular failure tissue, mitochondria had abnormal shape and size. Lastly, respirometric analysis demonstrated that mitochondria isolated from right ventricular failure tissue had a significantly reduced ADP- stimulated (state 3) rate for complex I. Conversely, functional right ventricular hypertrophy in the pulmonary artery banding model showed normal expression of peroxisome proliferator-activated receptor- coactivator-1α, whereas the expression of fatty acid oxidation genes was either preserved or unregulated. Moreover,

pulmonary artery banding-right ventricular tissue exhibited preserved transcription factor A mitochondrial expression and mitochondrial respiration despite elevated right ventricular pressure-overload. We conclude that right ventricular dysfunction, but not functional right ventricular hypertrophy in rats, demonstrates a gene expression profile compatible with a multilevel impairment of fatty acid metabolism and significant mitochondrial dysfunction, partially independent of chronic pressure-overload.

Chapter 1: General introduction to pulmonary hypertension and right ventricular failure. Rationale and outline of the thesis

Segments of this chapter have been previously published in:

Voelkel NF, **Gomez-Arroyo J**, et al. Pathobiology of pulmonary arterial hypertension and right ventricular failure. *Eur Respir J.* 2012 Dec;40(6):1555–1565.

"Further research is essential in order that the etiology of the disease to be discovered. Once the mechanism is known, perhaps it can be arrested or reversed […] Thus, the ultimate hope is for a discovery of the basic mechanisms which now are unknown"

N.F Voelkel and J.T. Reeves, 1979

1. 1 General introduction to pulmonary hypertension

Pulmonary hypertension (PH) or high blood pressure in the lung circulation, occurs in a broad spectrum of diseases of the lung and is defined as an elevation of the mean pulmonary artery pressure > 25 mmHg(210). Because many lung and systemic diseases can be associated with pulmonary hypertension, five World Heath Organization (WHO) meeting groups have worked to categorize PH, since the first classification of the disease in 1973. Indeed, nowadays the different etiologies of PH have been classified into 5 different groups (**Table 1**). Understanding the differences between the WHO groups is critical not only for medical management of the patient with PH but also for the understanding of the pathogenesis. For the purposes of this dissertation, one could simplify the causes of PH in two broad groups: 1) Diseases affecting the arterial (pre-capillary) component of the lung circulation, that is, lung vessels that take deoxygenated

blood from the right side of the heart (right ventricle) to the lungs and 2) Diseases affecting the venous (post-capillary) component of the lung circulation, which carries oxygenated blood to the left ventricle ready to be pumped into the systemic circulation. In addition to the hemodynamic criterion of a high mean pulmonary artery pressure (mPAP), the diagnostic definition of WHO Group 1, or pulmonary arterial hypertension (PAH), adds the criterion of a pulmonary arterial wedge pressure <15 mmHg, which largely rules out the presence of left heart disease. Although Groups 3, 4 and 5 include diseases or conditions associated with <u>arterial</u> lung vascular disease, the pathobiology of the diseases included in these groups is significantly distinct from Group 1. **<u>The reader should be aware that the entire dissertation is focused on Group 1, or pulmonary arterial hypertension (PAH).</u>**

As noted in **Table 1**, PAH includes conditions that range from congenital heart disease (different from WHO Group 2 which lists acquired left heart disease), infections, drug-induced, hepatopulmonary syndrome, as well as sporadic idiopathic (unknown) and hereditary idiopathic forms. All forms of PAH are characterized by elevated pulmonary arterial pressure and elevated blood flow resistance due to a precapillary pulmonary microangiopathy(243). However, although PAH is a disease originated in the lungs, patients with the disease die from right ventricular failure(49, 197).

Table 1. Classification of Pulmonary Hypertension

1. Pulmonary arterial hypertension (PAH)
1.1. Idiopathic PAH
1.2. **Heritable**
1.2.1. **BMPR2**
1.2.2. **ALK1, endoglin (with or without hereditary hemorrhagic telangiectasia)**
1.2.3. **Unknown**
1.3. Drug- and toxin-induced
1.4. Associated with
1.4.1. Connective tissue diseases
1.4.2. HIV infection
1.4.3. Portal hypertension
1.4.4. Congenital heart diseases
1.4.5. **Schistosomiasis**
1.4.6. **Chronic hemolytic anemia**
1.5 Persistent pulmonary hypertension of the newborn

1′. **Pulmonary veno-occlusive disease (PVOD) and/or pulmonary capillary hemangiomatosis (PCH)**

2. Pulmonary hypertension owing to left heart disease
2.1. **Systolic dysfunction**
2.2. **Diastolic dysfunction**
2.3. Valvular disease

3. Pulmonary hypertension owing to lung diseases and/or hypoxia
3.1. Chronic obstructive pulmonary disease
3.2. Interstitial lung disease
3.3. **Other pulmonary diseases with mixed restrictive and obstructive pattern**
3.4. Sleep-disordered breathing
3.5. Alveolar hypoventilation disorders
3.6. Chronic exposure to high altitude
3.7. Developmental abnormalities

4. **Chronic thromboembolic pulmonary hypertension (CTEPH)**

5. **Pulmonary hypertension with unclear multifactorial mechanisms**
5.1. **Hematologic disorders: myeloproliferative disorders, splenectomy**
5.2. **Systemic disorders: sarcoidosis, pulmonary Langerhans cell histiocytosis:** lymphangioleiomyomatosis, neurofibromatosis, vasculitis
5.3. **Metabolic disorders: glycogen storage disease, Gaucher disease, thyroid disorders**
5.4. **Others: tumoral obstruction, fibrosing mediastinitis, chronic renal failure on dialysis**

Table 1. Updated clinical classification of pulmonary arterial hypertension groups according the World Health Organization**.** *ALK1 = activin receptor-like kinase type 1; BMPR2 = bone morphogenetic protein receptor type 2; HIV = human immunodeficiency virus. Reproduced from Simonneau G, et al. Updated clinical classification of pulmonary hypertension. Journal of the American College of Cardiology. 2009 Jun 30;54(1 Suppl):S43–54. Copyright 2009, with permission from Elsevier.*

1.2 Brief historical and current perspective of the disease

Idiopathic pulmonary arterial hypertension (IPAH), formerly known as primary pulmonary hypertension, is the best-characterized form of PH. The term idiopathic refers to a disease of unexplained etiology and therefore patients diagnosed with IPAH do not have a coexisting cardiac or pulmonary disease(209). In other words, the diagnosis of IPAH remains a 'diagnosis of exclusion'. The disease was first described in 1891 by Romberg and later on by Ayerza in 1901 who reported patients with heart failure and severe cyanosis ('negros cardiacos') associated with 'brochopulmonary sclerosis'(247). The first systematic description was not reported until 1935 by Brenner(29) and did not become a clinical entity until 1951, when Dresdale and collaborators described its clinical and hemodynamic features(247). All forms of PAH, including IPAH, are characterized by a common histopathological feature: the presence of plexiform-like lesions (**Figure 1**) (243), hence the former name of 'unexplained plexogenic pulmonary arteriopathy'. This concept was further developed by Heath and Edwards who, in 1958, defined the structural vascular changes in the lungs of patients with PAH(247). After first anorexigen-induced (aminorex fumarate) epidemic of pulmonary hypertension in Europe in 1967-1970, the husband and wife Wagenvoort and Wagenvoort reported the largest series of autopsied patients providing the structural criteria for the diagnosis of PAH and its separation from other forms of pulmonary hypertension, which now are included in WHO Groups 2-5.

It should be noted that unlike other diseases, including infectious diseases, cancer or even pulmonary or cardiovascular (myocardial infarction, atherosclerosis, stroke)

diseases, PAH was a relatively unrecognized medical condition until rather recently.
As reviewed by Voelkel and Reeves, until the year 1979(241), researchers and clinicians
knew that PAH was a lung vascular disease predominantly affecting women (5:1), that it
could affect patients of any age but the highest incidence occurred between the ages of 25
and 29 years and perhaps, most importantly, it was well recognized that the disease had
no cure or treatment and therefore, upon diagnosis, the prognosis of the patient was
dismal. Indeed, the mean survival time of patients was 2 to 3 years after diagnosis(247).
Because of the heterogeneity of the data collected from rather small patient cohorts, in
1981, the Patient Registry for the Characterization of Primary Pulmonary Hypertension
was established by the National Heart, Lung, and Blood Institute of the National
Institutes of Health. This was the first prospective collection of data based on
standardized protocols, which included a initial diagnostic catheterization(49). A total of
194 patients from 32 medical centers in the United States were recruited and followed-up
in order to define survival patterns based on hemodynamic parameters. The data of this
registry provided for the first time a solid hemodynamic description of IPAH and
demonstrated that survival strongly correlated with the function of RV.
Five World Symposia on pulmonary hypertension have taken place in the past two
decades (the last in 2013) and scientists as well as clinicians have thoroughly categorized
the diverse forms of PH and have consolidated the data produced in many laboratories
and clinical centers around the world. Today, almost a quarter of a century after first NIH
national registry, the data from the Registry to Evaluate Early and Long Term PAH
Disease Management (REVEAL), the largest registry in the United States, indicate that
the phenotype of idiopathic PAH, has significantly changed. Today, up to 79% of patients

are obese women close to menopausal age (69). However, there is an apparent

discrepancy in the PAH phenotype between US and European registries(62, 105, 169),

suggesting, perhaps, currently unidentified regional environmental factors that could

contribute to the development and progression of the disease. Furthermore, PAH is no

longer an orphan disease(102). Unlike 20 years ago, three classes of drugs have been

developed and an increasing number of patients are being treated with a single drug or a

combination therapy (22, 104). The advent of PAH-specific therapies has improved the

survival of PAH patients in comparison the survival published in historic registries.

However, in spite of treatment, the mortality remains unacceptably high, as the

survival for incident patients continues to be as low as 54.9% at 3 years after diagnosis

(95% CI, 41.8 to 68.0)(107). **In other words, although new therapies improve**

survival, PAH remains an incurable and rapidly progressive disease. Indeed,

although the structural changes that explain the "fixed pulmonary hypertension" of PAH

patients have been described in recent decades (13, 181, 250) and new pathobiological

concepts of PAH have been described(199, 232), current PAH-specific drugs are

predominantly vasodilators(106) and do not stop the progression of the disease(213).

Figure 1.
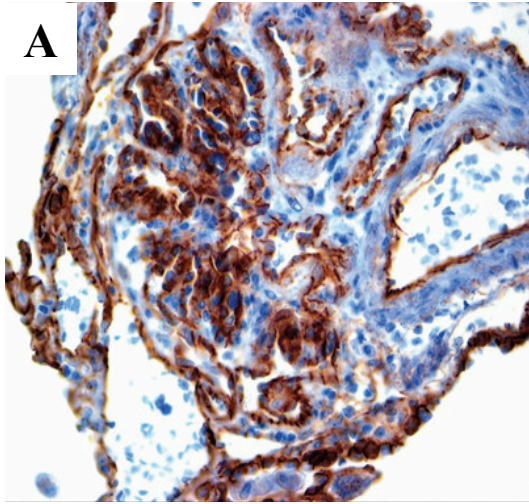
Lung vascular lesion
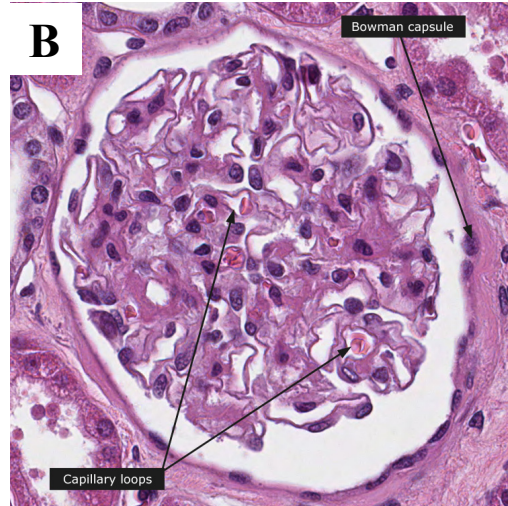
Normal kidney glomerulus

Figure 1. Comparison between a plexiform-like lesion from the lung of a patient with pulmonary arterial hypertension and a renal glomerulus. Micrographs obtained with a light-microscope illustrate the similarities between a classic plexiform-like lesion in a patient with pulmonary arterial hypertension (**A**) and a normal renal glomerulus (**B**). Complex vascular remodeling, as illustrated in panel A, is not present in the lung under normal conditions. *Panel A figure was reprinted with permission of the American Thoracic Society. Copyright © 2013 American Thoracic Society from Rai PR, et al. The cancer paradigm of severe pulmonary arterial hypertension. Am J Respir Crit Care Med. 2008,15;178(6):558–564 (Ref.* (178, 183)*).*

Official Journal of the American Thoracic Society. Panel B was reproduced from Pontén F et al. A global view of protein expression in human cells, tissues, and organs. Mol Syst Biol. 2009 5:337 (Ref (49, 178)*).*

1.3 Outline of the dissertation, justification and general hypothesis

The entire dissertation consists of seven chapters. **CHAPTER 2** is a compendium of the current literature discussing the pathobiology of PAH, which has significantly evolved from the early concepts proposed by many experts two decades ago. Although the data derived from cell-based models and human samples have provided the basis for the generation of novel hypotheses about the genesis of the disease, many questions remain unanswered. Because, animal models of the disease are fundamental not only to the better understanding of the disease but also for pre-clinical testing of new pharmacotherapies, in **CHAPTER 4** we broadly discuss the existing literature, as well as our own data, regarding the current animal models utilized to study PAH. Given that an 'ideal' animal model of pulmonary is not yet available, we sought to characterize the problems and prospects of the most prevalent animal model of pulmonary hypertension, the monocrotaline-injury and the SU5416/hypoxia rat models, as well as several transgenic mouse models reported in the literature and studied in our laboratory. **This chapter is of particular importance to the reader because it provides the necessary rationale for the use of the SU5416/hypoxia rat model of PH, the principal animal model used for the studies described in this dissertation**.

The direct consequence of the lung vascular remodeling present in patients with PAH are restricted blood flow and increased vascular resistance, all of which translates into increased right ventricular afterload (**Figure 2**)(246). Although, right ventricular failure (RVF) is the most frequent cause of death of patient with PAH(22, 49, 104, 197), the interactions between the remodelled lung circulation and the right ventricle (RV) are only

11

Figure 2.

Vascular Remodeling → ↑ Resistance Pressure → Right Ventricular Dysfunction /Failure
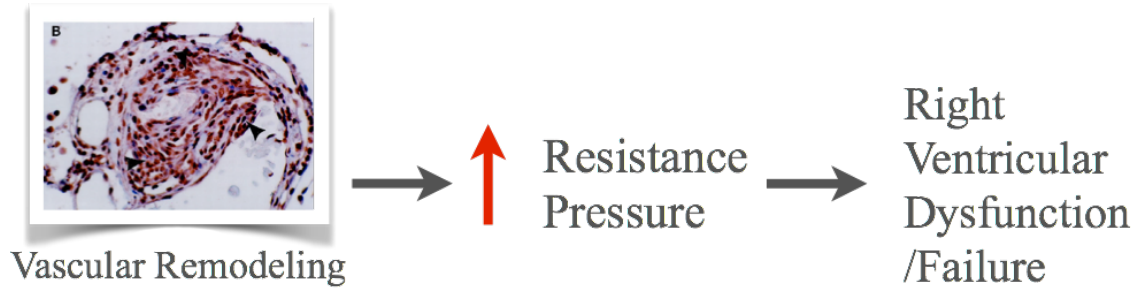
Figure 2. Pulmonary Arterial Hypertension: Natural history of disease. Schematic representation of the natural history of pulmonary arterial hypertension**.** Pulmonary vascular remodeling will be directly translated into increased blood flow resistance and therefore, increased pulmonary pressure. Right ventricular dysfunction and failure will be the direct consequence of increased pulmonary pressure (also known as RV after load). *Image of lung vascular lesion was reproduced from Rai PR, et al. The cancer paradigm of severe pulmonary arterial hypertension. Am J Respir Crit Care Med. 2008,15;178(6):558–564 (Ref.* (183)*).*

partially understood(246). Furthermore, a detailed description of the cellular and molecular mechanistic elements that explain RV failure ("RV failure program") is incomplete.

> **Given the prognostic importance of RV dysfunction/failure in PAH, understanding the mechanisms underlying the transition from adaptive (functional) to maladaptive (dysfunctional) right ventricular hypertrophy is critical, particularly if any to these mechanisms can be <u>prevented or reversed.</u>**

CHAPTER 3 discusses pertinent data highlighting unmet needs based on our current concepts of the pathobiology of RVF and provides an overall justification for the study of RV failure mechanisms. Chapter 3 also provides the basic cardiac physiology concepts that underlie the experimental approaches taken. As part of a preliminary project, we studied explanted hearts obtained from autopsy material of two different groups with pulmonary arterial hypertension and analyzed the differences in RV hypertrophy. These data are presented as part of Chapter 3.

Indeed, our knowledge of the pathobiology and pathophysiology of RVF has evolved from the state available two decades ago. New concepts such as fibrosis, capillary rarefaction, cardiac hibernation and cardiomyocyte apoptosis now complement the classical theory of load-dependent, wall stress-induced RV dysfunction. Because left ventricular failure, in the setting of chronic pressure overload (i.e systemic hypertension) is characterized by changes in energy substrate utilization and abnormal mitochondrial biology, we sought to characterize the changes in mitochondrial energy metabolism during RV failure.

We hypothesized that maladaptive RV hypertrophy, but not functional/adaptive RV hypertrophy would be characterized by abnormal cardiac metabolism and mitochondrial dysfunction.

To begin to address our research question, we utilized 2 different animal models of chronic RV pressure overload, the SU5416/hypoxia and the pulmonary artery banding models. **CHAPTER 5** provides a detailed description of the methodology used throughout the studies and the results are presented in **CHAPTER 6**. Lastly, **CHAPTER 7** includes published and unpublished data regarding additional therapeutic strategies utilized to reverse the metabolic changes and RV failure described in Chapter 6.

Chapter 2: Pathobiology of Pulmonary Arterial Hypertension

Segments of this chapter have been previously published in:

Voelkel NF, **Gomez-Arroyo J**, et al. Pathobiology of pulmonary arterial hypertension

and right ventricular failure. *Eur Respir J.* 2012 Dec;40(6):1555–1565.

CHAPTER 2

"Mexiform lesion" - © Jose Gomez-Arroyo

2.1 Introduction

As briefly stated in Chapter 1, our knowledge of the pathobiology of PAH has

significantly changed from what was initially proposed two decades ago(243). Early

hypotheses derived from autopsy studies and animal models of hypoxia-induced

pulmonary hypertension postulated that 1) vasoconstriction, 2) vascular remodeling and

3) thrombosis *in situ* were the main components contributing to the development of the

disease. Indeed these three components became the main targets for the therapies

designed to treat patients with PAH(106). However, whereas it is true that

vasoconstriction plays a role in the disease, that a small group of patients have a highly

vasorreactive (perhaps, completely different) form of PAH, and that thrombosis is frequently observed in small vessels(71), the use of vasodilator therapy and anticoagulants has not had a great impact on disease progression(72, 213). Therefore, new hypotheses based on human samples, cell-based and animal models have been developed. Although some of these concepts have been previously considered as part of the disease (**Figure 3**), mechanistic studies addressing the role of genetics, epigenetics and immune dysregulation in the pathogenesis of the PAH had not been reported until rather recently. This chapter intends to put in perspective the newly postulated pathobiological concepts of PAH, which reflect the progress made in the understanding of this complex pulmonary vascular disease.

2.2 Genetic influences and epigenetics in PAH

The pathogenesis of PAH is based on more than one hits, and genetic factors conferring a predisposition for the development or progression of severe PAH may be required as one of the hits (**Figure 4**)(136, 157, 175). Mutations of the Bone Morphogenic Type II Receptor (BMPR2) gene, a member of the transforming growth factor (TGF-β) superfamily, were first described in patients with familial/hereditary PAH (HPAH)(157). Although BMPR2 mutations in HPAH have a high prevalence (70%), limited numbers of patients with IPAH have mutations(136), and only 20% of the carriers ever develop PAH during their lifetime(136). BMPR2 mutation carriers at the time of PAH-diagnosis are younger (77, 175) and less likely have a vasoreactive component(59). A large number of mutations have

Figure 3. Early postulated hypothesis of the pathogenesis of pulmonary arterial hypertension.

IMMUNE
MECHANISMS
DRUGS
HYPOXIA
TOXINS
PERSISTENT
FETAL CIRCULATION

INDIVIDUAL
PULMONARY VASCULAR
HYPERREACTIVITY
(GENETIC DISPOSITION ?)

RIGHT VENTRICULAR
HYPERTROPHY

VASOCONSTRICTION ⟶ PA PRESSURE ↑
PVR ↑

INTIMA-ENDOTHELIAL CELL LESIONS
MEDIA HYPERTROPHY
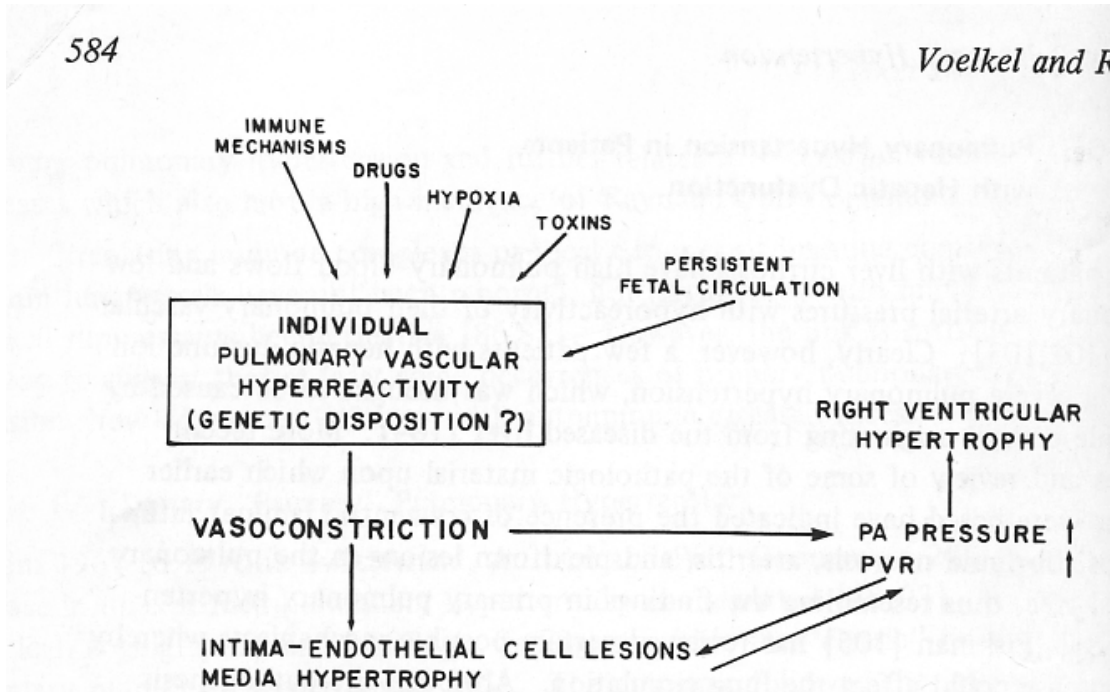
Figure 3. Data derived from the analysis of human samples and from the study of animal models of hypoxic pulmonary hypertension lead to the generation of early hypotheses that considered vasoconstriction a central component of the pathogenesis of pulmonary hypertension. *Copyright 1979. Reproduced with permission of the publisher. The image was obtained from Voelkel N, Reeves JT. Chapter 10: Primary Pulmonary Hypertension. In: Moser KM, editor. Pulmonary Vascular Diseases. New York: Marcel Dekker, Inc; 1979.*

been reported and the majority translate into a loss of function (137) or reduced BMPR2 expression(14). It has been reported that the disease appears to be more severe when patients carry a truncating BMPR2 mutation(15) however, this appears not to be the case in the French patients (77). Mechanistic studies indicate that BMPR2 mutations are permissive but not necessary for the development of severe PAH. BMPR2 may be one of the guardians of lung vessel homeostasis, as gene knockout and silencing experiments have clearly demonstrated that both apoptosis and cell proliferation of pulmonary vascular smooth muscle and endothelial cells are controlled by BMPR2(150). Intact BMPR2 signaling may be necessary for the execution of a normal lung vascular wound-healing program, preventing apoptosis-induced compensatory cell proliferation. BMPR2 loss makes cells more susceptible to apoptosis(226), however, vascular cell-apoptosis alone, is insufficient for angioproliferation to occur. BMPR2 signaling appears to define the cellular identity during reparative responses(230). BMP signaling is regulated at many different levels and each level could potentially contribute to abnormal BMPR2 function, without necessarily involving a mutation in the *BMPR2* gene(150). For example, mutations in the type I TGF-β receptor, ALK-1(76, 218, 229), have been observed in patients with severe PAH occurring in families with hereditary hemorrhagic telangiectasia. Moreover, although infrequent, mutations in the BMPR2-downstream mediators, the smad proteins, have also been described in PAH patients(155). In the aggregate the data indicate that BMP/TGF-β signalling plays an important role in the maintenance of the normal lung arteriolar structure.

Epigenetic mechanisms influence gene expression via modifications of the chromatin, histones and regulatory micro RNAs(95). At present, there is no firm evidence that PAH

Figure 4. Hallmarks of severe angioproliferative pulmonary arterial hypertension.
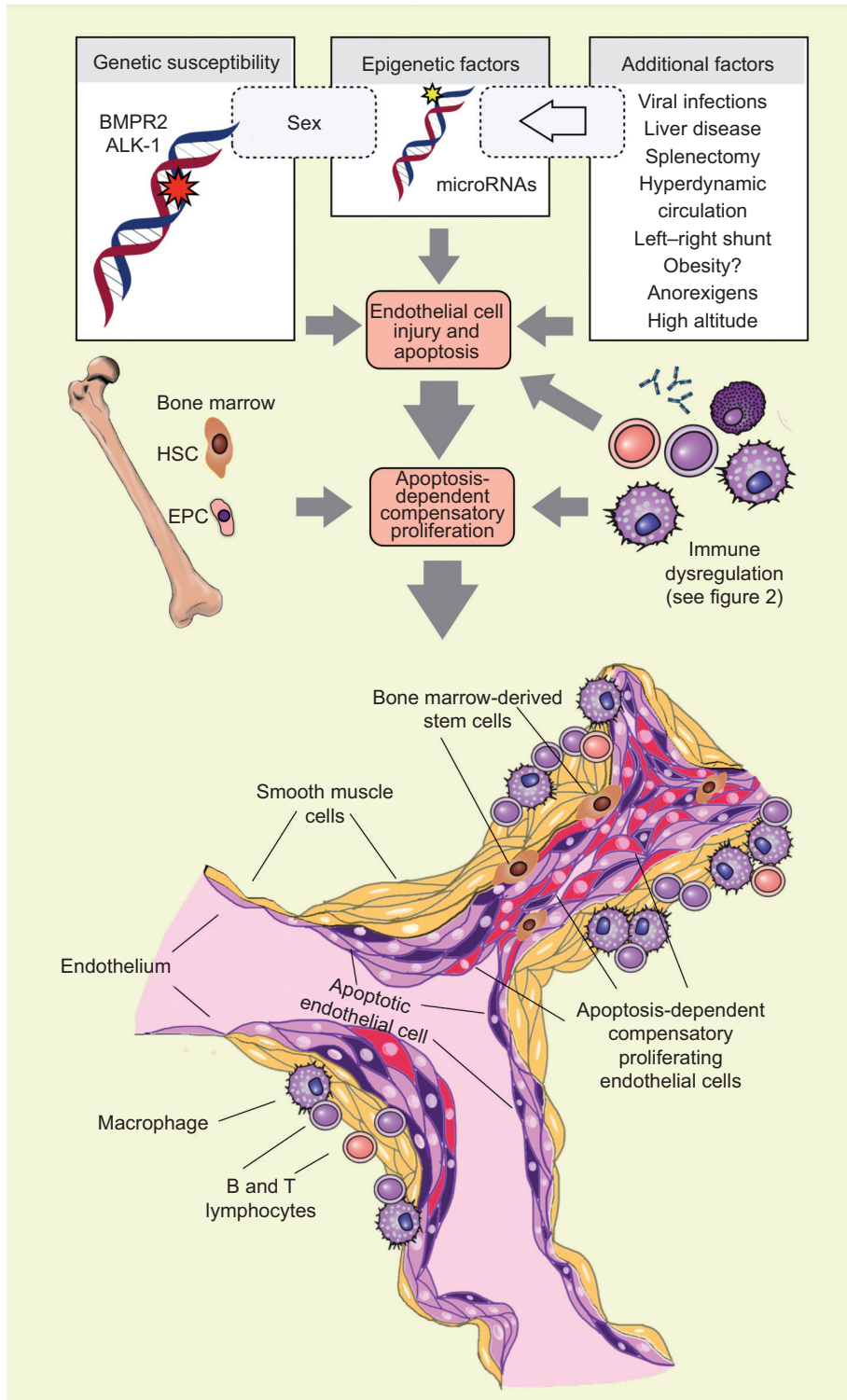
Figure 4. Genetic determinants, epigenetic factors and other conditions synergise and result in the injury and apoptosis of pulmonary arteriolar endothelial cells. Endothelial cell apoptosis triggers compensatory proliferation of phenotypically abnormal endothelial cells. Apoptosis may also be the initiating event, activating the bone marrow to release precursor and stem cells and eliciting a local immune response of the vascular wall. The end result is the complex vascular lesion, the plexiform lesion. These complex lesions obliterate the lumen of small arteries, predominantly localised to vessel bifurcations. The mature lesions are composed of endothelial cells (dark purple), smooth muscle cells (yellow), apoptotic cells (purple) and phenotypically altered apoptosis-resistant endothelial cells (red). These cells, together inflammatory cells, populate a microenvironment of exuberant cell growth. BMPR2: bone morphogenic type II receptor; ALK-1: activin A receptor type-II like-1; HSC: hematopoietic stem cell; EPC: endothelial progenitor cell. *Copyright 2012. Reproduced with permission of the publisher from Voelkel NF et al, et al. Pathobiology of pulmonary arterial hypertension and right ventricular failure. Eur Respir J. 2012 Dec;40(6):1555–1565.*

has an epigenetic component(119). Downregulation of BMPR2 expression has been

explained by activation of a STAT3/miRNA-17-92 microRNA axis in normal human

lung endothelial cells after interleukin-6 exposure(31). Interestingly, mice overexpressing

IL-6 develop severe pulmonary hypertension(214) and, unlike other PH mice models ,

also develop angioobliterative vascular remodelling and robust RV hypertrophy(82).

Overexpression of miR-17 also increases proliferation of human pulmonary artery

smooth muscle cells and inhibition with an specific miR-17 antagomir ameliorated PH in

two experimental models(180). Another microRNA, miRNA-204, has been found

downregulated in pulmonary artery smooth muscle cells isolated from patients with

PAH(44). Upregulation of miR204 seems to induce an apoptosis-resistant phenotype in

smooth muscle cells.

2.3 The paradigm shift: From vasoconstriction to cell growth.

Terms like "cell phenotype switch," "apoptosis-resistance" and "angiogenic niche" have

introduced a new vocabulary which can be used to explain the pathobiology of

PAH(183). The early pioneers of PH research focused their attention on hypoxic

vasoconstriction(254), and because the arachidonic acid-derived prostacyclin is a

powerful inhibitor of hypoxic pulmonary vasoconstriction(242), it was thus intuitive to

establish prostacyclin infusion as the first treatment for severe PAH(17). Since then, rapid

progress has been made. Our knowledge of the cellular and molecular components

involved in the pathobiology of PAH has expanded and these new insights are likely to

change our future approach to the treatment of PAH. We now regard the plexiform

pulmonary vascular lesions as a product of an angioproliferative process leading to

vascular occlusion (angioobliteration)(183, 232) and we appreciate that these lesions are

composed of a multitude of cell types, among them, actively dividing and phenotypically abnormal apoptosis-resistant endothelial cells with a monoclonal origin(129), progenitor cells(148) and immune cells(40, 171, 172). Immunohistochemistry, using antibodies directed against cell surface epitopes and nuclear markers of cell activation, identifies different cell phenotypes with their expressed genes and proteins(183). Hallmarks of cancer in angioproliferative PAH have been described, in particular angiogenesis(232), metabolic changes(262) and apoptosis-resistant cells(193). Based also on the therapy refractoriness of PAH, a hypothesis of "quasi-malignancy" has been proposed(183): apoptosis may be the initiating event followed by the selection of proliferating apoptosis-resistant cells –some of which may be stem cells **(Figure 4)**. PAH plexiform lesions also show decreased expression of the tumor-suppressor protein peroxisome proliferator activated receptor (PPAR) gamma(9), while exhibiting increased expression of β-catenin, CXCR4 (a receptor that mediates metastatic cell homing), and survivin, among other(183). Survivin, an inhibitor of apoptosis, is expressed in essentially all cancers, and cultured cells isolated from the lungs of PAH patients exhibit a markedly increased expression of survivin. Moreover, experimental gene therapy targeting this protein suppresses proliferation and ameliorates PAH in rats(141). Another hallmark of cancer is the metabolic switch towards glycolysis (Warburg effect, perhaps as a defense against oxidative damage). Pulmonary arterial endothelial cells from IPAH patients cultured *in vitro*, demonstrate reduced oxygen consumption, reduced mitochondrial respiration and increased glycolytic metabolism(262).

The "quasi-malignancy" disease model also accommodates the concept of a cancer stem cell/angiogenic niche(183). Precursor cells can be transported into the pulmonary

vascular adventitia via vasa vasorum(263), stem cells can divide and migrate from a niche at the media-adventitia border zone(61) and pulmonary microvascular endothelial cell stem cells of small arteries(8) may proliferate to the point of lumen obliteration. It is presently unclear whether stem- and precursor cells are friends or foes. For example, autologous endothelial progenitor cells transplantation therapy for PAH has reported positive results(252). However, this early trial has been criticized(228) because the cells utilized for the clinical trial were not "true" progenitors. Conversely, anti c-Kit (a stem cell marker) treatment for PAH with the tyrosine kinase inhibitor imatinib mesylate, has demonstrated anectodal positive results(75). Stem cell-based gene therapy is currently being investigated in a clinical trial (NCT00469027).

Growth factors and receptor tyrosine kinases

Many potent cell growth factors are overexpressed in IPAH vascular lesions, and it is likely that these growth factors and their receptor tyrosine kinases contribute to cell growth and vessel obliteration. The Platelet Derived Growth Factor (PDGF) has been extensively studied in PAH(173), and it has been shown that PDGF can induce the proliferation and migration of SMCs and fibroblasts. PDGF has been proposed as a key mediator in the progression of several fibroproliferative disorders. It was postulated that PDGF receptor blockers could reverse PAH, based on the case report of a patient with end-stage IPAH, treated with imatinib mesylate. Subsequently, a clinical safety trial evaluating imatinib mesylate as a treatment of advanced forms of PAH was performed(74). The data showed a significant decrease in pulmonary vascular resistance (PVR) and a moderate increase in cardiac output, but no significant change in pulmonary artery pressures, leading to the conclusion that imatinib mesylate may have a limited role

in the treatment of IPAH patients. Other tyrosine kinase inhibitors for PAH are being studied(78, 160). It is important that the tyrosine kinase inhibitors imatinib, sorafenib and nilotinib were shown in animal studies to be acute pulmonary vasodilators(2). However, the vasodilator effect in clinical studies of PAH was not prominent. This is an example, that identifying highly specific molecular targets in PAH animal models that do not reproduce the salient features of human PAH, may be misleading and the drug effect may be lost in translation(81, 82). Paradoxically, dasatinib, a multi-tyrosine kinase inhibitor, has been associated with the development of PAH(94, 147).

2.4 Inflammation and Immune Response

The association of autoimmune disorders with PAH and the presence of antinuclear and antiphospholipid antibodies in the serum of patients with IPAH has been appreciated for many years(158). There is more evidence that lymphoid neogenesis occurs in IPAH; macrophages, mast cells, T- and B- lymphocytes, plasma cells and anti-endothelial cell antibodies are present in and around the complex pulmonary vascular lesions in IPAH patients(171, 232). Serum levels of IL-1 and IL-6 are high in IPAH patients(103), and serum IL-6 levels negatively predict patient survival(211). However, whether inflammation and aberrant immune responses in IPAH are cause or consequence remains unknown. Likely PH occurs when an inflammatory pulmonary arteriolar injury is not resolved by (normally) protective, innate anti-inflammatory mechanisms. Regulatory T-cells (Tregs) control not only other T-cells but also regulate monocytes, macrophages, dendritic cells, natural killer cells and B-cells(192), and recent evidence suggests that decreased Treg cell number or function may favour the development of PH(221). For example, conditions associated with PAH, such as HIV, systemic sclerosis, systemic

lupus erythematosus, Hashimoto's thyroiditis, Sjogren's Syndrome and the

antiphospholipid syndrome are characterized by abnormal CD4$^+$ T-cell number and

function(28, 45, 139, 167, 182, 212). At the experimental level, athymic rats, lacking T-

cells, develop pronounced PH after vascular injury with a vascular endothelial growth

factor receptor blocker. The lungs in these animals are populated by infiltrating

macrophages, mast cells and B cells, similar to human PAH lesions(221, 224). Most

importantly, PH is prevented by immune reconstitution of Tregs prior to the induction of

vascular injury(221). All together, it is a possibility that aberrant Treg-cell function in the

face of vascular injury can result in heightened innate and adaptive immune responses

that could initiate and/or propagate the development of PH (120)(**Figure 5).** Despite the

increasing evidence suggesting a role for immune deregulation in PAH, there is only

limited anecdotal evidence suggesting that PH associated with connective tissue disorders

–such as systemic lupus erthyematosis and systemic sclerosis or viral infections, such as

human herpes virus-8 – can respond to gluococorticoids or targeted B cell depletion(93,

116). Sanchez et al(196) and Jais et al(111) reported on treatment of patients with mixed

connective tissue disease - or systemic lupus erythematosus – associated PH, where

corticosteroid and cyclophosphamide has been used as first-line drugs. The effectiveness

of B cell depletion is currently being put to test with an NIH-trial examining the

effectiveness of rituximab – a chimeric monoclonal antibody against the protein CD20,

primarily expressed by B-cells – for systemic sclerosis-associated PH (NCT01086540).

Figure 5. Participation of the immune system in pulmonary vascular remodelling.
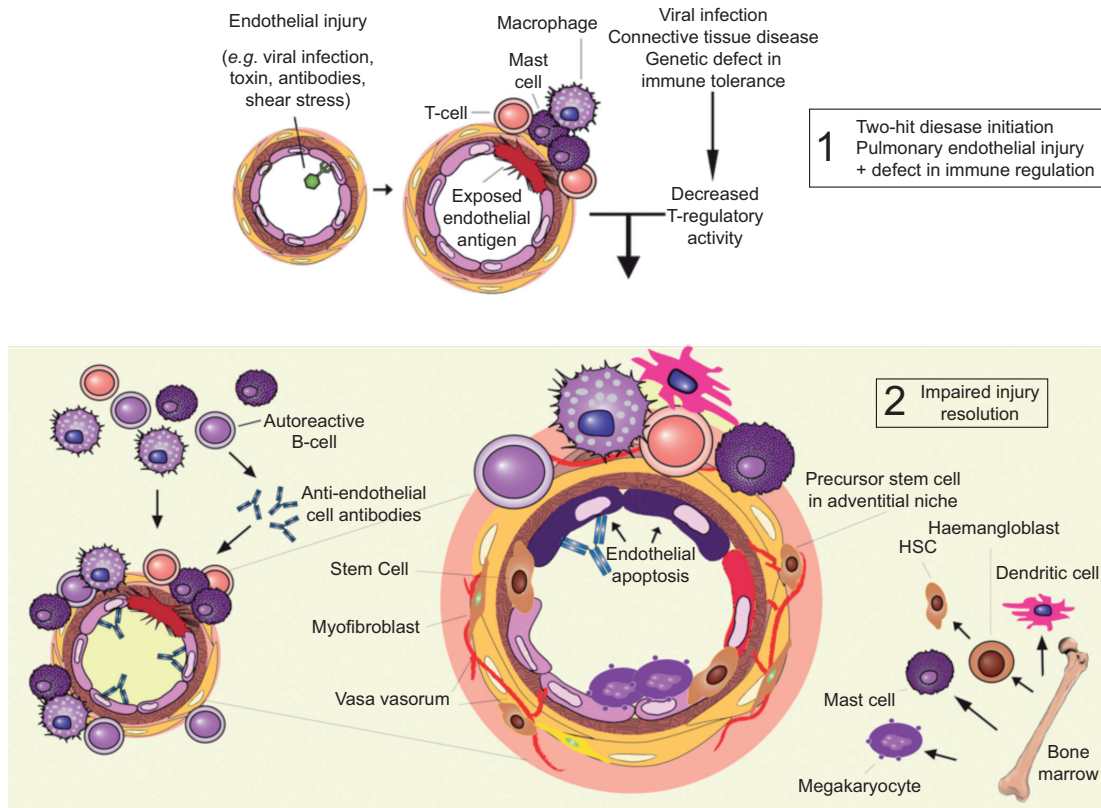
Figure 5. The initial arteriolar endothelial cell injury can be due to mechanical stress, toxins or antibodies. The ''two-hit'' hypothesis considers that defective immune regulation, such as in HIV/AIDS and scleroderma, participates in the lumen-obliterating cell growth [1] and in the impaired injury resolution [2]. The disease model depicted here reflects the complexity of multicellular interactions within and around the vascular wall and the active role of the bone marrow and inflammatory and immune cells in the pathobiology of pulmonary arterial hypertension. The multi-growth factor-producing mast cell was the first of several immune cells to be identified in the perivascular space of pulmonary arterioles in lungs from patients with severe pulmonary hypertension. It may populate these vessels because of hyperplasia (in situ expansion of mast cell number) or after being recruited from the bone marrow. An impaired activity of regulatory T-cells may facilitate the angio-obliteration. HSC: hematopoietic stem cell. *Copyright 2012. Reproduced with permission of the publisher from Voelkel NF et al, et al. Pathobiology of pulmonary arterial hypertension and right ventricular failure. Eur Respir J. 2012 Dec;40(6):1555–1565*

It is becoming apparent that circulating factors can likely amplify lung vascular injury, attract immune cells and/or repair cells which respond to a variety of chemotactic stimuli, suggesting perhaps, a systemic disease component contributing to the development or progression of PAH. In the "modern era" of PAH treatments, where standard vasodilation therapies have failed to reverse or stop the progression of PAH, novel targets such as discrete immune pathways hold promise. However, new drugs and clinical trials will require to assess which patients may respond to anti-inflammatory treatment strategies.

2.5 Summary and Conclusions

PAH is increasingly recognized not as one disease but as a group of diseases where genetic susceptibility renders patients vulnerable to a chronic pulmonary microangiopathy. Further explorations of the molecular mechanisms of cell reprogramming in PAH, in both the lung vessels and the heart, should lead to a better understanding of this group of diseases. The classical pathophysiology of PAH which operates with the mechanical concepts of pressure, flow, shear stress, RV wall stress and impedance, should be complemented with the new pathobiological concepts of cell injury and repair and interactions of complex multicellular systems (**Figure 6**). Precursor-and stem cells derived from the bone marrow and resident lung vascular stem cells should also be considered as active players in the process of pulmonary vascular wound healing "gone awry". Integrating the new pathobiological concepts will become critical as we design new medical therapies in order to change the prognosis of the patients with this fatal group of diseases.

Figure 6. Integration of haemodynamic and cellular events that characterise the cardiopulmonary disease of severe pulmonary arterial hypertension (PAH).
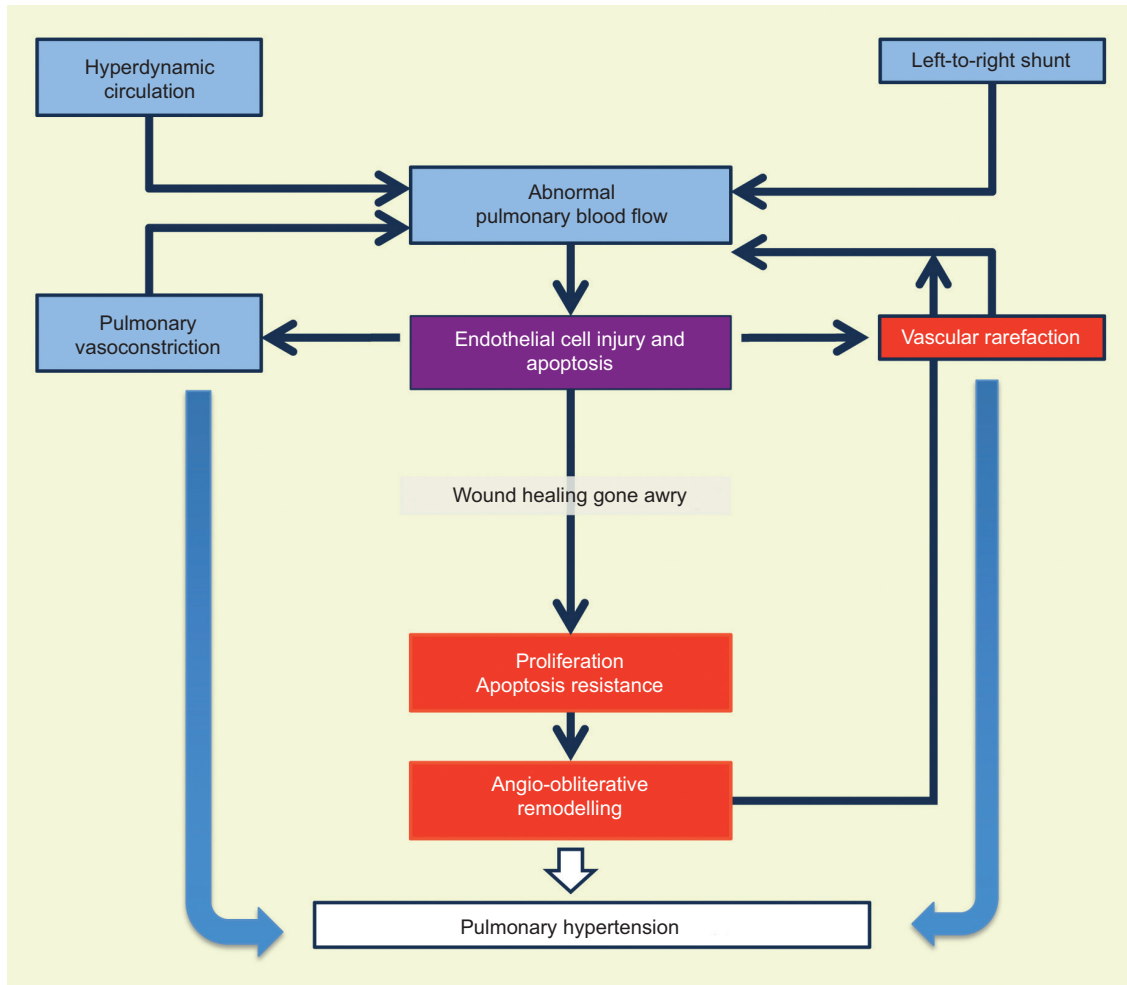
Figure 6. The pathophysiology of PAH, which operates via mechanical concepts, is complemented with concepts of cell injury and repair and interactions of complex multicellular systems. The model is built on the principle of abnormal pulmonary blood flow. Regional blood flow abnormalities underlie the pulmonary vascular remodelling, which in turn causes further alterations of the regional blood flow, perpetuating a cycle of cell death and cell proliferation. Vascular rarefaction occurs in the form of pruning of the small lung vessels, and in the right ventricle in the form of myocardial capillary rarefaction. *Copyright 2012. Reproduced with permission of the publisher from Voelkel NF et al, et al. Pathobiology of pulmonary arterial hypertension and right ventricular failure. Eur Respir J. 2012 Dec;40(6):1555–156*

Chapter 3: Function and Dysfunction of The Right Ventricle

Segments of this chapter have been previously published in:

Gomez-Arroyo J et al. Differences in Right Ventricular Remodeling Secondary to

Pressure-Overload in Patients with Pulmonary Hypertension. *Am J Respir Crit Care Med*.

2013. *In Press*.

Voelkel NF**, Gomez-Arroyo J**, et al. Mechanisms of right heart failure-A work in

progress and a plea for failure prevention. *Pulm Circ*. 2013 Jan;3(1):137–143.

.

CHAPTER 3

"Severe damage of right ventricle free wall (of the dog) had no apparent effect on

hemodynamics."

Starr I., et al.

American Heart Journal, **1943**

3. 1 Introduction

The right ventricle (RV) of the heart, which pumps blood through a low pressure, low resistance "lesser" circulation, is now receiving more attention by researchers and clinicians, after many years of benign neglect(23, 30, 85, 246). Some of the many reasons for neglecting the RV assumed that 1) In the context of global cardiac performance the RV was not very important (246) and 2) That the cellular and molecular mechanisms of RV failure (RVF) were not different from those responsible for LV failure. Perhaps the biggest knowledge gap originated from the lack of experimental studies modeling the development of RVF, and from attempts to extrapolate mechanisms of chronic RVF from studies originally designed to study acute RVF. These likely explain why "pressure overload" is the most frequent – and sometimes exclusively – quoted mechanism of RVF. Indeed, patients with chronic, progressive pulmonary vascular disease, most frequently die of RV failure(249). However, as we increment our

knowledge in the pathobiology of RVF, we should also begin to consider RVF as a "progressive," but not necessarily "chronic" phenomenon.

3.2 The case for investigating the Right Ventricle

We propose that the outcome of the patient with pulmonary arterial hypertension (PAH) is not only determined by pathophysiological characteristics germane to the lung disease – vasoconstriction and pulmonary vascular remodeling – but rather by the response of the RV to increased afterload and to additional mechanistically important factors imposed on the RV such as neuroendocrine system activation (23, 26) and perhaps, factors released from a "sick-lung circulation" (243)(**Figure 7**). In the management of patients with severe PAH we still face (as a barrier) the fact that prevention of RV failure is not a realized treatment goal. For the past 15 years, clinical studies have utilized vasodilator drugs expecting to significantly reduce pulmonary arterial pressure, halt or delay the progression of the lung vascular disease, reduce RV afterload and prevent the development of RVF. However, this goal is not often accomplished in the clinical setting, as a recent meta-analysis of PAH clinical trials reported a weighted mean reduction in mean pulmonary arterial pressure of 3 mmHg after treatment(72). Moreover, it has been demonstrated that even after many years of vasodilator therapy (at least with epoprostenol treatment), pathological lung vascular remodeling does not stop(213). Lastly, a recent cardiac MRI study from the Netherlands' pulmonary hypertension center reported that the survival of medically treated patients with PAH was not determined by a vasodilator-induced decrease of the pulmonary vascular resistance, but rather by an improved RV ejection fraction (RVEF) (237).

36

Figure 7: The sick lung circulation–right heart failure axis.
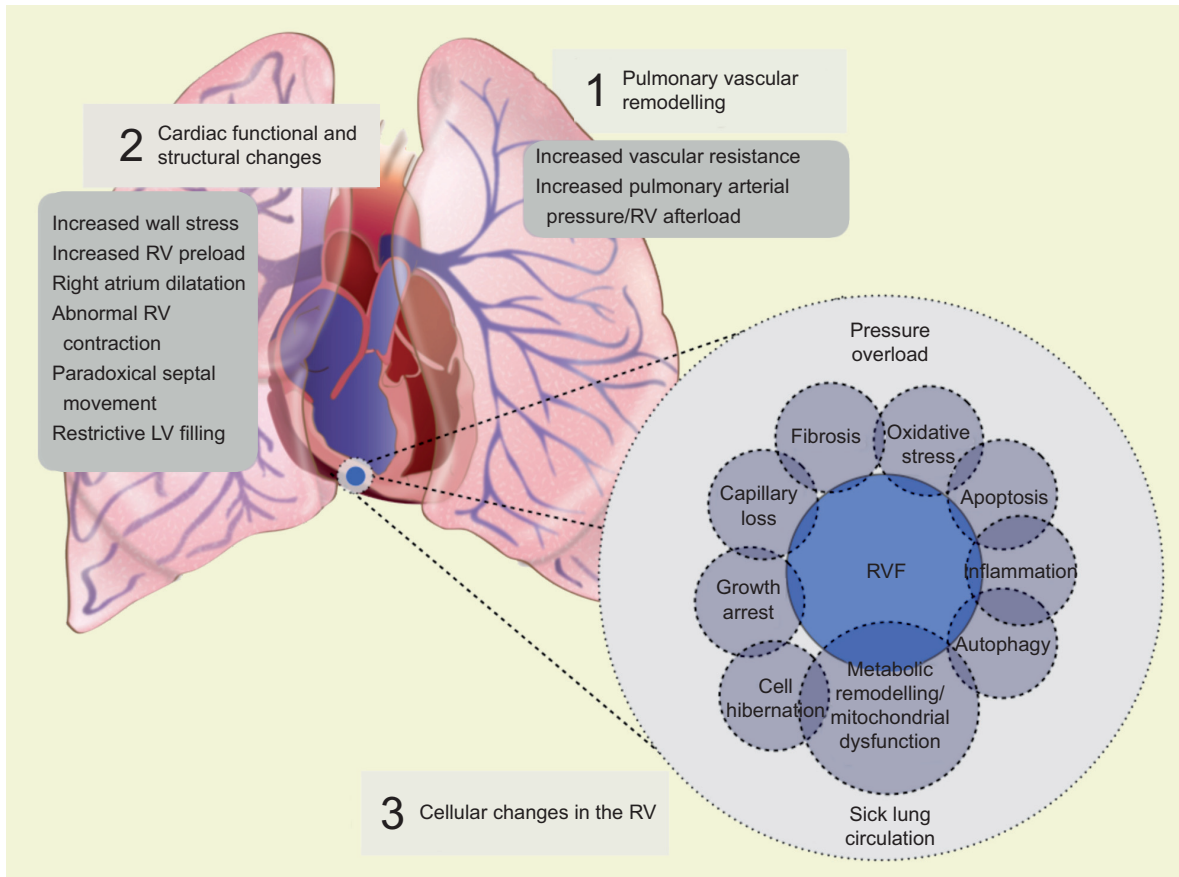
Figure 7: Increased pulmonary vascular resistance generates a significant afterload for the right ventricle resulting in right ventricular hypertrophy. The structural and functional changes during the development of right ventricular failure can be characterized clinically(249). Right ventricular dysfunction is probably associated with multiple cellular changes(23), such as oxidative stress, apoptosis, inflammation, fibrosis and metabolic remodelling. These factors also contribute to right ventricle (RV) dysfunction and failure. The cellular changes are either the result of chronic RV pressure overload or the effect of circulating factors released from the sick lung circulation. RVF: right ventricle failure; LV: left ventricle. *Copyright 2012. Reproduced with permission of the publisher from Voelkel NF et al, et al. Pathobiology of pulmonary arterial hypertension and right ventricular failure. Eur Respir J. 2012 Dec;40(6):1555–1565.*

Thus, if current vasodilator drugs have failed to reverse the vascular disease, should we not start thinking about RV-targeted therapies while we wait for new PAH lung-specific therapies to get in the pipeline?

The prevailing paradigm holds that increased RV afterload is sufficient as an explanation of RV failure, but there are several conflicts with this view:

- Under most circumstances the RV adequately adapts to chronic pressure overload (in contrast to acute pressure overload). In average, at least 55% of incident patients with PAH live (with chronic progressive pressure overload) for 3 years(22).

- Even in the pre-pulmonary hypertension "drug era" (prior to 1991) there were long-term PAH patient survivors(241), most prominently patients diagnosed with aminorex- (appetite suppressant) induced PAH(127).

- There are patients with severe PAH that remain highly functional (NYHA functional class I) for many years without developing RV failure(22).

- Experimental studies show that after pulmonary artery banding (PAB), the RV develops adaptive hypertrophy which is more resistant to pressure overload and does not necessarily develop failure(25).

Perhaps, the best example to argue against pressure-overload as the unique insult responsible for the development of RVF are the patients with Einsemenger Syndrome.

3.3 Differences in Right Ventricular Remodeling Secondary to Pressure-Overload in Patients with Pulmonary Hypertension: The 'Unique' Right Ventricle of Patients with Eisenmenger Syndrome

Patients with Eisenmenger Syndrome (EMS), develop PAH secondary to a systemic-to-pulmonary shunt. In other words, a congenital heart defect (mainly nonrestrictive post-tricuspid defects) initially allows blood to shunt the left side compartment to shunt towards the right ventricle or pulmonary artery, either by means of a ventriculoseptal defect or a *patent ductus arteriosus*. If not corrected a certain age, the shunt allows large amounts of blood to be pumped into the lung circulation (volume-overload) and this overload eventually leads vascular remodeling and pulmonary hypertension(97). Once PH has developed, the pressure in the right ventricle will eventually be high enough to reverse the shunt and pump venous (deoxygenated) blood into the left (systemic) circulatory compartment, explaining the remaining features of the Eisenmenger syndrome: Cyanosis, chronic hypoxemia, polycythemia and finger clubbing(97)..

Most importantly, the 'resilient' RV of EMS patients appears to be better adapted to increased pressure-overload compared to the RV of patients with idiopathic PAH (IPAH) or other forms of PAH(98). Indeed, whereas most patients with IPAH frequently present with decreased cardiac output at the time of diagnosis(22), patients with EMS maintain a normal cardiac output and right atrial pressure in spite of a similar degree of pressure overload(96), at least until later stages of the disease(96). Interestingly, whereas the hemodynamic differences between IPAH and EMS patients have long been recognized(96), and some structural differences of the RV have been described by

cardiac tomography(98), an anatomo-pathological comparison between the hearts of patients with EMS and IPAH has so far not been reported.

As a preliminary project, we performed a post-mortem morphometric analysis of the left and right ventricles of patients with IPAH (n=6) or EMS (n=6) who died from RV failure, and sought to characterize the differences in RV hypertrophy.

3.3.1 Patient's characteristics and methods

All patients with EMS included in this study had a patent ductus arteriosus as the systemic-to-pulmonary shunt. Age-matched patients who died from non-cardiac, non-pulmonary disease where used a controls (n=6). The majority of patients died before any PAH-specific therapies were available. However, we excluded any patient that had been treated with PAH-specific drug later in time. Informed consent was obtained from the family of each patient. The study protocol conformed to the ethical guidelines of the 1975 Declaration of Helsinki and was approved by the Instituto Nacional de Cardiología "Ignacio Chávez" Institutional Review Board.

We measured the anterior-to-posterior and septum-to-free-wall diameters, as well as RV and LV wall thickness at the base, middle and apex levels (**Figure 8A-B**). Annular dimensions of tricuspid and mitral valves were also measured. Utilizing the RV diameters we estimated the RV-chamber area using the formula $A= (\pi * dAP * dSW)/4,$ were A represents the RV-chamber area, $ChamberArea = \frac{\pi*dAP*dSW}{4}$ dAP represents the anterior-to-posterior diameter and dSW represents the septum-to-free wall diameter. This formula was derived from the formula to calculate the area of a circle. All results are reported as mean ± standard deviation. Differences between groups were assessed by one-way or

two-way ANOVA and a Bonferroni's post-hoc test was used to assess significant differences between groups. A *p-value*< 0.05 was accepted as significant. Correlation analysis was done using a Spearman's test.

The mean age for all groups was 28 ± 10 years. Both EMS and IPAH patients had severe pulmonary hypertension (56 ± 14 mmHg in IPAH *versus* 78 ± 14 mmHg in EMS, *p=0.023*). **Figure 8C-E** illustrates that the RV in both groups of patients responded to pressure-overload with significant hypertrophy as evidenced by increased RV wall thickness. Interestingly, EMS patients also exhibited increased left ventricular (LV) wall thickness at the base and middle levels but not at the apex level (**Figure 8F-H**). In contrast to what has been reported by cardiac magnetic resonance in patients with increased RV afterload secondary to chronic thromboembolic pulmonary hypertension[89], we did not find a reduction in LV wall thickness in the group of patients with IPAH. **Figure 9A-C** illustrates the correlation between the wall thickness at the base, middle and apex levels with their respective RV-chamber area. Patients with IPAH developed significant RV hypertrophy compared to control right ventricles but significantly less hypertrophy compared to EMS patients. Most importantly, compared to EMS group, the RV of IPAH patients had significantly less hypertrophy (RV thickness) in relationship to the RV-chamber area **(Figure 9A-C)** and this relationship between area and wall thickness seemed to be more disproportionate at the apex level.

It should be noted, however, that EMS patients had significantly a higher mean pulmonary arterial pressure and this finding could in fact explain the differences in RV

Figure 8. Right and Left Ventricles Wall Thickness in Patients with Pulmonary Arterial Hypertension
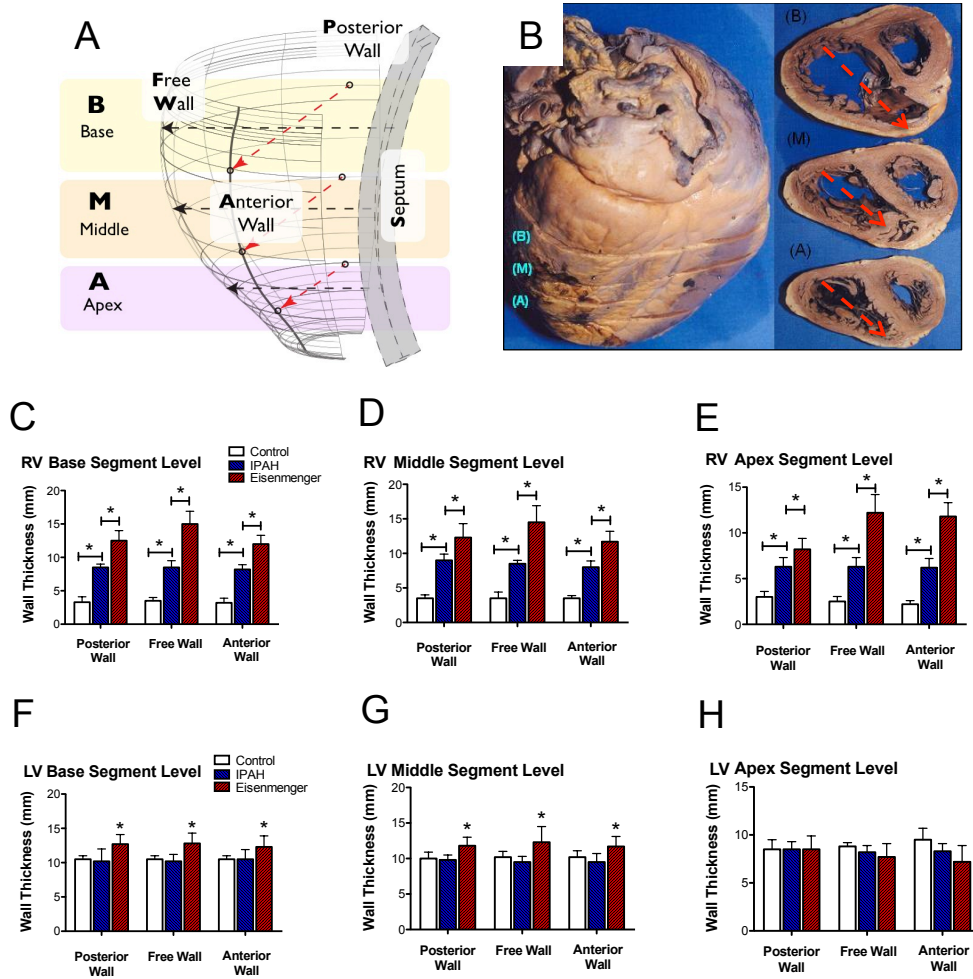
Figure 8. A-B) Schematic representation and gross anatomy of the RV illustrating the location where each measurement level was taken. **C-E)** Right ventricular posterior wall, anterior wall and free wall thickness at base, middle or apex segment levels. **F-H)** Left ventricular posterior wall, anterior wall and free wall thickness at base, middle or apex segment levels. *Figure was reprinted with permission of the American Thoracic Society. Copyright © 2013 American Thoracic Society* **Gomez-Arroyo J** *et al. Differences in Right Ventricular Remodeling Secondary to Pressure-Overload in Patients with Pulmonary Hypertension. Am J Respir Crit Care Med. 2013. In Press.*

hypertrophy. However, as it can be appreciated in **Figure 9F-H**, the LV of these patients

is also larger and thicker, which could suggest the presence of a stimuli, not directly

associated with increased RV pressure-overload, that lead to generalized growth of the

heart. However, to what extent the remodeling of the RV in EMS patients is independent

of pressure-overload will remain to be investigated. Interestingly, despite the fact that the

RV of EMS patients was exposed initially to volume and later by pressure-overload, the

RV underwent concentric **(Figure 9M)** rather than eccentric hypertrophy. This is a

particularly interesting finding given the fact that volume-overload of the left ventricle

frequently leads to dilated cardiomyopathy. It is also important to underline that all

patients in the EMS group had a post-tricuspid defect (patent ductus arteriosus) and our

findings may not be true for all congenital heart defects leading to Einsenmenger

physiology. For instance, it has been shown that pre-tricuspid defects (such as atrial

septal defects) exhibit different cardiac remodeling compared to post-tricuspid defects

(98). To further investigate cardiac remodeling in the two groups of patients, we analyzed

collagen deposition by Masson Trichrome staining. We demonstrated that both

conditions were associated with significant perivascular and interstitial RV fibrosis

(Figure 9 K-L). However, EMS patients appear to exhibit less RV fibrosis, which could

contribute to better diastolic function. The mechanisms underlying the difference in the

amount of cardiac fibrosis will remain to be investigated.

In the aggregate, based on the data derived from our study of patients with ESM

and from the current literature, one could suggest that chronic, progressive

pressure overload might be the initial component responsible for triggering

maladaptive changes in the RV, however, not necessarily the only one. Other factors

such as ischemia, inflammation, oxidative damage, epigenetics and abnormal cardiac

energetics could equally contribute to the development of RVF (**Figure 7**).

Figure 9. Correlation Between Wall Thickness and Chamber Area in Patients with

Pulmonary Arterial Hypertension
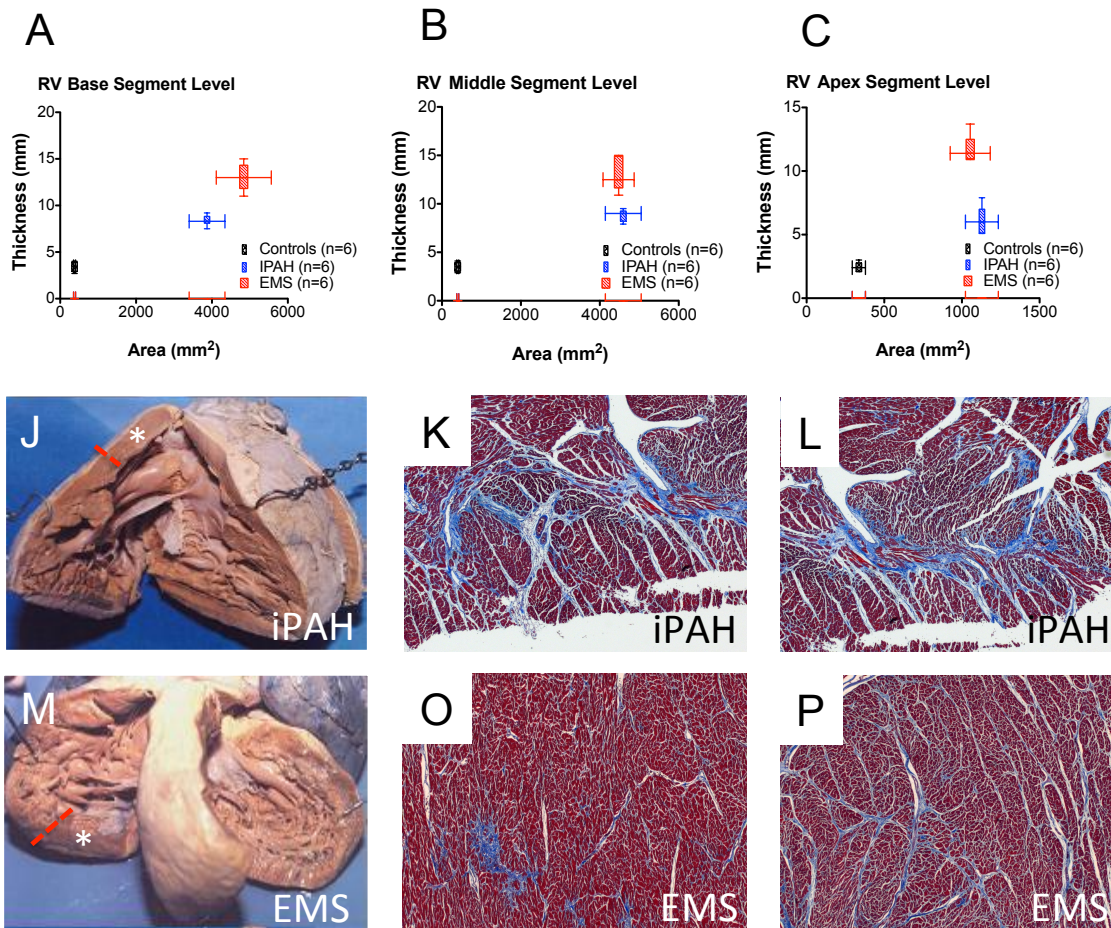
Figure 9. A-C) Correlation between free wall thickness and RV chamber area.

Horizontal and vertical whiskers represent the standard error bars for both variables. **J)**

Autopsy material shows the thin RV-free wall (asterisk) of a patient with idiopathic

pulmonary hypertension (IPAH), compared to the RV of an Eisenmenger's Syndrome

patient **(M). K-L)** Micrographs of Masson Trichromatic-Stained slides illustrate

significant collagen deposition (blue) in the RV of the IPAH patient compared to the

EMS patient **(O-P).** *Figure was reprinted with permission of the American Thoracic*

Society. Copyright © 2013 American Thoracic Society **Gomez-Arroyo J** *et al.*

Differences in Right Ventricular Remodeling Secondary to Pressure-Overload in Patients

with Pulmonary Hypertension. Am J Respir Crit Care Med. 2013. In Press.

3.4 Mechanisms of Right Ventricular Failure

3.4.1 Right ventricular ischemia

Patients with severe PAH can develop chest pain which may be due to RV

ischemia(241). Wolferen et al (239) have shown changes in the right coronary artery

blood flow pattern in patients with PAH, while Gómez, Sandoval and collaborators

employed stress myocardial scintigraphy using technetium sestamibi to demonstrate RV

ischemia associated with a RV end-diastolic pressure elevation(83). Unfortunately human

histological studies of the RV from patients with chronic severe PAH are unavailable,

and it has never been demonstrated whether the ratio of RV muscle-to-capillary density,

in patients with severe PAH, is altered as it has been reported in LV failure or in

experimental RVF(25). Hein *et al* studied LV tissue biopsies obtained at the time of heart

surgery for aortic stenosis valve replacement, and described capillary rarefaction and

discuss their finding of autophagy. In order to explain RV ischemia in the setting of PAH,

investigators have pointed towards increased RV-wall stress (92) and myocardial fibrosis,

but it is presently unclear whether RV-wall microcirculation impairment, RV wall stress,

RV fibrosis – or all these factors in combination – conversely contribute to RV

myocardial ischemia. In the SU5416/ chronic hypoxia (Su/Hx) model of severe PAH and

RV failure (to be discussed in Chapter 4) (25), Bogaard et al. have demonstrated a

dramatic reduction in the number of *perfused* myocardial capillaries using *in vivo* tomato-

lectin endothelial cell (EC) labeling. Histologically we have also showed diffuse

myocardial fibrosis(25). Capillary rarefaction has also been reported in the monocrotaline

(MCT) model of PAH(86). Surprisingly, the capillary density in the RV from rats with

pulmonary artery banding (mechanically induced RV hypertrophy) is only mildly

decreased [17]. We asked whether the Su/Hx model of PAH presents with additional functional alterations of the remaining RV capillaries. Thus, we used electron microscopy to show damaged EC in cardiac capillaries (**Figure 10)**.

Based on our results, we propose three mechanisms that could account for the capillary rarefaction observed in experimental RVF: 1) EC apoptosis and/or 2) Endothelial cell mesenchymal transformation, as proposed by Zeissberg *et al*(268). 3) Insufficient angiogenesis in a context of rapid myocardial hypertrophy. EC death could be partially explained by a decreased expression of the angiogenic protein vascular endothelial growth factor (VEGF), as it has been observed in the failing RV from Su/Hx animals(25). This hypothesis is largely based on the data generated by Eli Keshet's group, which has shown that genetically engineered, reversible reduction of VEGF expression in the mouse myocardium results in capillary rarefaction, suggesting that VEGF signaling is necessary for the maintenance of myocardial capillaries(140). Handoko *et al* and others have also reported decreased VEGF and RV-capillary rarefaction in rats treated with MCT(86, 168). Taken together, the work from several laboratories supports the notion that there are microcirculatory problems in the failing RV. However, whether impaired microcirculation function is sufficient to explain the rest of maladaptive changes observed in the failing RV remains to be investigated.

3.4.2 Inflammation

As mentioned in Chapter 2, the role of a dysregulated immune system in the pathobiology of human PAH has become more apparent in recent years (90, 158, 251). Interestingly, only one single study has reported leukocyte infiltration in the right ventricles obtained from patients with idiopathic PAH (IPAH) and PAH associated with

systemic sclerosis (SScPAH) (165). The authors reported a higher number of CD45+ and CD68+ cells in SScPAH when compared with RV samples from IPAH patients. Although inflammatory cells have been localized in the RV from rats with monocrotaline-induced PAH(81, 86), no systematic study has been undertaken to examine the role of inflammatory cells or inflammatory mediators in RV failure. A recent experimental study of LV failure in mice generated a novel concept of a toll-like receptor 9 (TLR-9) – dependent failure component. In this model of chronic severe LV pressure overload mitochondrial DNA from damaged heart cells generated a cardiac inflammatory response via TLR 9(163).

3.4.3 Oxidative Stress

Oxidative cell damage and oxidant-dependent transcriptional control occur and participate in inflammatory organ and tissue responses. Little is known about the role of oxidant stress in RV failure with the exception of the important study of Yet *et al*(264). These authors exposed hemeoxygenase-1 KO mice to 5 weeks of chronic hypoxia and found that the RV, but not the LV was damaged and dilated. Thus, it appears that the HO-1 function is required for a successful adaptation of the RV to pressure overload. The expression of HO-1 in the RV tissue from the Su/Hx pulmonary hypertensive rats is reduced, perhaps reflecting an impaired response to oxidant stress(25).

3.4.4 MicroRNA

Several recent publications have demonstrated microRNA dependent regulation of gene expression in association with pulmonary artery cell growth (44, 57, 180) and plasma microRNA expression patterns after acute myocardial infarcts or in patients with right heart failure (185). In mouse models, miRNAs play a role in the development of heart

Figure 10. Electron Microscopy Demonstrating Damaged Capillaries in Right

Ventricular Failure Tissue
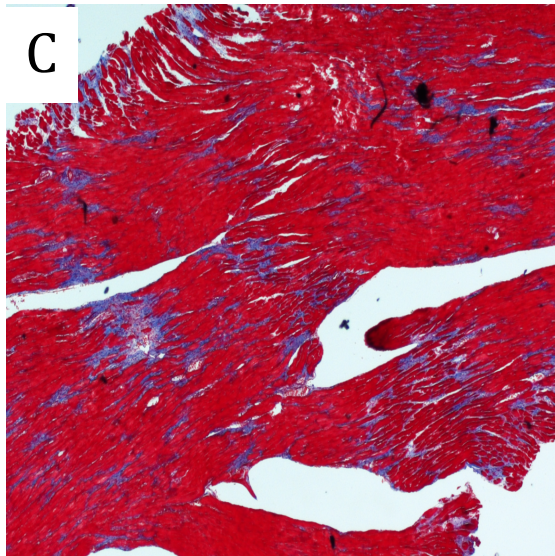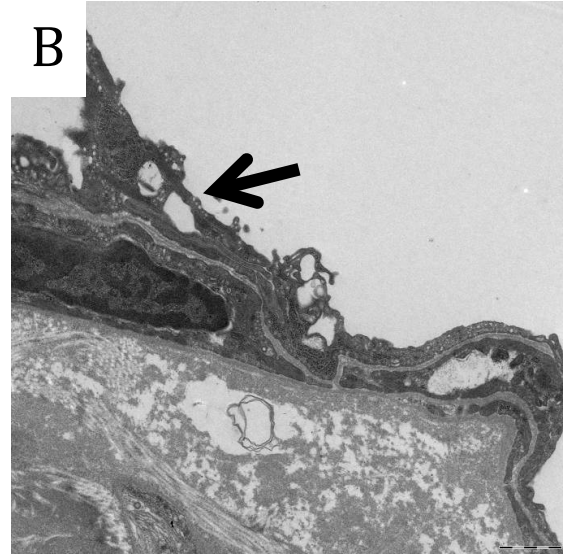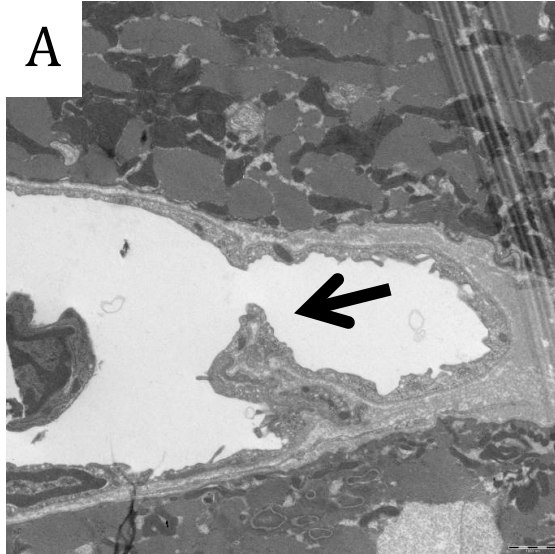
Figure 10. Micrographs obtained by electron microscopy demonstrate the presence of "blebbing" (A, arrow) and holes (B, arrow) which are a representation of endothelial cell damage of the microvessels of RV tissue obtained from rats with severe pulmonary hypertension and right ventricular failure. Figure C is a microphotograph of RV tissue obtained from a rat with RV failiure, stained with a Masson-Trichromatic staining which marks collagen in blue.

failure and the literature on cardiac microRNAs is still expanding(238). The transition of the RV from hypertrophy to failure has been investigated in the rat Su/Hx model and we reported a decrease in miR 21,34c, 133a and 139-3p in Su/Hx-induced RV failure when compared to PAB-induced RV hypertrophy(55). More recently Reddy *et al* reported RV-specific microRNA expression changes in a murine model(185). Unfortunately, the mechanisms by which miRNAs could affect gene and protein expression during RVF, are incompletely understood.

3.4.5 Other mechanisms: Apoptosis, fibrosis and mitochondrial dysfunction

Indeed, other mechanisms could contribute to the development of RV failure, by directly affecting the contractile machinery. For instance, Bogaard *et al.* in our group has demonstrated that RV tissue obtained from animals with severe RVF exhibit positive Terminal deoxynucleotidyl transferase dUTP nick end (TUNEL) staining which is utilized to label cells with severe DNA damage and serves as a surrogate marker for cellular apoptosis(26). Cell death could potentially contribute to the formation of replacement fibrosis which has been demonstrated in human and experimental RV failure (**Figure 9** and **10**). Abnormal cardiac metabolism has long been recognized as a problem in chronic left heart failure(156, 220). Similarly, data derived from experimental models of PH suggest that the failing RV is also characterized by a certain degree of "metabolic remodeling". In the SU/Hx rat model, the RV exhibits increased expression of glycolysis-related genes(55), whereas dysfunctional RV hypertrophy in the monocrotaline rat model of PH is associated with increased glycolysis enzymatic rates(176). Unfortunately, a complete characterization of RV "metabolic remodeling" in human PAH is still lacking. Positron emission tomography studies have shown increased accumulation of the glucose

analog 18F-2-Deoxy-2-Fluoro-D-Glucose (18-FDG) in the RV of PAH patients(35, 161).

However, 18-FDG uptake studies have multiple limitations and the physiological

interpretation is not straightforward (i.e 18-FDG uptake studies do not directly measure

glycolysis). RV oxygen consumption can also be measured by [11C]-acetate PET

scanning(259). However, such studies are limited to a few specialized centers and are

difficult to perform(249). Based on these studies, we sought to characterize the metabolic

transcriptional profile and mitochondrial function of RV tissue in normal, adaptive and

maladaptive RV hypertrophy. The results are presented and discussed in Chapter 5.

3.5 Summary and Conclusion

Right heart failure is characterized by morphological and functional changes. We wish to

advance the concept that the RV afterload by itself is insufficient as an explanation of the

mechanism of RV failure. Other factors should be taken into account when studying and

treating RVF, as they pose a critical paradox: While the remodelled lung circulation in

PAH is characterized by angiogenesis, apoptosis-resistance and cell proliferation

(Chapter 2), the failing RV suffers from ischemia(83), capillary rarefaction and

cardiomyocyte apoptosis(25), conditions that could be worsened by pharmacotherapy

targeting pulmonary vascular remodelling.

Chapter 4: Animal Models of Pulmonary Arterial Hypertension and Right Ventricular Chronic Pressure-Overload

Segments of this chapter have been previously published in:

Gomez-Arroyo JG, et al The monocrotaline model of pulmonary hypertension in perspective. *Am J Physiol Lung Cell Mol Physiol.* 2012 Feb 15;302(4):L363–9.

Gomez-Arroyo JG, et al A Brief Overview of Mouse Models of Pulmonary Arterial Hypertension: Problems and Prospects. *Am J Physiol Lung Cell Mol Physiol*. 2012 May 15;302(10):L977-91

CHAPTER 4

4.1 Introduction

Animal models of disease are of pivotal importance for the investigation of normal organ function, the pathobiology of frequent and rare disorders as well as for preclinical proof of principle treatment studies. As mentioned in the previous Chapters, it has been increasingly noticed that there is a substantial gap between our knowledge of left ventricular and right ventricular failure (RVF) mechanisms and that the concepts of RVF mechanisms have been mainly adapted from models of left ventricle failure or extrapolated from models of acute RVF(246).

Different animal models of pulmonary hypertension have been described many investigators and therefore, the aim of this Chapter is to briefly describe the current models of adaptive and maladaptive RV hypertrophy with or without lung vascular remodeling. This Chapter also provides the rationale for using the SU5416/hypoxia model for the experiments conducted for this dissertation and discusses the pros and cons of the other models such as the Monocrotaline-injury rat model. Lastly, we discuss the limitations of genetically engineered mice for the study of PH and RV failure.

4.2 The Monocrotaline-injury Model of Pulmonary Hypertension in Perspective

For the past three decades, two rat models have been central to the investigation of pulmonary hypertension (PH): The chronic hypoxia exposure model and the monocrotaline (MCT) lung injury model (215). Although the mechanisms of hypoxia-induced vascular remodeling are understood to some degree, the complex obliterative lesions found in human patients with severe PAH do not develop in this rodent model

(248). The monocrotaline rat model continues to be a frequently investigated model of PAH as it offers technical simplicity, reproducibility and low cost compared to other models of PAH. While the MCT rat model has contributed to a better understanding of vascular remodeling in pulmonary hypertension. However, multiple features of the "monocrotaline syndrome" do not resemble human PAH: liver failure, lung injury and myocarditis. Therefore, based on a literature review and our current data we questioned whether this model remained productive as a preclinically relevant model of severe plexogenic PAH.

4.2.1 Monocrotaline pyrrole toxicity and the "monocrotaline syndrome"

Monocrotaline (MCT) is an 11-membered macrocyclic pyrrolizidine alkaloid derived from the seeds of the *Crotalaria spectabilis* plant (**Figure 11A and B**). The MCT alkaloid is activated to the reactive pyrrole metabolite dehydromonocrotaline (MCTP) in the liver, a reaction that is highly dependent on CYP3A4 (cytochrome p450) (187, 257). Specific metabolic inducers of this cytochrome increase the MCTP production by the rat liver, whereas specific anti-CYP3A4 antibodies inhibit it (114, 187). When ingested, MCT induces a syndrome (**Table 2**) characterized – among other manifestations – by pulmonary hypertension, pulmonary mononuclear vasculitis (acute necrotizing pulmonary arteritis in about one-third of the animals) and right ventricular hypertrophy (117, 125).

Although it has been reported that MCT injures pulmonary endothelial cells (190) (117), the exact toxicological mechanisms by which MCT initiates lung toxicity remain unclear.

Table 2.

Characteristic	Dose range (mg/kg)	Reference
Acute lung injury	60 -100	(58, 122, 188, 200, 216)
Interstitial pulmonary fibrosis	2.4 - 100	(91, 145, 146)
Necrotizing pulmonary arteritis	Not quantified	(117, 125, 257)
Pulmonary hypertension	45 - 60	(27, 117, 159, 176, 198, 200, 266, 267)
RV hypertrophy	45 - 60	(27, 34, 86, 117, 159, 176, 198, 200, 266, 267)
Myocarditis	50 - 60	(4, 34, 86)
Hepatic venooclusive disease	60 - 300	(41-43, 47, 48, 51, 60, 138, 142, 170, 256, 257)

Lee and Sehgal, have shown that pulmonary arterial endothelial cells (PAEC) exposed to MCT develop megalocytosis characterized by an enlarged Golgi apparatus, displacement of endothelial nitric oxide synthase and decreased cell-surface/caveolar nitric oxide (128). MCT-treated endothelial cells demonstrate marked disruptions of intracellular membrane trafficking that affect several cell membrane proteins (204). Huang and Mathew have reported that MCT-induced loss of membrane proteins, results in the activation of proliferative and antiapoptotic factors, and deregulation of nitric oxide signaling, leading to lung vascular changes (100). The initial MCT-induced endothelial cell damage has also been linked to BMPRII (Bone Morphogenetic Protein Receptor II) dysfunction and BMP signaling disruption, as well as increased expression of intracellular elements involved in the sequestration and inhibition of the BMPR II activity (184). Nakayama and Wilson demonstrated that in human PAEC, the monocrotaline pyrrole significantly induced the Nrf2-mediated stress response pathway and increased caspase-3 activation (154).

Paradoxically, although there is vast evidence to suggest that MCT elicits PAEC dysfunction in multiple levels, the MCT PAH model is characterized predominantly by pulmonary arterial medial hypertrophy (**Figure 11D**) but not by endothelial cell-mediated angioobliteration, as it is present in the human disease or in the SU5416/hypoxia model of severe PAH (**Figure 11E**). It remains unclear whether an initial MCT-induced damage of pulmonary endothelial cells stimulates smooth muscle cell proliferation and/or endothelial cell mesenchymal transition; it is also elusive whether endothelial cell dysfunction is a consequence of non-PAEC damage or systemic inflammation triggered by MCT exposure. A detailed mechanistic explanation connecting the initial endothelial

cell injury and subsequent medial hypertrophy is still missing. Another major concern is the relation between the kinetics of MCT and development of pulmonary hypertension. MCT causes a short intense insult with a rapid loss of the starting compound because MCTP is rapidly degraded in aqueous solutions such as plasma (32, 63, 257). Of interest, significant changes in pulmonary artery pressures, medial thickness of small pulmonary arteries and RV hypertrophy do not occur until the third or fourth week after MCT exposure (124, 235). This issue has been partially explained by the accumulation of MCTP in erythrocytes, where it conserves its capability to interact with lung tissue (63, 166, 257). Furthermore, although a time-dependent effect of MCT has been described (88, 235), an adequate dose-response study has not yet been reported.

Many publications have demonstrated pulmonary vessel remodeling in MCT-treated rats and dogs, leading to pulmonary hypertension (84, 215, 257). Mitchel Botney (164) originally described that when used in combination with pneumonectomy (a "second hit"), MCT-treated rats developed angioobliterative changes in the pulmonary vasculature resembling those of human disease or the SU5416/hypoxia rat model (255). However, plexiform-like vascular lesions have not been described after a "single hit" of monocrotaline alone, while other pathological changes have been reported as a consequence of MCT exposure. MCT not only injures the pulmonary arteries, but also induces alveolar edema, alveolar septal cell hyperplasia and occlusion of pulmonary veins (58, 126). MCT-induced interstitial pulmonary fibrosis has also been described in mice (with variable doses and timepoints) (58, 91). Electron micrographs of MCT-treated animals, revealed degeneration of both lung endothelial and type I epithelial cells, as well as marked interstitial hypercellularity and fibrosis (145, 146). Hayashi and Hayashi

reported that a single dose of 100 mg/kg, is sufficient to induce severe pulmonary fibrosis and/or interstitial pneumonia in mice (91), whereas other investigators have reported that pulmonary fibrosis seems to be only a late manifestation of monocrotaline exposure (58). The MCT pyrrole has also been described as an anti-mitotic agent (47, 174). In astrocytes, the MCT pyrrole can induce DNA damage by generating DHP-derived DNA adducts, which induce DNA-crosslinks, DNA-celullar protein conjugates and apoptosis (154, 208, 253). MCT-induced DNA damage is reflected in persistent cell cycle arrest and is responsible for the cyto- and karyomegaly (megalocytosis) described in pneumocytes, human pulmonary endothelial cells, glial cells and hepatocytes of MCT-treated animals (128, 208, 256, 257). Particularly, type II pneumocytes seem to be highly affected by MCT-induced mitotic inhibition (260), which is partially mediated by altered polyamine metabolism (20). Confirming these previously reported data, when compared to the SU5416/hypoxia model of angioobliterative pulmonary hypertension, the MCT-treated animals demonstrate marked perivascular edema (**Figure 11F**), significant alveolar septal thickening (**Figure 11G**), and type I pneumocyte megakariocytosis (**Figure 11H**).

4.2.2 Monocrotaline-induced myocarditis

MCT treated rats develop significant pulmonary hypertension and marked right ventricular (RV) hypertrophy (**Figure 12 A**, also see references (27, 117, 176, 198, 225). Traditional concepts suggest that the RV dysfunction of MTC-treated rats is a direct consequence of pressure overload. Interestingly, despite having lower pulmonary artery pressure and a similar degree of RV dysfunction compared to the SU5416/hypoxia model

of pulmonary hypertension (**Figure 12 B-C**), MCT treated rats exhibit a significantly

higher mortality (**Figure 12 D**). Several investigators have utilized MCT to induce

Figure 11. The monocrotaline pyrrole and the lung changes characteristic of the

monocrotaline syndrome
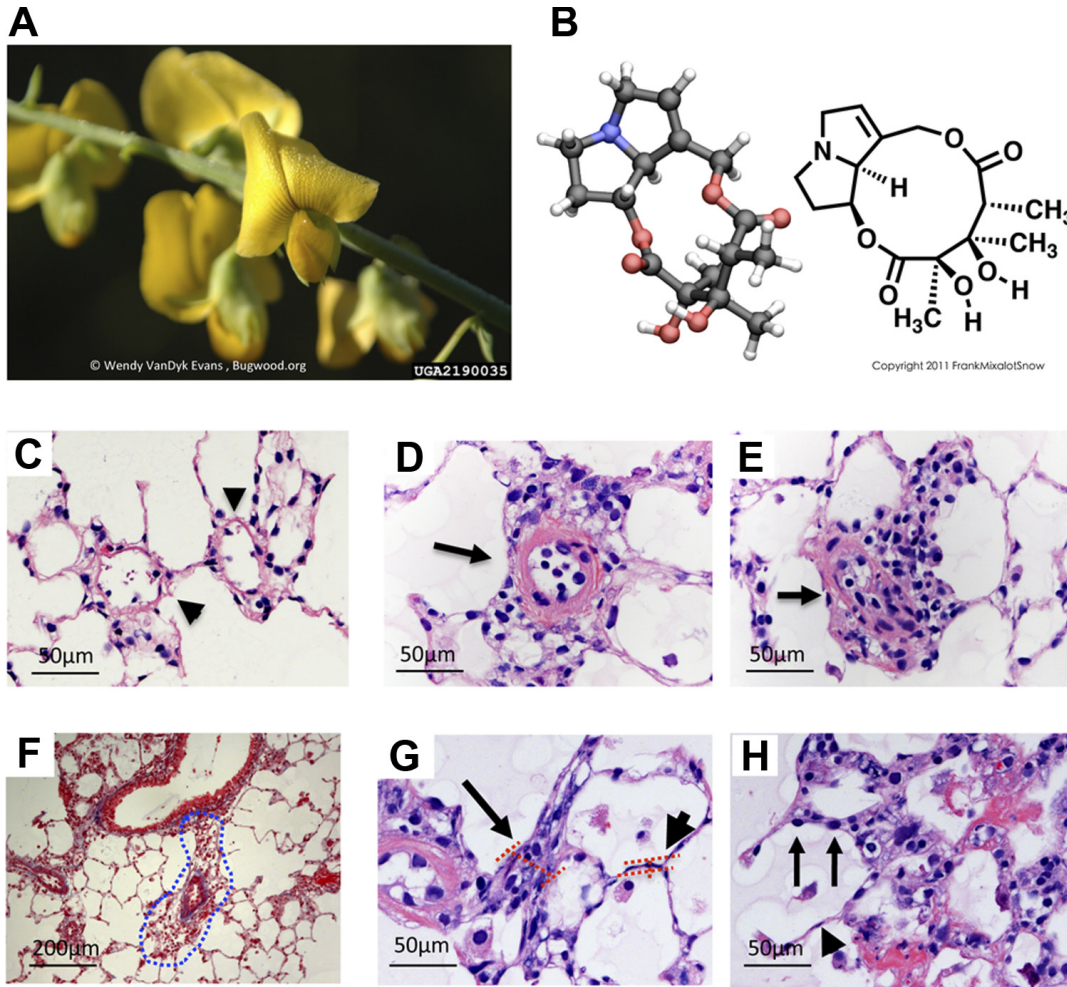
Figure 11. *A*: *Crotalaria spectabilis*, image re- produced with permission of Wendy Van-Dyk Evans, Bugwood.org. *B*: monocrotaline pyrrole chemical structure, reproduced with permission of chembase.com-chemical com- pounds database. Monocrotaline-treated rats (*D*) exhibit pulmonary vascular media hyper- trophy and mononuclear cell infiltration compared with control rats (*C*). In contrast to monocrotaline-treated rats, the model of SU5416/hypoxia (*E*), characterized by ab- normal endothelial cell proliferation, shows complete vascular obliteration. In addition to the vascular changes, monocrotaline-treated rats exhibit marked perivascular edema (*F*, blue line), alveolar septal thickening (*G*, long arrow; arrowhead marks a normal septa), and megalocytosis of type I pneumocytes (*H*, long arrows; arrowhead marks a normal type I pneumocyte nucleus).

pulmonary hypertension, assuming that MCT has no direct cardiac effect; however, others have investigated the potential role of load-independent maladaptive mechanisms that could contribute to RV failure in MCT-treated rats. For instance, in addition to RV hypertrophy, MCT treatment has been associated with increased [67]Galium uptake by scintigraphy (34) and marked neutrophil migration into the RV myocardium, even during early stages of the monocrotaline syndrome (34). Whether this neutrophil infiltration was a consequence of RV pressure overload or consequence of a direct cardiac effect (perhaps microvascular endothelial cell damage) of monocrotaline remains undetermined. Handoko *et al* have also demonstrated a widespread leukocyte infiltration of the right ventricle in MCT-treated rats (86). Our own data confirm the presence of multiple inflammatory cell foci throughout the RV (**Figure 12 F-G**). When characterized by immunohistochemistry, the majority of the leukocyte infiltrates were positive for CD20, a marker for B-lymphocytes (**Figure 12 K**), while CD68 (a macrophage marker) was negative. CD8 (a cytotoxic T-cell marker) was positive as well, but to a lesser extent. These results suggest perhaps that monocrotaline induces a lymphocytic myocarditis. We also observed, marked infiltration of inflammatory cells within the left ventricle, associated with coronary arteriolar wall thickening (**Figure 12 H**) and marked perivascular fibrosis (**Figure 12 I**). The MCT-induced myocarditis may be responsible for significant left ventricular systolic dysfunction and impaired diastolic relaxation, also described by Akhavein and Rohlicek (4). Benoist and collaborators have described a pro-arrhytmogenic substrate in the hearts of MCT-treated animals (21). Whether MCT-induced myocarditis or arrhythmias (21, 144) are the cause of death in rats – which can

Figure 12. Changes in the Right Ventricle Associated with Monocrotaline Exposure
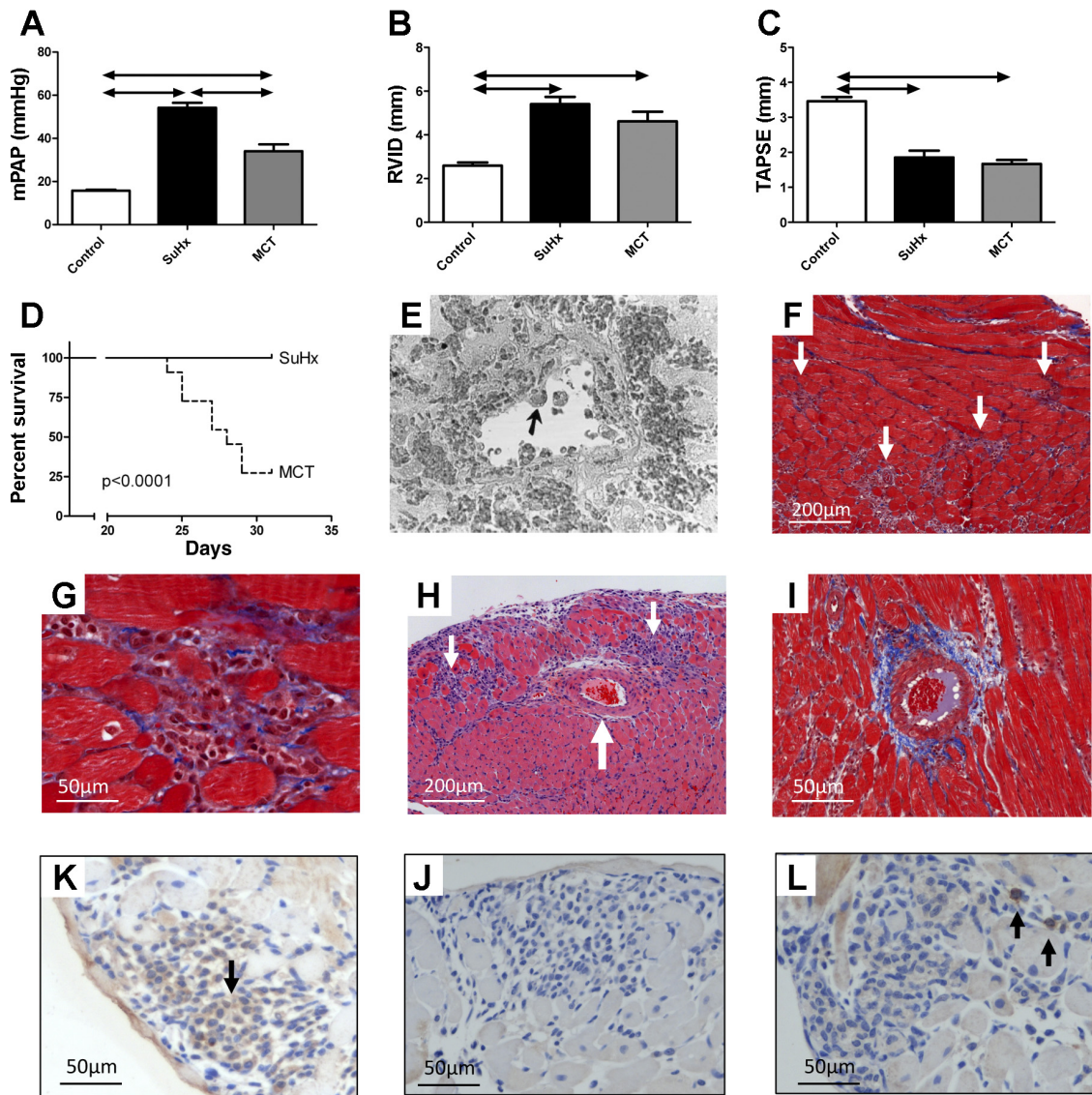
Figure 12. Both monocrotaline (MCT) and SU5416/hypoxia animals develop pulmonary hypertension, however, MCT-treated rats present with a lower degree of pulmonary hypertension compared with the SU5416/hypoxia model (*A*). Both models develop a similar degree of right ventricular (RV) dysfunction assessed by increased RV internal diameter (*B*) and decreased tricuspid annular planar systolic excursion (TAPSE, *C*), two heart rate-independent variables to evaluate RV function by echocardiogram. Although the pulmonary artery pressure is lower in MCT-treated rats, and RV dysfunction is similar in both models, MCT-treated rats exhibit a higher mortality rate compared with the SU5416/hypoxia model (*D*). Rats treated with a dose of 160 mg/kg or higher develop liver alterations consistent with hepatic venooocclusive disease [*E*]. Histological analysis of MCT-treated right ventricles demonstrated a severe inflammatory infiltrate in the RV (*F* and *G*). A similar inflammatory infiltrate was present in the left ventricle of MCT-treated rats (*H*, arrows) and was associated with medial hypertrophy of coronary arterioles (*H*, arrowhead) and marked perivascular fibrosis (*I*). Immunohistochemistry reveals that the majority of the inflammatory infiltrates are prominently positive for the B cell marker CD20 (*K*), negative for CD68+ (*J*), and identifies few CD8+ cells (*L*). These results are consistent with an MCT-induced lymphocytic myocarditis. SuHx, SU5416/hypoxia-exposed rats; mPAP, mean pulmonary arterial pressure; RVID, right ventricular internal diameter.

tolerate higher levels of RV afterload – remains undetermined but should be considered. Indeed, as mentioned in Chapter 3, although inflammatory cells have been found present in patients with pulmonary hypertension associated with systemic sclerosis(165), a mechanistic role for these cells is still incomplete and, conversely, they could serve as confounders for the development of RV failure.

4.2.3 Limitations of the Monocrotaline-Injury Model of PAH: Do rats die with PH or from PH?

As reviewed in the Chapter the monocrotaline rat model of pulmonary hypertension remains a model favored by many investigators, continues to impact preclinical PAH research (215), and a significant amount of time and funding continues to be invested in testing new drugs in this model (245). We are skeptical and of the opinion that the MCT model is not an appropriate model of human severe PH. Pulmonary vasoconstriction seems to be an important mechanistic component of the MCT-model (37, 143, 162, 202), and while that is shared in a certain subpopulation of patients with PAH (those documenting a large vasoconstriction component), pulmonary interstitial edema, myocarditis and hepatic venoocclusive disease (not to mention renal alterations (123)), which are part of the monocrotaline syndrome, are certainly not associated with the human forms of severe PAH (renal insufficiency is however a late manifestation (205)). Whereas the "two hits" model of monocrotaline/pneumonectomy can reproduce the pertinent pulmonary vascular pathology of human PAH, the other components of the monocrotaline syndrome may be cofounding. Also importantly, in contrast to the SU5416/hypoxia model (225), a very large number of drugs and compounds have either prevented or improved pulmonary hypertension in the MCT-alone (single-hit) model.

Paradoxically the animals, when untreated, die from undetermined causes. Hence the question: do MCT-treated rats die with PH or from PH? As a preclinical model of severe PAH, the MCT-alone model may be misleading as the particular syndrome associated with the development of PH (after a single injection of MCT) and the successful treatment of the MCT syndrome with practically any drug investigated (215), may have little in common with human forms of severe PH.

4.3 Pulmonary artery banding: A model for Adaptive (functional) Right Ventricular Hypertrophy

Many researchers have utilized the pulmonary artery banding (PAB) model to study the effects of mechanically-induced pressure-overload of RV. As mentioned in Chapter 3, increasing impedance, and therefore the afterload of the RV, by means of a band around the pulmonary artery would theoretically lead to RV dysfunction and eventually RV failure. Indeed, the transverse aortic constriction model is commonly used to reproduce systemic hypertension and left ventricular failure(12). Because the RV seems to adapt to increased pressure overload in a certain group of patients (mainly patients with Eisenmnger Syndrome, as studied in Chapter 3), Bogaard et al. (25) revisited the rat PAB model and compared the measurements obtained with the SU5416/hypoxia model, a model of severe pulmonary hypertension and RVF (see below). Interestingly, and in contrast to what would be expected, the PAB rats were able to tolerate high RV systolic pressures for a remarkably long time and TAPSE (tricuspid annular plannar systolic excursion), a heart-rate independent measurement of RV longitudinal contractility commonly used to evaluate RV function in patients with PAH, was similar to that of control rat RVs (3.25mm in PAB versus 3.46 in controls). In order to explain why the RV

of PAB rats was more 'resilient', microarray-based gene expression analysis of the

compensated rat RVH was performed. This analysis allowed the characterization of a

'RV failure transcriptional signature'(55). Following PAB surgery, rats showed an

increased expression of IGF-1 (insulin-like growth factor-1) mRNA, normal levels of

phosphorylated Akt and VEGF protein levels, as well as and an increased amount of

apelin (another pro-angiogenic factor) when compared to RV tissues from rats with RVF

(SU5416/hypoxia rats)(25). These results were in line with what Faber et al. reported

when evaluating right and left ventricular function in PAB rat(64). The authors

demonstrated that 6 weeks of pressure overload resulted in enhanced baseline RV

contractility while LV baseline contractility remained unaffected. In contrast, Fang,

Archer and collaborators showed that 4 weeks after PAB, the cardiac output and treadmill

distance were significantly reduced in the PAB vs. control animals(65). Possible

explanations for this discrepancy could be the differences in pulmonary artery lumen

reduction and the time allowed for RV adaptation.

Another interesting feature are the changes in the RV when compared to the LV

subjected to pressure-overload in rodents. The Stanford pediatric cardiology group

performed PAB in mice and then analyzed the RV and LV tissues with mRNA

microarrays(234). Animals with moderate pulmonary stenosis had a 50% survival of >50

days. Importantly, the right ventricular end-diastolic pressure increased 6 hours

postoperatively in mice with severe stenosis, but remained within the normal range in the

animals with moderate outflow tract stenosis. Furthermore, the authors demonstrated a

differential expression of genes between the pressure-overloaded right ventricles when

compared to the left counterparts. Altogether, the published data suggest that PAB can be used as a model of RV pressure-overload with associated adaptive hypertrophy.

4.4 The SU5416/hypoxia rat model of pulmonary arterial hypertension: A brief summary

The combined VEGF receptor 1 (Flt) and 2 (KDR) blocker, SU5416, was one of the first agents discovered by screening for growth inhibitory activity of cultured endothelial cells incubated with the potent angiogenic VEGF ligand (68). Kindly provided by Dr. Peter Hirth (Sugen, South San Francisco, CA), for preclinical studies, SU5416 was tested with the hypothesis that inhibition of VEGF signaling would result in pulmonary emphysema. Indeed, a single subcutaneous injection of 20 mg/kg of SU5416 caused airspace enlargement and mild PH in adult rats (115). Unexpectedly, rats injected with SU5416 (20 mg/kg) were exposed to chronic hypoxia in a hypobaric chamber, as an attempt to worsen the airspace enlargement. The results of these experiments were published in 2001 (223). Surprisingly, the combination of SU5416 and chronic hypoxia (hereafter SUHx) resulted in the development of severe PAH which was not reversible when the animals were returned to Denver altitude (223) or in later experiments to sea level (**Figure 13**) (25). The PH was associated with angioobliterative pulmonary lesions which were preventable by treating the animals concomitantly with a pan-caspase inhibitor, indicating that apoptosis was necessary for the development of pulmonary vascular lesions (223). This rat model has served as a model for preclinical drug studies designed to examine whether the PH and pulmonary vascular disease in the SuHx rats could be reversed once established.

Figure 13. Comparison between a normal lung vessel and the vascular lesions present in the SU5416/hypoxia rat model of severe pulmonary arterial hypertension.
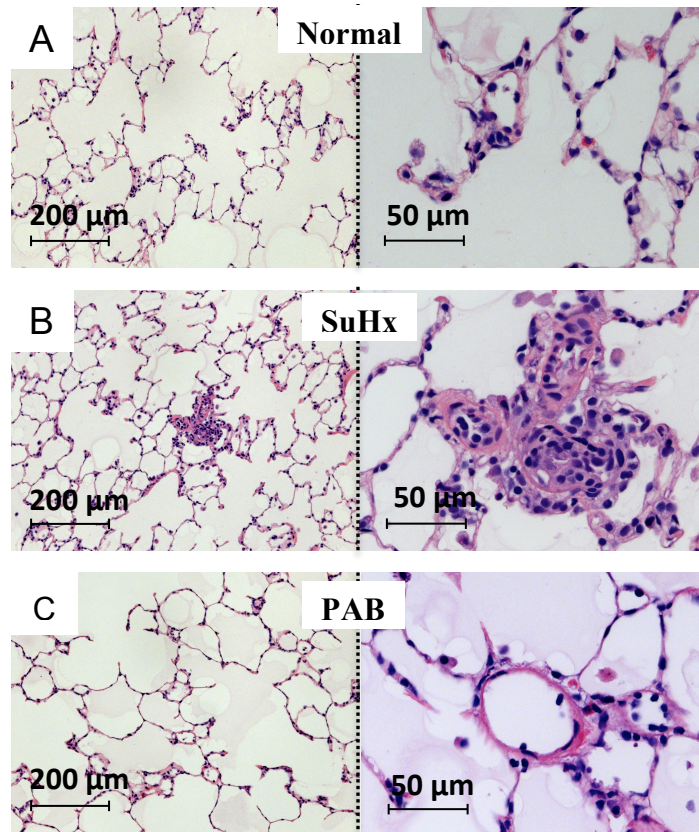
Figure 13. Microphotographs showing the histological differences in the lung

vasculature between controls (A), SuHx (B) and Pulmonary Artery Banding (PAB) (C).

Because in this rat model the PH is severe, is accompanied by plexiform-like lesions and is largely refractory to treatment, it was concluded that the SUHx rat model of angioobliterative severe PH had a number of features which resembled the human disease. Moreover, Abe *et al* has shown the histopathological similarities of the SUHx lung vascular lesions in comparison to the plexiform lesions in human disease (1). In addition to severe PH, rats treated with SU5416 and exposed to chronic hypoxia also develop severe RV failure characterized by a cardiac output reduction, decreased TAPSE, increased RV diastolic diameter, capillary rarefaction, RV fibrosis and cardiomyocyte apoptosis (25, 27, 162).

The SUHx model has been modified to uncover immunological mechanisms in the pathobiology of severe PAH. We have shown that treatment of athymic rats with SU5416 is sufficient to cause severe angioobliterative PAH— indicating that hypoxia is not necessary (224), and that early immune reconstitution with rat regulatory T lymphocytes prevents the development of severe PAH (222, 224). For further information regarding the SuHx model the reader is referred to ((25, 194, 195, 223)).

4.5 Mouse Models of Right Ventricular Failure: Problems and Prospects

The advent and development of genetically modified mice, as tools to dissect cellular and molecular signaling pathways, created an understandable desire to generate mouse models for PH studies. In recent years a considerable number of transgenic mice have been generated in order to investigate mechanisms of pulmonary hypertension (See Ref (82)). In particular, the report of associations between mutations in the *BMPR2* gene with both familiar and idiopathic forms of pulmonary arterial hypertension (PAH) (101, 137, 157, 218), led to multiple attempts to generate novel animal models of PAH. In addition

to BMPR2 knock out (KO) mice, researchers have targeted other genes suspected to be involved in the pathogenesis of PAH. Very likely the transgenic mouse studies have strongly influenced the way we think of the pathogenesis of PAH and helped shift the early mechanical concepts of pressure – and flow – dependency, towards disease models built on cell-to-cell interactions, immune dysregulation, metabolic changes and abnormal cell phenotypes (50, 149, 181, 183, 224, 251, 262). However, although somewhat useful for the study of lung vascular remodeling, mice exhibit multiple limitations as a model of right ventricular failure.

RV hypertrophy is easy to measure by separating the RV-free wall from the rest of the heart (70). In rats, the RVSP is strongly correlated with the RV/LV+S (162) suggesting that the RV responds to an increased afterload with a corresponding degree of hypertrophy. Rat models of PAH – such as the SU5416/hypoxia and monocrotaline-injury models – generate robust RV hypertrophy (mean RV/LV+S 0.67-0.76) (25, 80). In contrast to rat models, only mice overexpressing interleukin-6 seem to develop a comparable degree of hypertrophy (average RV/LV+S 0.69) and pulmonary hypertension (214). When plotting data extracted from the reviewed mouse PH studies (**Figure 14B-D**), there seems to be an "uncoupling" between RVSP and RV/LV+S for the majority of PH-mouse studies, even after hypoxia exposure. For example, Xu *et al* (261) demonstrated that mice lacking the adenosine A2A receptor develop spontaneous PH (RVSP 39 mmHg), however the RV/LV+S was only 0.26, a value that is within normal limits for C57BL6/J WT mice (219). In contrast, Chen and collaborators (39) reported that mice overexpressing

Figure 14. Brief analysis of the hemodynamics and right ventricular hypertrophy of mice

models of pulmonary hypertension
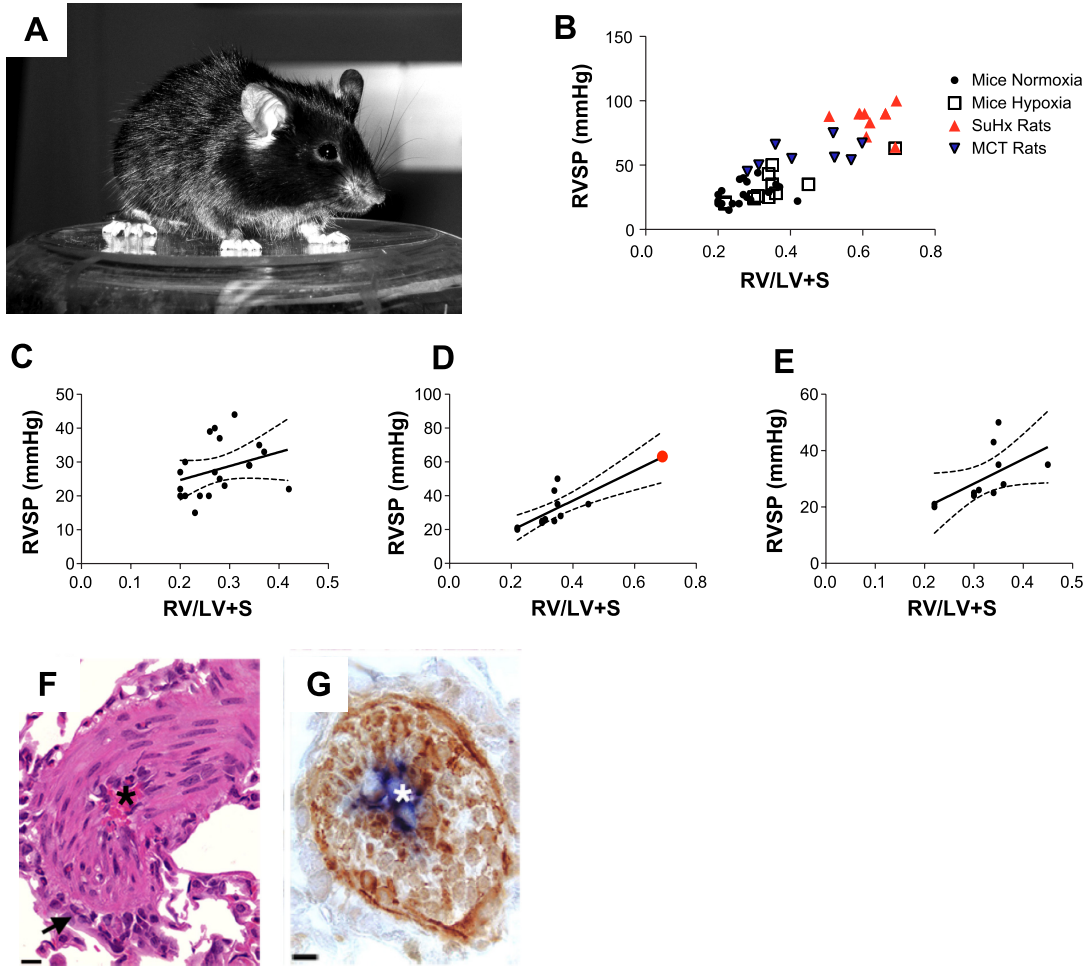
Figure 14 A: C57BL6 mouse. *B*: correlation between right ventricular systolic pressure (RVSP) and right ventricle (RV) to left ventricle (LV) plus septum (S) ratio (RV/LV+S) in mouse pulmonary hypertension (PH) models exposed to normoxia and hypoxia, compared with the combination of SU5416 and chronic hypoxia (SuHx) and monocrotaline (MCT)-injured rat models. *C*: correlation between RVSP and RV/LV+S in mouse models exposed to normoxia. Pearson coefficient 0.32, *P* <0.150. *D*: correlation between RVSP and RV/LV+S in mouse models exposed to hypoxia. If all mouse models are included, the Pearson coefficient is 0.82, *P* < 0.0008. However, the correlation seems to be driven by an outlier, the IL6-OE mice (red dot). Thus, if the latter is not included in the statistical calculations, the coefficient becomes nonsignificant (*r* =0.58, *P* < 0.057) (*E*). *F*: hematoxylin and eosin (HE)-stained lung section of a pulmonary vessel obtained from wild-type C57BL6 mice chronically exposed to ovalbumin. The mice develop severe pulmonary arterial muscularization without pulmonary hypertension. The vascular remodeling does not involve endothelial cell proliferation (*G*; brown staining is smooth muscle actin and blue is von Willebrand factor). *F* and *G* are reprinted from Daley et al. (2008), doi:10.1084/jem.20071008

connective tissue growth factor (CTGF) generate modest PH (average RVSP 22 mmHg

versus 10 mmHg in WT controls) but develop significant RV hypertrophy (RV/LV+S

0.42).

Three of the published mouse models of PH have provided unpredicted and puzzling

results which ought to be followed-up to better understand the integrated response of the

lung circulation/heart axis, in the setting of PAH and chronic hemodynamic stress. For

instance, Daley *et al* (50) reported very pronounced pulmonary artery muscularization,

but no RV hypertrophy. In contrast, the studies of Shifren *et al* (206) demonstrate that

mice lacking elastin develop impressive elevation of RVSP without RV hypertrophy.

Finally, in hemeoxygenase-1 knock out mice, Yet *et al* demonstrated that after chronic

hypoxia exposure, mice did not develop RV hypertrophy, but developed RV dilatation

(264). All together, these last three studies exemplify that in mice: 1) Severe

muscularization does not necessarily indicate pulmonary hypertension 2) PH is not

always translated into RV hypertrophy 3) RV remodeling could happen in the absence of

PH. Whether increased pulmonary arterial pressure and right ventricular remodeling are

two mechanistically distinct processes which are usually coupled in PAH remains to be

investigated.

4.6 Summary and Conclusions

Animal models serve as a powerful tool to evaluate human disease. Unfortunately, none

of the current models is perfect and each one of the presented in this Chapter offers

unique, and perhaps, complementary features for the researcher interested in studying RV

failure. The pulmonary artery banding model in rats and mice could offer tremendous

opportunities to study genes or proteins required for RV adaptation to chronic pressure

overload. Conversely, models of established RV failure such as monocrotaline or SU5416/hypoxia have been used to describe the mechanisms potentially involved in the transition from adaptive to maladaptive RV hypertrophy and can therefore serve to identify and study key molecular players involved in the reversal of RV failure.

Chapter 5: Methodology and Statistical Analysis

Segments of this chapter have been previously published in:

Gomez-Arroyo J, et al. Metabolic gene remodeling and mitochondrial dysfunction in failing right ventricular hypertrophy secondary to pulmonary arterial hypertension. *Circ Heart Fail*. 2013 Jan 1;6(1):136–144.

CHAPTER 5

5. 1 Generation of Animal Models

5.1.2 SU5416/Hypoxia model

Male Sprague-Dawley rats (weight 200-250 g) received a single injection of SU5416 suspended in 0.5% (w/v) carboxymethylcellulose sodium, 0.9% (w/v) sodium chloride, 0.4% (w/v) polysorbate 80, and 0.9% (v/v) benzyl alcohol in deionized water, according to our protocol and previously published literature(79, 223), at a dose of 20 mg/kg subcutaneously and were exposed in a hypoxia (nitrogen dilution) chamber simulating an approximate altitude of 5000 m. for 4 weeks. As previously described, the RV in the SuHx rat model responds to pulmonary hypertension with a robust degree of hypertrophy, followed by dysfunction and failure(162). The RV in this rat model is characterized by fibrosis, capillary rarefaction and cardiomyocyte apoptosis(25), which are associated with decreased cardiac output, markedly dilated RV and decreased exercise capacity(26). Also, as previously described, the SuHx RV dysfunction model reproduces some features of human RV dysfunction, such as paradoxical septal movement and RV dilatation.

5.1.2 Pulmonary artery banding

Male Sprague-Dawley rats (weight 180-200 g) were anesthetized with isoflurane inhalation (5% and 2%, respectively, in oxygen-enriched room air). After intubation, the animals are mechanically ventilated with the use of a volume-controlled respirator.

Positive endexpiratory pressure was maintained at 4 cmH2O. A left thoracotomy as performed, where the pulmonary artery was carefully dissected free from the aorta. A silk thread was then positioned underneath the pulmonary artery, while we also placed an 8-gauge needle is placed alongside the pulmonary artery. A suture was tied tightly around the needle, and the needle rapidly removed to produce a fixed constricted opening in the lumen equal to the diameter of the needle. After the banding, the thorax was closed in layers, and postoperative pain relief was obtained by applying buprenorphine (15μg/kg s.c.). For more information about the procedure please refeer to Bogaard, et at. Circulation 2009 (25). The PAB rats were sacrificed to collect organs 6 weeks after the surgery, to allow for significant hypertrophy as reported by Bogaard *et al*(24, 25). As a model of strictly mechanical RV pressure overload, the PAB rat model demonstrates preserved RV function despite generating significantly high RV afterload and hypertrophy(24, 25) (See Chapter 4). Thus, the PAB-model was utilized as a model of non-dysfunctional RV hypertrophy.

5.2 Human samples

Human RV tissue samples were obtained from 4 patients diagnosed with PAH and RVF that underwent cardiac transplantation. All human samples were kindly donated by the Bosch Institute, University of Sydney, Sydney, Australia. Control RV samples were obtained from a normal donor heart, carefully matching age and gender. Clinical information regarding the human samples can be found **Table 3**.

Table 3. Demographic and clinical information of patients with right ventricular

dysfunction and pulmonary hypertension

Patient			Age	Gender	NYHA Class	Clinical Data
Control			42	Female	I	Brain death due to subarachnoid hemorrhage. No previous cardiac or pulmonary disease.
EMS 1	21	Female	II			Large VSD and pulmonary hypertension.
EMS 2	46	Female	IV			Large VSD and pulmonary hypertension.
PAH 1	38	Female	IV			Familiar IPAH, mean pulmonary pressure 80 mmHg, wedge pressure 10, cardiac index 1.76. Negative vasoreactive test. No specific PAH treatment.

Table 3. Demographic and clinical information of patients with right ventricular dysfunction and pulmonary hypertension. Heart samples from free RV wall were obtained after cardiac transplantation, immediately frozen and stored. *NYHA* = New York Heart Association Functional Classification at the moment of cardiac transplantation; *EMS* = Eisenmenger's Syndrome; *IPAH* = Idiopathic Pulmonary Arterial Hypertension; *VSD* = Ventriculoseptal defect

5. 3 Echocardiography

Doppler echocardiography was performed using the Vevo770 imaging system (VisualSonics, Toronto, Canada) directly after the hypoxic exposure (baseline) and again 4 weeks later after treatment. Superficial anesthesia with ketamine/xylazine was used to obtain two-dimensional, M-mode and Doppler imaging in both long axis and short-axis views, using a 30-MHz probe. Measurements were made of the RV inner diameter in diastole (RVID; long axis) and tricuspid annular plane systolic excursion (TAPSE; long axis). The presence of pulmonary hypertension before treatment was evaluated by measuring the pulmonary artery acceleration time and mid-systolic notching with pulsed-wave Doppler recordings, as previously reported (235).

5.4 Hemodynamic measurements

Four weeks after SU5416 administration or four weeks after the first dose of carvedilol (eight weeks after SU5416 injection), hemodynamic measurements were made using a 4.5 mm conductance catheter (Millar Instruments, Houston, TX) and the Powerlab data acquisition system (AD Instruments, Colorado Springs, CO). The rats were anesthetized with an intramuscular injection of ketamine at a dose of 100mg/kg and xylazine 15 mg/kg. Rats were then were intubated through tracheotomy and placed in a supine position. After a median sternotomy the RV outflow tract was punctured with a 23G needle and the catheter was introduced ante grade to measure pulmonary artery pressures.

5.5. Tissue preparation for molecular analysis

Upon sacrifice, the right lung and the total heart were removed. The RV was carefully dissected from the rest of the heart to measure the RV/LV+S. RV weight over left ventricle and septum weight (LV/+S) weight is the standard assessment for hypertrophy,

as previously reported(25, 79, 82). After dissection the lung, RV and LV+S tissues were frozen with liquid nitrogen until the isolation of mRNA and protein was performed. The left lung was inflated with 0.5% low-melting agarose at a constant pressure of 25cm H_2O, fixed in 10% formalin for 48 hours and used for histological evaluation of the lungs and IHC analysis, as reported previously(25, 109).

5.6 Gene expression studies

Using the FastPrep®- 24 instrument (MP Biomedicals, Solon, OH), 25mg of RV or LV or Lung tissue were homogenized with Triazol® (Qiagen, Valencia, CA) in Lysing Matrix D impact-resistant 2ml tubes (MP Biomedicals, Solon, OH). mRNA was carefully isolated using a RNeasy (Qiagen, Valencia, CA) isolation kit according to manufacturers protocol. Total RNA (1 μg) was reverse transcribed into first complimentary DNA (cDNA) using the High-Capacity cDNA Reverse Transcription Kit (Applied Biosystems, Foster City, CA). First strand cDNA was diluted 10 times and RT-QPCR performed using Power SYBR® Green PCR Master Mix (Applied Biosystems) along with murine specific primers (**Table 4**).

All PCR reactions were performed with a LightCycler480 PCR system (Roche Diagnostics, Meylan, France). The cycling parameters were the following: initial denaturation at 95°C for 15 min, followed by 50 cycles of denaturation at 94°C for 15s, annealing at 55°C for 15 s, and extension at 72°C for 15 s. The α-actinin 1 and 18 S genes were used as the reference gene for mRNA relative quantification. All gene expression results were normalized to controls, and expressed as mean± SEM unless otherwise specified.

5.7 Western Blotting

Whole cell lysate from isolated right ventricle was prepared using RIPA (Radio-Immunoprecipitation Assay) buffer (Sigma, St. Louis, MO), and the protein concentration was determined using BioRad Protein DC Protein Assay (BioRad, Hercules, CA). Thirty micrograms of whole cellular protein per lane was separated by SDS-PAGE with a 4-12% Bis-Tris NUPAGE gel (MES SDS running buffer) and blotted onto a PVDF membrane. The membrane was incubated with blocking buffer (5% non-fat dry milk/PBS 0.1%/Tween 20) at room temperature for 1 hour. The membrane was then probed with the primary antibodies diluted in blocking buffer overnight at 4˚C. Subsequently, membranes were incubated with horseradish peroxidase-conjugated anti-mouse or anti-rabbit antibody diluted 1:1000 in blocking buffer. Blots were developed with ECL (PerkinElmer, Waltham, MA) on GeneMate Blue Basic Autorad Films (BioExpress, Kaysville, UT). Blots were scanned and densitometry analysis was done with ImageJ (National Institutes of Health 1997-2011, Bethesda, MD; http://imagej.nih.gov/ij). Rabbit anti-PGC1α antibody was acquired from Cell Signaling Technology, Inc., Beverly, MA. Rabbit anti-ACADM and ACADVL antibody were acquired from Abcam plc, Cambridge, MA. Rabbit anti-PPARα antibody, ND4L and CytB were purchased from Santa Cruz Biotechnology, Inc., Santa Cruz, CA) and rabbit anti-estrogen related receptor alpha (EPR46Y) was purchased from Millipore, Billerica, MA.

Table 4. List of Primers Used

Gene	NCBI Gene Ref.	Forward Sequence	Reverse Sequence
α-actinin 1	81634	5' TCAGTTGGAAGGATGGTCTTG 3'	5' AAGGCTGTGTTCAGGTTTGTG 3'
ACADM	24158	5' GACGGAGCAGCAGAAAGAGTT 3'	5' CTTGATGAGAGGGAACGGGTA 3'
ACADVL	25363	5' AAGTGAATGACCCTGCCAAGA 3'	5' ATGCCCCCAGTTCTTTGAGTC 3'
ACADS	64304	5' CTGGATTGTGCCGTGAAGTAC 3'	5' GCTTGAACTGGATGTTTTGGA 3'
ACSL1	25288	5' GGGTACTACTGAGGGTGTCCG 3'	5' CTCTGGAAGCCATCGTACATC 3'
CD36	29184	5' GTTATTGGTGCTGTCCTGGCT 3'	5' CCGTTTTCACCCAGTTTTTGA 3'
COUP-	11398	5'	5'

TF1	4	CTTTTGCTTCGTCTCCCTT CC 3'	ATGGGGGTTTTACCTACCAA A 3'
CPT-1α	25757	5' GGCATGATCGCAAAGAT CAGT 3'	5' GCCACCCAGAGCCCTGTAC CA 3'
CPT-1β	25756	5' AAGAACACGAGCCAACA AGCA 3'	5' TACCATACCCAGTGCCATCA C 3'
CPT-2	25413	5' GCTGCCTATCCCTAAACT TGA 3'	5' AACGCTTCTGTTCTCCTGAA C 3'
CS	170587	5' CTGAGTGCCAGAAACTG CTAC 3'	5' GTGAGAGCCAAGAGACCTG TT 3'
ERRα	293701	5' CACAAGGAGGAGGAGGA TGG 3'	5' AGGCGTTTGGGTAGAGAGC T 3'
ERRγ	360896	5' TCCCCAGACCAAGTGTG AATA 3'	5' AGTGATACCCAGAGGCGAT GT 3'
GLUT-1	24778	5' TTCCTGCTCATCAATCGT AAC 3'	5' ACCCTCTTCTTTCATCTCCT G 3'

89

Hexokinase 1	25058	5' TGATGGAGGTGAAGAAGAGGC 3'	5' GGCAGCATTTTGACAGTAGCT 3'
Hexokinase 2	25059	5' GAAGATGATTAGCGGGATGTA 3'	5' TAAGGAGTTCTGGGCTGAGTT 3'
IDH1	24479	5' CACACAGTTCCTTCCAAATGG 3'	5' GCGTCCATCATACTTCTTCAG 3'
PDHb	289950	5' GCTGAGATTTGTGCGAGAATT 3'	5' CGTAAGGCATAGGGACATCAG 3'
PDK-1	89813	5' CGAAACAGACATCATAATGTG 3'	5' GAATATGAGGATGTGCTGGTT 3'
PGC-1α	83516	5' ACCCCAGAGTCACCAAATGA 3'	5' GCAGTTCCAGAGAGTTCCAC 3'
PPAR-α	25747	5' GGTCCTCTGGTTGTCCCCTT 3'	5' GTGAGTTACGCCCAAATGCA 3'
PPAR-δ	25682	5' AACTTCAGCAGCCTCTTC	5' ACCAGCAGTCCGTCTTTGTT

		CTC 3'	G 3'
PPAR-γ	25664	5' CGGTTGATTTCTCCAGCA TT 3'	5' TCGCACTTTGGTATTCTTGG 3'
SP-1	24790	5' AGCAGCAATACCACCCT TACA 3'	5' GACAGTTGAGCAGCATTCA CA 3'

5.8 Isolation of mitochondria

Isolation of a single population of cardiac mitochondria was conducted as described previously (217), except that approximately 100 mg of right ventricle tissue were used. Briefly, tissue was washed in a modified Chappell-Perry (CP) buffer (buffer CP1 at pH 7.4: 100 mM KCl, 50 mM MOPS, 1 mM EGTA, 5 mM MgSO$_4$·7H$_2$O, 1 mM ATP), dried with Whatman filter paper, weighed, minced and homogenized in CP1 buffer using a polytron tissue blender (Kinematica, Bohemia, NY). The homogenate was supplemented with 5 mg/g (wet weight) trypsin (#T0303, Sigma-Aldrich), incubated with stirring for 15 min at 4 ^{o}C followed by addition of 3 ml of CP2 buffer (CP1 buffer containing 0.2% BSA (#A7030, Sigma-Aldrich) to attenuate trypsin activity). Digested tissue was further homogenized by two strokes using a digital steady-stirring tight Teflon pestle/glass tube homogenizer set at 600 rpm (Fisher Scientific, Pittsburgh, PA). Undigested tissue and heavier cell fractions in the remaining volume were pelleted by centrifugation at speed 500g for 10 min at 4 ^{o}C. The mitochondria-containing supernatant was centrifuged at 3000g for 10 min at 4 ^{o}C. The mitochondrial pellet was washed with 1 ml of KME buffer, pH 7.4 (100 mM KCl, 50 mM MOPS, 0.5 mM EGTA). Mitochondria were re-suspended in KME and used within 4 h after isolation or frozen. The protein concentration was measured by Lowry (134) using BSA as a standard and sodium deoxycholate as a detergent.

5.9 Mitochondrial oxidative phosphorylation

Oxygen consumption by intact mitochondria was measured using a Clark-type oxygen electrode (Strathkelvin Instruments, North Lanarkshire, UK) at 30 ^{o}C in respiration buffer at pH 7.4 (80 mM KCl, 50 mM MOPS, 1 mM EGTA, 5 mM KH$_2$PO$_4$, 1 mg/ml defatted

BSA) as previously described (38, 132). Briefly, substrates for complex I (20 mM glutamate), complex II (20 mM succinate with 7.5 μM rotenone), and complex IV (1 mM N,N,N′,N′-tetramethyl-p-phenylenediamine (TMPD)/20 mM L- ascorbate with 7.5 μM rotenone) were used and state 3 (0.2 mM ADP-stimulated), state 4 (ADP-limited) respiration, respiratory control ratio (RCR), maximal rate of state 3 respiration (2 mM ADP), and ADP/O ratio were determined.

5.10 Chromatography Electrospray Ionization Tandem Mass Spectrometry

Eicosanoids were analyzed from frozen heart samples as follows. Briefly the frozen heart tissues were thawed on ice and homogenized using an Omni TH tissue homogenizer to obtain a 10% (w/v) solution in PBS. 200 μl of the solution thus obtained was diluted 1ml of LCMS grade ethanol containing 10 ng of each internal standard and 0.05% BHT. The internal standards used were, (d4) 6k PGF1α, (d4) 8-iso PGF2α, (d4) PGF2α, (d4) PGE2, (d4) PGD2, (d4) LTB4, (d4) TXB2, (d4) LTC4, (d5) LTD4, (d5) LTE4, (d8) 5-hydroxyeicosatetranoic acid (5HETE), (d8) 15-hydroxyeicosatetranoic acid (15HETE), (d8) 14,15 epoxyeicosatrienoic acid, (d8) Arachidonic Acid, and (d5) Eicosapentaenoic acid. The mixture thus obtained was agitated to homogeneity using a bath sonicator and the resultant suspension was incubated in the dark at 4 ^{0}C for 5 hours with periodic sonication. Following incubation, the insoluble fraction was precipitated by centrifuging at 6000g for 20 minutes and the supernatant was transferred into a new glass tube. This supernatant was dried under vacuum followed by reconstitution in 100 μl of 50:50 EtOH:dH2O for quantitation via LC/MS/MS. A 30 minute reversed-phase LC method utilizing a Kinetex C18 column (150 x 2.1mm, 1.7μm) was used to separate the eicosanoids at a flow rate of 200μl/min at 50°C. The column was equilibrated with 100%

Solvent A [acetonitrile:water:formic acid (10:90:0.02, v/v/v)] for five minutes and then 10 μl of sample was injected. 100% Solvent A was used for the first minute of elution. Solvent B [acetonitrile:isopropanol (50:50, v/v)] was increased in a linear gradient to 25% Solvent B to 3 minutes, to 45% until 11 minutes, to 60% until 13 minutes, to 75% until 18 minutes, and to 100% until 20 minutes. 100% Solvent B was held until 25 minutes, then was decreased to 0% in a linear gradient until 26 minutes, and then held until 30 minutes. The eicosanoids were analyzed using a hybrid triple quadrapole linear ion trap mass spectrometer (QTRAP5500® ABSciex) via multiple-reaction monitoring in negative-ion mode. Eicosanoids were monitored using precursor → product MRM pairs. The mass spectrometer parameters used were: curtain gas: 30; CAD: High; ion spray voltage: -3500V; temperature: 500°C; Gas 1: 40; Gas 2: 60; declustering potential, collision energy, and collision cell exit potential vary per transition.

5.11 Statistical analysis

Differences between groups were assessed with one-way or two-way ANOVA or Kruskall-Wallis tests. Bonferroni's and Dunn's post-hoc tests were used to assess significant differences between groups. A p-value < 0.05 was accepted as significant. Correlation analysis was done with Spearman's test. Results are reported as means±SEM, or fold-change mean±SEM unless specified otherwise. Four-to-six rats were used per group, unless otherwise specified. Statistical analysis was done with PASW V.18 (IBM, Armonk, New York) and GraphPad Prism (La Jolla, CA).

Chapter 6: Metabolic gene remodeling and mitochondrial dysfunction in failing right ventricular hypertrophy secondary to pulmonary arterial hypertension

This entire chapter has been previously published in:

Gomez-Arroyo J, et al. Metabolic gene remodeling and mitochondrial dysfunction in failing right ventricular hypertrophy secondary to pulmonary arterial hypertension. *Circ Heart Fail*. 2013 Jan 1;6(1):136–144.

CHAPTER 6

6.1 Introduction

As discussed in Chapter 2 and 3 pulmonary arterial hypertension (PAH) is a severe and often rapidly progressive group of diseases which are characterized by a chronically and frequently progressive increase in the right ventricular (RV) afterload(197). Increased RV afterload is partially compensated by RV hypertrophy but eventually leads to RV dysfunction (RVD), RV failure and untimely death, regardless of medical treatment(197). Human and experimental chronic **left** heart dysfunction is characterized by decreased oxidative metabolism(156), abnormal mitochondrial respiration(189) and impaired mitochondrial biogenesis(113). These changes have in part been explained by a deregulated expression of critical transcription factors such as the peroxisome proliferator-activated receptor (PPAR) alpha(16), the estrogen-related receptor (ERR) alpha(108) and the master regulator of oxidative metabolism, the PPAR-gamma coactivator-1alpha (PGC-1α)(12).

Akin to left heart failure, it has been postulated that RVD is characterized by abnormal energy metabolism(186, 231). Studies in animal models have demonstrated that RVD exhibits an increased expression of glycolysis-related genes(54) and increased enzymatic glycolysis rate(176). However, is largely unknown to what extent this switch in cardiac bioenergetics (also known as metabolic remodeling(236)) involves changes in fatty acid oxidation (FAO), whether metabolic remodeling is a response to chronic pressure overload, or to what extent mitochondrial structure and function are also compromised in RVD. Thus, we sought to 1) characterize the metabolic gene expression profile associated

with RV dysfunction, 2) determine whether pressure overload is sufficient to explain

metabolic gene remodeling, 3) assess the structure and function of mitochondria in the

dysfunctional RV.

6.2 Results

6.2.1 RV dysfunction is characterized by a load-independent downregulation of

PGC-1α, PPAR-α and ERR-α.

Drake et al. have previously reported that dysfunctional RVs from SuHx-rats,

differentially express multiple gene signalling pathways when compared with non-

dysfunctional hypertrophied RVs(55). Importantly, we reported that RVD is associated

with gene expression changes that suggest an abnormal metabolism, with a particularly

strong signal relating to the peroxisome proliferator-activated receptor (PPAR) signaling

pathways. Therefore, as a first step, we measured the expression of PGC-1α, a direct

coactivator and master regulator of the PPAR family of transcription factors. PGC-1α

regulates oxidative metabolism and many aspects of mitochondrial biology(67).

Western blots of protein samples obtained from SuHx RV tissues showed a significantly

decreased amount of PGC-1α protein (**Figure 15A**). qPCR analysis revealed a significant

downregulation of PGC-1α mRNA levels (**Figure 15B**) indicating that the change in

PGC-1α expression also occurred on the transcription level. Decreased PGC-1α gene

expression was accompanied by a decreased expression of the ERR-α and PPAR-α genes

(**Figure 15B**). To evaluate whether pure mechanical RV pressure-overload was sufficient

to downregulate PGC-1α expression, we measured PGC-1α transcript levels in PAB-RV

tissues and found that the expression of PGC-1α, ERR-α and PPAR-α was not

Figure 15. Gene and protein expression of PGC-1α, ERR-α and PPAR-α in SuHx RV

tissue and its relationship with RV function.
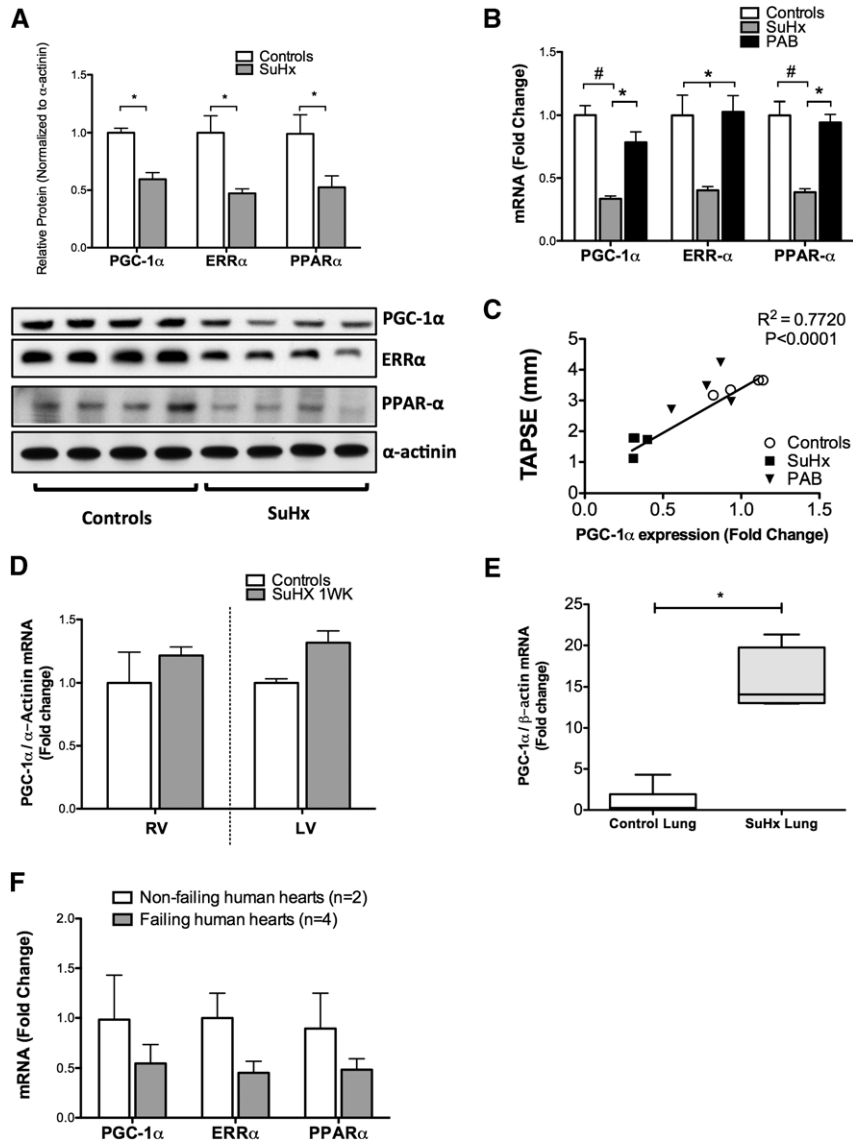
Figure 15. **A**, Western blots on SU5416/ hypoxia (SuHx) right ventricular (RV) whole tissue lysates show a downregulation of peroxisome proliferator-activated receptor (PPAR)- coactivator-1α (PGC-1α), estrogen-related receptor (ERR)-α, and PPAR-α on the protein level. **B**, Quantitative reverse transcription-polymerase chain reaction mRNA expression analysis from right ventricles of control, SuHx, and pulmonary artery banding (PAB) animals. Compared with controls and PAB, SuHx-RV tissue exhibits decreased PGC-1α transcript levels along with a decreased expression of the nuclear receptors ERR-α and PPAR-α. **C**, PGC-1α correlation with right ventricular function (tricuspid annular plannar systolic excursion [TAPSE]). **D**, Quantitative polymerase chain reaction analysis shows no change in PGC-1α expression in RV and left ventricle (LV) of SuHx rats at 1 week after SuHx had been initiated. **E**, mRNA expression of PGC-1α in SuHx lung tissue. **F**, PGC-1α, ERR-α, and PPAR-α mRNA transcript levels in human RV samples. Data are shown in fold changes±SEM over controls; **P<0.001; #*P*<0.0001. *Reproduced with permission from* **Gomez-Arroyo J, et al.** *Metabolic gene remodeling and mitochondrial dysfunction in failing right ventricular hypertrophy secondary to pulmonary arterial hypertension. Circ Heart Fail. 2013 Jan 1;6(1):136–144.*

significantly decreased in the non-failing hypertrophied RVs of PAB rats, despite the high RV pressure and RV hypertrophy (**Figure 15B**). **Figures 15C** and **Figure 16 2A-B** illustrate that PGC-1α (R^2=0.72, p=0.001), PPAR-α (R^2=0.72, p=0.001) and ERR-α (R^2=0.76, p=0.002) transcript levels strongly correlated with the tricuspid annular plane systolic excursion (TAPSE), a heart-rate independent variable of RV function.

We have previously described that SU5416 treatment alone does not induce RV dysfunction and has a limited impact on gene expression(55). However, because decreased expression of PGC-1α could be a direct effect of the combination of SU5416 and hypoxia rather than a consequence of RVD, we measured the expression of PGC-1α at one week after the SuHx protocol had been initiated. At one week no RVD is present and indeed, as shown in **Figure15D**, PGC-1α expression is not decreased in the RV or in the LV. In addition, we measured the expression of PGC-1α in rat lung tissues after four weeks of SuHx, a time-point where plexiform-like lesions have already formed, and we found a significant increase in PGC-1α expression (**Figure 15E**). To further evaluate a potential toxic effect of SU4516 in the setting of RV pressure overload, we examined the RV gene expression of PAB animals exposed to SU4516 and found no change in the PGC-1α, ERR-α or PPAR-α mRNA transcript levels (**Figure 16C**). Next, we measured the expression of PGC-1α in LV tissue obtained from animals sacrificed four weeks after initiation of the SuHx protocol. Although somewhat decreased, the SuHx-LV tissue did not show a significant change in PGC-1α expression (**Figure 16D**). In the aggregate, the data indicates that the decreased expression of PGC-1α is unlikely due to a toxic effect of SU5416.

Figure 16.
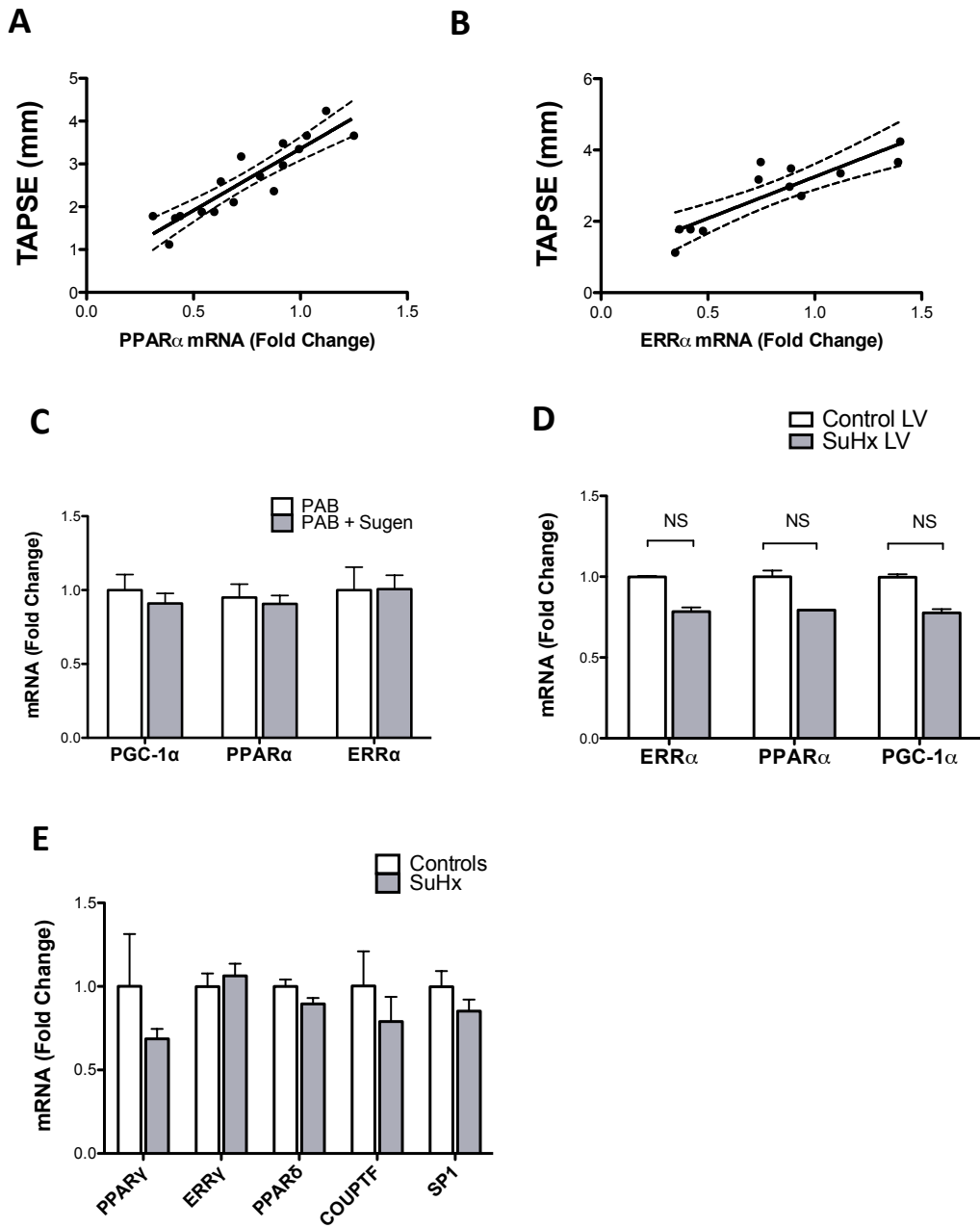
Figure 16. Gene expression of PGC1α and other nuclear receptors involved in fatty acid transition from fetal to adult hearts. Scatter-plot illustrating correlation between TAPSE and mRNA expression of ERR-α (A) and PPAR-α (B). RT-PCR analysis reveals no difference in the gene expression of PGC-1α, PPAR-α or ERR-α in the PAB model after exposure to SU5416 (C) or in SuHx left ventricle tissue (D). E) mRNA transcript levels of transcription factors other than PGC-1α that regulate cardiac energetics. N= 4-8 per group. Data are shown in fold-change mean ± SEM. * p=<0.05, #p=<0.001. *Reproduced with permission from **Gomez-Arroyo J, et al.** Metabolic gene remodeling and mitochondrial dysfunction in failing right ventricular hypertrophy secondary to pulmonary arterial hypertension. Circ Heart Fail. 2013 Jan 1;6(1):136–144.*

Because nuclear receptors other than PGC-1α have been implicated in phenotypic metabolic changes which occur during normal cardiac development, we decided to evaluate the expression of the estrogen related receptor gamma (ERR-γ), and of the transcription factors COUP-TF1 and SP1 (5, 191). QPCR analysis showed that the expression of these transcription factors was not affected in dysfunctional RV tissues (**Figure 16E**). Lastly, to examine whether the changed expression of the metabolic gene pattern was also observed in human myocardium, we examined the gene expression of PGC-1α, PPAR-α and ERR-α in RV tissue samples from patients with PAH. Indeed, we found a comparable expression pattern in the human RV tissue as we had observed in the SuHx RV rat tissue (**Figure 15F**).

6.2.2 Dysfunctional RV hypertrophy is characterized by decreased expression of genes involved in fatty acid and glucose oxidation

Figure 17A illustrates that multiple PGC-1α/PPAR-α/ERR-α target genes encoding critically important proteins, required for fatty acid transport into the cardiomyocytes and into the mitochondria, were downregulated in the SuHx dysfunctional RVs. In addition, the expression of genes encoding proteins required for beta-oxidation (ACADM, ACADVL and ACADS) was decreased (**Figure 17B**). Western blot analysis confirmed the decreased expression of ACADM and ACADVL in RVD (**Figure 17C**). Supporting the observation of normal expression of PGC-1α/PPAR-α/ERR-α, non-failling hypertrophied (PAB) RVs demonstrated a normal expression of ACADM and a significantly increased expression of ACADS and ACADVL. These Acyl-CoA

Figure 17.
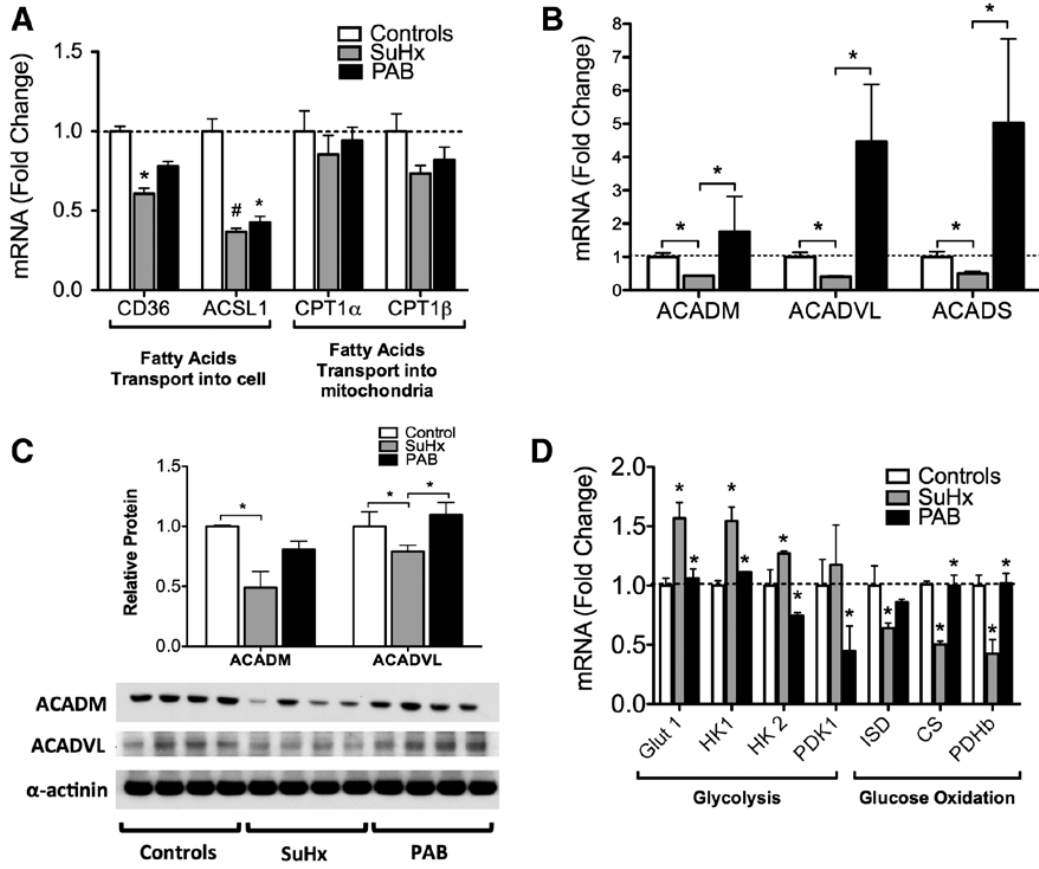
Figure 17. Gene and protein expression of PGC-1α target genes required for fatty acid oxidation. mRNA levels of genes encod- ing key rate-limiting enzymes involved in fatty acid transport into the cell (*CD36*) and transport into the mitochondria (*ACSL1, CPT1α*, *CPT1β*, and *CPT2*) were decreased. **B**, Genes encoding a family of acyl-coen- zyme A (CoA) dehydrogenases specific for fatty acid à-oxidation (*ACADS*, *ACADM*, and *ACADVL*) also were downregulated

in dysfunctional SU5416/hypoxia (SuHx) right ventricles but significantly increased in pulmonary artery banding (PAB) right ventricular (RV) tissue. **C**, Western blotting on cytosolic protein extracts obtained from RV tissue lysate shows decreased protein expression of ACADM and ACADVL in SuHx-RV tissue. **D**, Genes encoding key rate-limiting enzymes for aerobic glucose oxidation (Kreb cycle) were downregulated, whereas genes encoding enzymes neces- sary for glycolysis were upregulated. Data are shown in fold changes±SEM over con- trols; *$P<0.01$; #$P<0.0001$. *Reproduced with permission from* **Gomez-Arroyo J, et al.** *Metabolic gene remodeling and mitochondrial dysfunction in failing right ventricular hypertrophy secondary to pulmonary arterial hypertension. Circ Heart Fail. 2013 Jan 1;6(1):136–144.*

dehydrogenases are required to metabolize medium, short and long fatty acids, respectively.

In accordance with our previous reports(55), dysfunctional RV hypertrophy in the SuHx rats was characterized by increased expression of GLUT1 and Hexokinase-1; these two genes play an important role in glycolysis (**Figure 17D**). In contrast, we found a downregulation of genes that encode enzymes involved in aerobic glucose catabolism, such as the genes encoding the Krebs cycle enzymes citrate synthase and isocitrate dehydrogenase. Furthermore, the beta subunit of pyruvate dehydrogenase – an important link between glycolysis and glucose oxidation – showed a 50% decreased mRNA expression, whereas the gene expression of pyruvate dehydrogenase kinase (PDK-4), an enzyme controlling pyruvate dehydrogenase activity was upregulated. Conversely, non-failing hypertrophied PAB RVs exhibited a normal expression of glycolysis-related genes, a significantly lower expression of PDK-4 and normal expression of isocitrate dehydrogenase and citrate synthase (**Figure 17D**).

6.2.3 RVD is characterized by abnormal mitochondrial ultrastructure, impaired mitochondrial respiration and abnormal mitochondrial biogenesis**.**

PGC-1α regulates mitochondrial biogenesis along with oxidative metabolism(67). Therefore, we sought to explore abnormalities in mitochondrial biology. PGC-1α exerts pleiotropic effects by direct coactivation of an array of nuclear and non-nuclear receptors employed in the control of cellular metabolism(67). Among them, TFAM regulates mitochondrial DNA replication and maintenance, and is required for cellular and mitochondrial viability(118, 240). Associated with the decreased expression of PGC-1α, SuHx-RVD tissue had a decreased expression of TFAM (**Figure 18A**). Because, reduced

Figure 18.
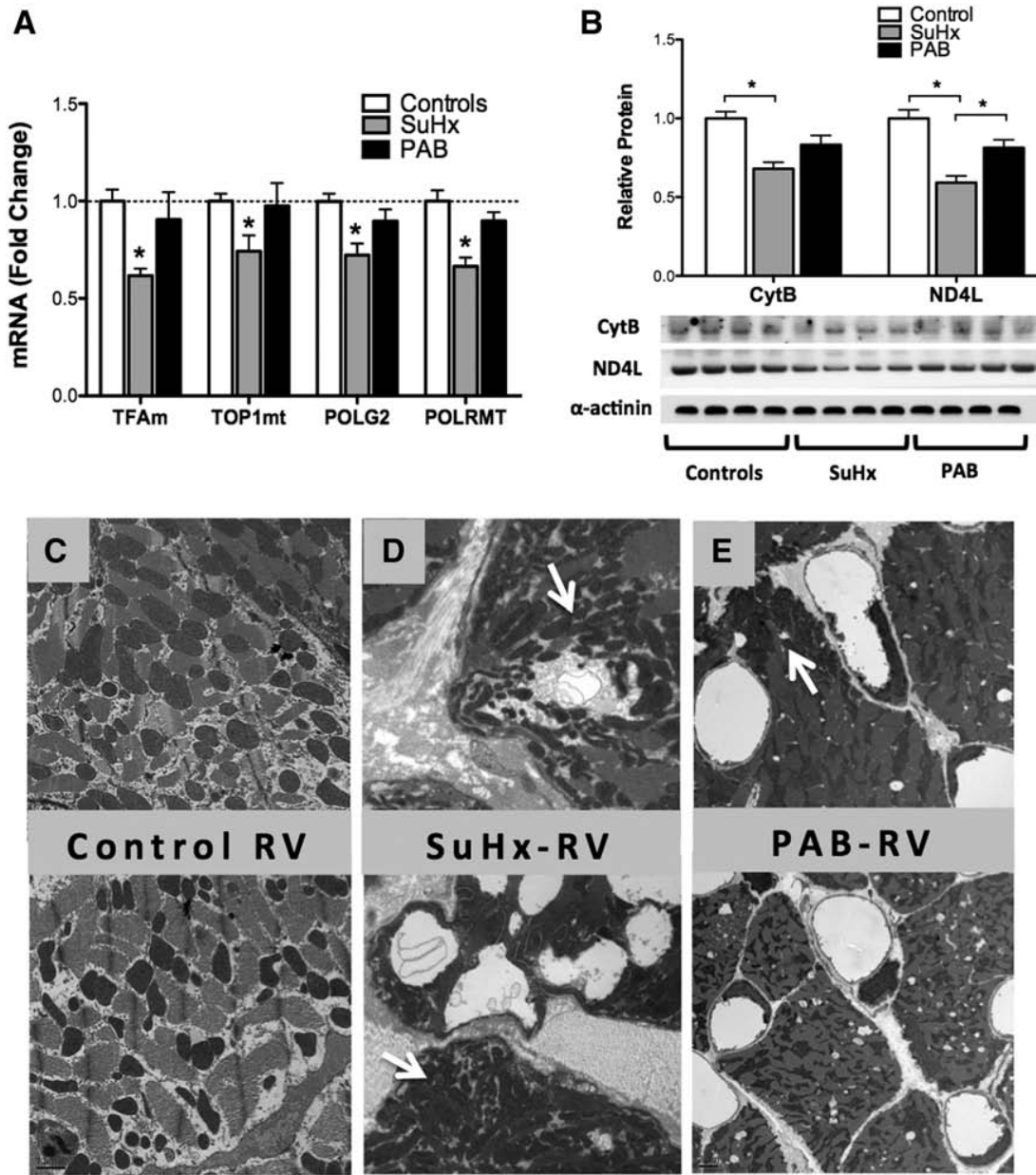
Figure 18. **Changes in mitochondrial biology in RV failure tissue.** mRNA transcript levels of genes required for mitochondrial bio- genesis and mitochondrial DNA (mtDNA) replication and transcription. **B**, Western blotting of right ventricular (RV) tissue demonstrates a significantly decreased protein expression of mtDNA-encoded proteins in SU5416/hypoxia (SuHx)-RV dysfunction. **C** and **D**, Electron microscopy demonstrates abnormal ultrastructure of mitochondria in RV dysfunction. Data are shown in fold changes±SEM compared with controls; *P<0.01; #P<0.0001. *Reproduced with permission from* **Gomez-Arroyo J, et al.** *Metabolic gene remodeling and mitochondrial dysfunction in failing right ventricular hypertrophy secondary to pulmonary arterial hypertension. Circ Heart Fail. 2013 Jan 1;6(1):136–144.*

TFAM mRNA levels is associated with alterations in mitochondrial biogenesis, we measured the expression of *Top1mt*, *POGL2* and *POLRMT*, a set of genes that encode enzymes required for the replication of mtDNA and mitochondrial biogenesis(113, 118). All three genes were downregulated in dysfunctional (SuHx) RV hypertrophy but not in PAB-induced RV hypertrophy as illustrated in **Figure 18A**. To test for decreased mtDNA transcription, we measured the expression of two mtDNA-encoded proteins proteins: NADH-ubiquinone oxidoreductase subunit 4L (ND4L) and cytochrome B (CytB). These two proteins are subunits of the mitochondrial electron-transport chain complexes I and III respectively. As illustrated in **Figure 18B**, the relative protein expression of ND4L and CytB was significantly decreased in SuHx-RVs.

High-power magnification electron microscopy demonstrated that the mitochondrial ultrastructure in RVD tissue was highly abnormal. In comparison to controls (**Figure 18C**), mitochondria in SuHx RVs were consistently abnormal in shape and size, and clumped together in clusters (**Figure 18D**). Although clustering of mitochondria was also present in the PAB RVs (**Figure 18E,** arrow), the overall distribution of mitochondria was similar to that of control RVs. Upon isolation, RVD tissues exhibited a significantly decreased amount of mitochondria, as evidenced by mitochondrial yield and by citrate synthase activity (**Figure 19A-B**). Isolated mitochondria were studied by respirometry to evaluate the efficiency of oxidative phosphorylation. RVF-mitochondria demonstrated a significantly decreased ADP-stimulated (State 3) respiration rate when utilizing glutamate (**Figure 19C**) but not when utilizing succinate as electron donors to complex I and II, respectively.

Figure 19
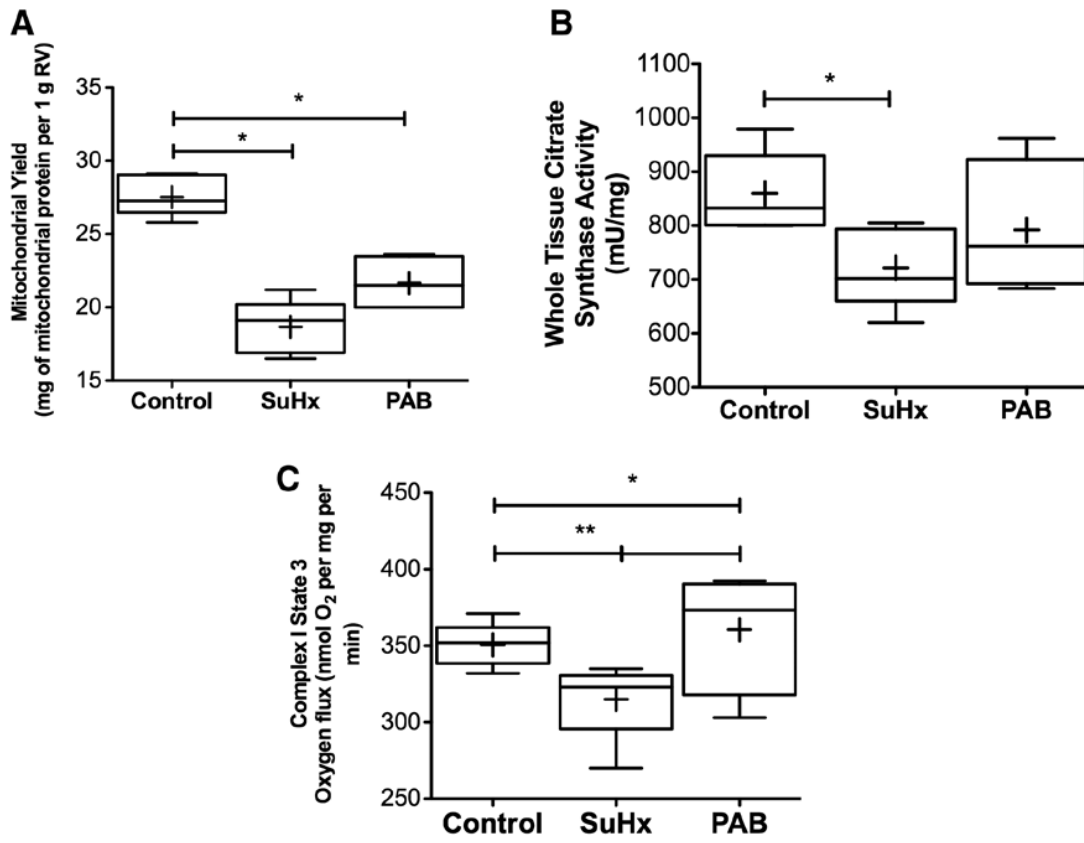
Figure 19: A, Amount of mitochondrial protein per 100 mg of right ventricular (RV) tissue. SU5416/hypoxia (SuHx) and pulmonary artery banding (PAB) RV tis- sues demonstrate significantly decreased mitochondrial yield when compared with control RV tissue. **B**, Whole tissue citrate synthase activity assay demonstrates that SuHx has a reduced oxidative capacity when compared with control RV. **C**, State 3 respiration with complex I substrate (gluta- mate) is significantly decreased in SuHx RV dysfunction when compared with control or PAB RV tissues. The lines in the box- and-whiskers plots illustrate the median, whereas the + sign illustrates the mean. *$P<0.01$; #$P<0.0001$.

Reproduced with permission from the published from **Gomez-Arroyo J, et al.** *Metabolic gene remodeling and mitochondrial dysfunction in failing right ventricular hypertrophy secondary to pulmonary arterial hypertension. Circ Heart Fail. 2013 Jan 1;6(1):136–144.*

Since mitochondrial dysfunction could contribute to the generation of reactive oxygen species (ROS), we measured the levels of 8-isoprostane (8-*iso*Prostaglandin F$_{2\alpha}$) in RVD tissues. 8-Isoprostane has been proposed as a marker of antioxidant deficiency and enhanced oxidative stress(151). Analysis from LC tandem mass spectrometry of SuHx RV tissue demonstrated no change in the amount of 8-isoprostane in comparison to controls (**Figure 20A**) but increased levels in the lungs (**Figure 20B**). However, whereas the amount of ROS generated might have not been sufficient to cause significant lipid peroxidation in whole RV tissues, ROS could still induce damage. mtDNA is particularly susceptible to ROS-induced damage(207) and a common marker of mtDNA damage is the formation of 7,8-dihydro-8-oxoguanine (8-oxoG), a mutagenic base byproduct that results from direct exposure of DNA to ROS(18). **Figure 21** shows that 8-oxo-G positive staining in dysfunctional RV tissues, particularly in the endomyocardial area.

Figure 20
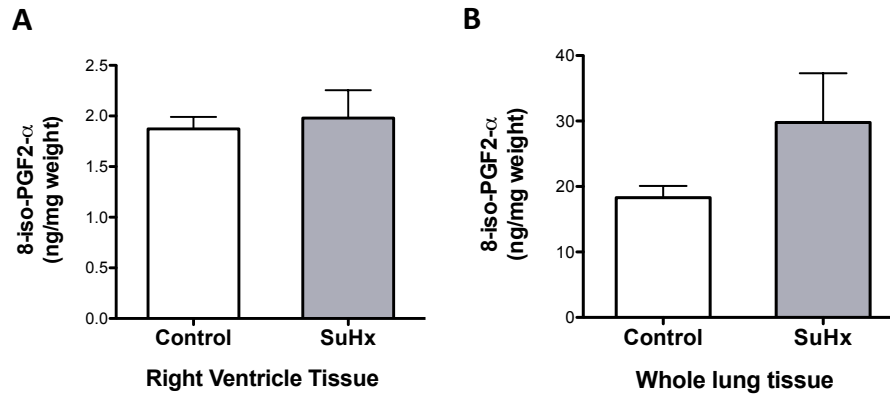
Figure 20. LC-tandem mass spectrometric measurement of 8-iso- PGF-2α (8-isoprostane) in the RV (A) and lung (B) tissue of SuHx rats. N= 4 rats per group. There were no statistically significant differences between groups. *Reproduced with permission from **Gomez-Arroyo J, et al.** Metabolic gene remodeling and mitochondrial dysfunction in failing right ventricular hypertrophy secondary to pulmonary arterial hypertension. Circ Heart Fail. 2013 Jan 1;6(1):136–144.*

Figure 21.
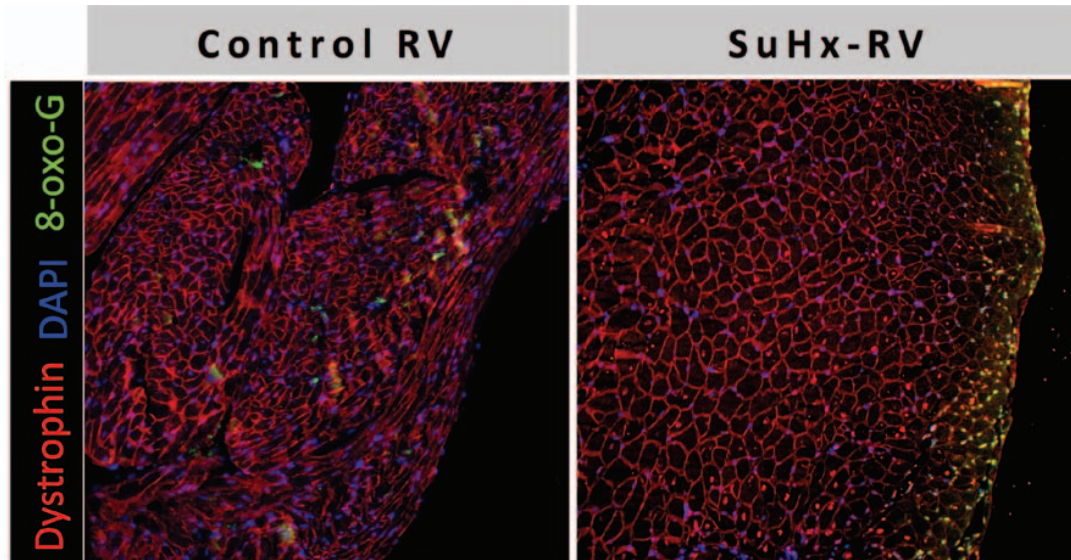
Figure 21. Immunofluorescence shows increased 7,8-dihydro-8-oxoguanine (green) in right ventricular dysfunction (RVD) tissue vs SU5416/hypoxia (SuHx)-RVD. *Reproduced with permission from* **Gomez-Arroyo J, et al.** *Metabolic gene remodeling and mitochondrial dysfunction in failing right ventricular hypertrophy secondary to pulmonary arterial hypertension. Circ Heart Fail. 2013 Jan 1;6(1):136–144.*

6.3 Discussion

Right ventricular failure is a common consequence of severe chronic pulmonary hypertension and the most frequent cause of death in patients with PAH(197). Although RV dysfunction plays a important prognostic role in patients with PAH(237, 244), there are relatively few experimental data shedding light on the mechanisms of chronic RV dysfunction (RVD) and failure(23, 246). Whereas it has been proposed that RVD is associated with metabolic gene remodeling(231), a comprehensive metabolic gene profile of the failing RV is still lacking.

Here we demonstrate that dysfunctional RV hypertrophy – in rats and patients with PAH – exhibit a significant reduction in the expression of PGC-1α and its corresponding nuclear receptors (PPAR-α and ERR-α). Interestingly, the change in PGC-1α expression appears to be largely independent of the RV pressure overload and hypertrophy. Moreover, multiple PGC-1α target genes encoding proteins required for fatty acid metabolism were significantly decreased in expression in RVD tissues. Particularly, the expression of genes encoding the acyl-CoA dehydrogenases which are specific for fatty acid β-oxidation, was significantly decreased in dysfunctional SuHx-RV hypertrophy but not in adaptive PAB-RV hypertrophy. Conversely, functional PAB-RV hypertrophy was associated with a high expression of ACADS and ACADVL, the latter being the most important heart acyl-CoA dehydrogenase for FAO. Altogether the gene and protein expression data suggest that in RVD, FAO is impaired on multiple levels (**Figure 22**). Along with the metabolic gene remodeling, we show evidence for an abnormal mitochondrial ultrastructure and decreased mitochondrial respiration at the level of complex I of the electron transport chain. Moreover, RVD is characterized by decreased

Figure 22.
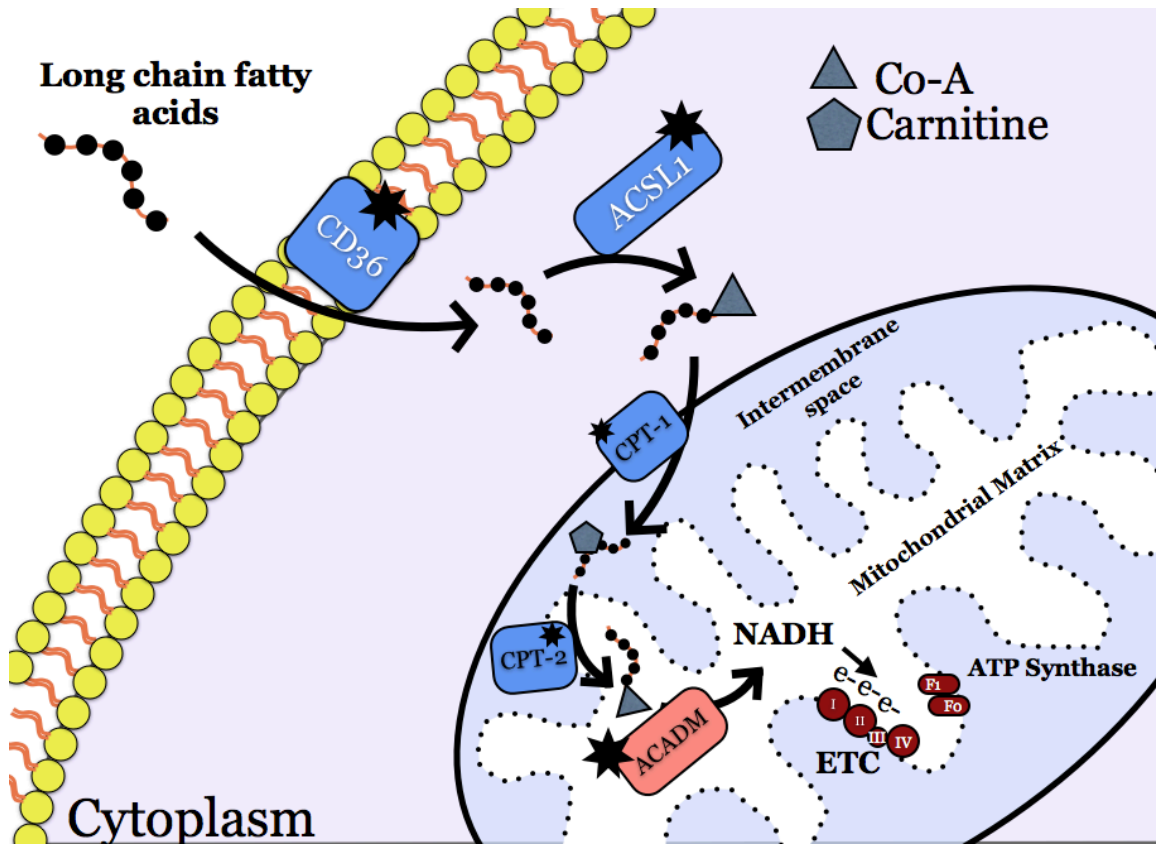
Figure 22. Schematic representation of the multiple steps affected in fatty acid metabolism during right ventricular failure (black stars). *ETC= Electron transport chain.*

expression of genes encoding proteins required for mitochondrial biogenesis such as TFAM, *Top1mt*, *POGL2* and *POLRMT*. RVD also demonstrated a significantly low mitochondrial yield in comparison to control RVs. Finally we demonstrate that RVD exhibits high levels of 7,8-dihydro-8-oxoguanine, consistent with ROS-induced DNA damage.

We decided to focus on central transcriptional regulators such as PGC-1α and its corresponding nuclear receptors ERR-α and PPAR-α, because multiple gene knockout studies have illustrated that these proteins play an important role during the functional bioenergetic adaptation of the heart to pressure overload(67, 237, 244). PGC-1α is preferentially expressed in tissues with high oxidative capacity and coordinates several biological processes of mammalian energy metabolism by activating genes involved in cellular uptake and mitochondrial oxidation of fatty acids(179). Heart tissue obtained from PGC-1α knockout mice displays a reduced palmitoyl-L-carnitine state 3 respiration, suggesting reduced FAO, and a reduction in the amount of ATP generated per oxygen consumed (131). Of equal importance, in the absence of PGC-1α, the expression of mitochondrial genes in the heart is suppressed, the activities of mitochondrial enzymes are altered and ATP production is reduced (11). As it has been shown in models of left heart failure(11, 12, 130), the SuHx model of severe PAH and RVD is characterized by reduced PGC-1α expression. We consider this reduced expression as a central component of RV metabolic remodeling. Whereas downregulation of PGC-1α is a feature of dysfunctional hypertrophy, it remains unclear what drives the downregulation of PGC-1α expression during RVD. As the SuHx model is characterized by capillary rarefaction(25), ischemia and hypoxia could potentially drive the metabolic remodeling. However, PGC-

1α expression is not decreased until RVD occurs. Because PGC-1α expression is an HIF-independent hypoxia-inducible gene(10), it is unlikely that the downregulated expression of PGC-1α and the associated metabolic remodeling profile would be entirely explained by hypoxia or by HIF activation. Whereas decreased PGC-1α mRNA expression has been reported in human left heart failure (203), recent studies using samples of left ventricles obtained from patients with heart failure have demonstrated a relatively normal expression of PGC-1α(113). Perhaps these discrepant results may be explained by different drug treatments of the patients with LV failure.

Whereas impaired glucose oxidation has been well characterized in the monocrotaline-injury model of RVD, changes in fatty acid metabolism are less clear(177). In our study, the downregulation of PGC-1α, ERR-α, and PPAR-α expression was coupled to a decreased expression of genes encoding FA transport proteins and FAO, which suggests to us that FA catabolism in the failing RVs is likely compromised on the levels of regulation, transport and catabolism. Others have reported that changes in FAO occur in the monocrotaline-injury model of PH, mainly in CPT-1β expression(33), and few case reports have shown reduced uptake of radiolabeled fatty acid analogues in the RV of patients with PAH(121). However, it remains unclear whether the changes in FA metabolism are beneficial or detrimental in the overall function of the RV. In the left ventricle, multiple studies have shown that the rate FAO is preserved or increased in physiological/adaptive hypertrophy, and that FAO decreases during the progression of heart failure(3). Similarly, we demonstrate a normal/increased expression of ACADM, ACADS and ACADVL in adaptive PAB-RV hypertrophy. These results are supported by the data of Fang and Archer, who demonstrated that rats with PAB-RV hypertrophy

exhibit higher rates of FAO(65). We postulate that along with capillary rarefaction, fibrosis and ROS-induced damage, mitochondrial metabolic remodeling in RVD is pathological. It has been reported that FAO inhibition may have a therapeutic potential(65) however, it will remain to be tested whether further inhibition of FAO is beneficial in the model of SuHx RVD.

While it has been reported that RVD is associated with mitochondrial hyperpolarization(152), a comprehensive analysis of mitochondrial respiration in RVD is still lacking. Here we demonstrate that RVD is associated with significant mitochondrial dysfunction, reduced mitochondrial yield and reduced overall oxidative capacity. Surprisingly, although the expression of PGC-1α and TFAM was unchanged in PAB-RV hypertrophy, mitochondrial yield and citrate synthase activity were similarly decreased in both SuHx-RVD and PAB-RV hypertrophy. Because PGC-1α regulates mitochondrial biogenesis, our results would suggest an "uncoupling" between PGC-1α expression and mitochondrial biogenesis in adaptive PAB-RV hypertrophy. Yet, abnormal mitochondrial biogenesis can occur in the presence of normal PGC-1 levels(113). We speculate that preserved PGC-1α and TFAM expression could explain the better preserved mitochondrial respiration in PAB-RV hypertrophy when compared to SuHx-RVD, as both proteins play a critical role in mitochondrial function(67, 118).

6.4 Study Limitations and Future Directions

We do not know whether a decrease of in PGC-1α expression is a consequence or a cause of RVF. Nonetheless, our results show that decreased PGC-1α gene expression is not explained by a toxic effect of SU5416, hypoxia or RV pressure overload. Several mechanisms may participate in the downregulation of PGC-1α expression in RVD and

119

the associated gene metabolic remodeling. We did not explore whether the metabolic remodeling-dependent gene and protein expression profile affects enzymatic activity.

6.5 Conclusions

Our data illustrate that right ventricular dysfunction is associated with a complex multilevel disturbance of fatty acid oxidation and mitochondrial respiration that are not entirely explained by pressure overload or hypertrophy. We propose that RV metabolic remodeling is a consequence of decreased PGC-1α expression. To what extent metabolic remodeling or mitochondrial dysfunction is of functional importance for the development of RVD remains to be investigated.

6.6 Clinical Perspective

Our experiments demonstrate that in the setting of severe pulmonary arterial hypertension, load-independent alterations of cardiac energy metabolism and mitochondrial efficiency are associated with RVD. Because RV failure determines the outcome in patients with severe PAH, the cellular and molecular mechanisms which underlie RVF need to be understood for they could be reversible. As we design RV-targeted therapies, the use of metabolic modulators should aim to restore not only substrate utilization but also mitochondrial function.

Chapter 7: Pharmacotherapies Tested to Reverse Metabolic Remodeling and Improve Right Ventricular Failure in the SU5416/hypoxia Model of Severe PAH

Segments of this chapter have been previously published in:

Drake JI, **Gomez-Arroyo J,** et al. Chronic carvedilol treatment partially reverses the right ventricular failure transcriptional profile in experimental pulmonary hypertension. *Physiol. Genomics*. 2013 Apr 30;

CHAPTER 7

7.1 Introduction

As it was discussed in Chapter 3, studying the mechanisms that contribute to the development of right ventricular failure is critical in order to develop new therapeutic strategies. Although we characterized the transcriptional profile in maladaptive RV hypertrophy (Chapter 6), we still do not know whether these changes in fatty acid oxidation are indeed adaptive or maladaptive or whether the use of metabolic modulators could improve function of the failing RV. Therefore, in this chapter, we sought to:

1) Evaluate whether further blockade of fatty acid oxidation improved function of the failing right ventricle.

2) Evaluate whether other metabolic modulators that do not affect substrate utilization but rather mitochondrial biogenesis improved function of the failing right ventricle.

3) Evaluate whether treatment with the adrenergic receptor blocker, carvedilol, modified the metabolic transcriptional profile observed in maladaptive RV hypertrophy.

7.2 Pharmacotherapies Used

7.2.1 Etomoxir (D-enantiomer) treatment

A group of SuHx animals was treated with the fatty acid oxidation blocker Etomoxir. Etomoxir was purchased as a D-enantiomer from Sigma-Aldrich (St Louis, MO). It was dissolved in PBS pH 7.4 (phosphate buffered saline 1x) and administered intraperitoneally in a standard dose of 7 mg/kg/day (equivalent to 15mg/kg/day of racemic Etomoxir) (133, 201, 233) for 2 weeks, starting once RV failure was established (as confirmed by echocardiogram). The D-enantiomer of etomoxir was used because it is more accurate to quantify and administer when compared to the racemic form.

7.2.2 Resveratrol treatment

Resveratrol dissolved in with propylene glycol and water 50/50 was orally administered 10mg/kg daily by oral gavage for 4 weeks starting once RV failure was established (as confirmed by echocardiogram).

7.2.3 Recombinant human TFAM treatment

A recombinant human mitochondrial transcription factor A (rhTFAM) produced and purified by Gencia Corporation, (Charlottesville, VA), kindly shared by Dr. James Bennett and collaborators. rhTFAM was stored in 50% sorbitol, and dialyzed against 5% glycerol in 1x PBS then filtered through 10,000 Amicon ultracentrifugal filter units (MWCO) right before injection. rhTFAM was administered at a dose of .67mg/kg and injected intravenously through rat tail vein once per week for 4 weeks.

7.2.4 recombinant human TFAM protein sequence and characteristics

For detailed information about the recombinant protein please refer to Reference (110, 227). Briefly, RhTFAM is a translational fusion protein is composed by an HA epitope placed after an 11-Arginine protein transduction domain (PTD) which facilitates cytosolic escape of transduced protein after macropinocytosis(110). rhTFAM includes an N-terminal protein transduction domain to allow rapid translocation across cell membranes, followed by an SOD2 mitochondrial localization signal to stimulate uptake through the TOM-TIM mitochondrial translocases. RhTFAM enters the mitochondrial compartment of cells rapidly and can also transport mtDNA cargo into mitochondria. The nucleotide sequence corresponding to PTD-HA-MLS-TFAM is shown below:

 [6X-His]-[SUMO3]-[11Arg PTD]–[HA]-[SODMLS]-[MatureTFAM]

[MGHHHHHHGG]-[MSEEKPKEGVKTENDHINLKVAGQDGSVVQ
FKIKRHTPLSKLMKAYCERQGLSMRQIRFRFDGQPINETDTPAQLE
MEDEDTIDVFQQQTGG]-[RRRRRRRRRRR]-[GEGDIMGEWGNEIFGAI
AGFLGGE]-[MLSRAVCGTSRQLPPVLGYLGSRQ]-[SSVLASCPKKPVSSY LR
FSKEQLPIFK AQNPDAKTTELIRRIAQRWR ELPDSKKKIYQD
AYRAEWQVYKEEISRFKE QLTPSQIM SLEKEIMD KHLKRKAM TKKKEL
TLLGKPKRPRSAYN VYVAERFQEA KGDSPQEKLK TV KENWKNLS
DSEKELYIQH AKEDETRYHN EMKSWEEQ MIEVG RKD LLRRTIKKQR
KYGAEEC) KGDSPQEKLK TVKENWKNLS DSEKELYIQH AKEDETRYHN
EMKSWEEQ MIEVGRKD LLRRTI KKQR KYGAEEC](110).

7.2.5 Adrenergic Receptor Blockage treatment

Carvedilol treatment has been shown to improve RV function in experimental PAH (27).
One group of SuHx (n=4-6) and one group of MCT (n=4-6) animals were treated with
carvedilol (15mg/kg; Sigma-Aldrich, St Louis, MO) dissolved in 20% DMSO and water
and administered once daily per oral gavage for 4 weeks, starting after RV failure was
confirmed by echocardiogram. Another group of SuHx rats was treated with a β-1
selective adrenergic receptor blocker (metoprolol). Metoprolol was administered in a
dose of 150 mg/kg/day, dissolved in the drinking water. Both carvedilol and metoprolol
doses have been validated previously (27).

Results and Discussions for Each Pharmacological Approach

7.3 Pharmacological inhibition of fatty acid β-oxidation with Etomoxir does not improve function nor prevent deterioration of right ventricular function.

To begin to address whether the changes in metabolic substrate utilization in the failing RVs, described in Chapter 6, were an adaptative or a maladaptative mechanism, we treated a group of SuHx animals (with established RVF assessed by echocardiogram) with a standarized dose of etomoxir (133, 201, 233), a potent carnitine-palmitoyltransferase-1 (CPT-1) blocker. CPT-1 catalyses a rate-limiting (133) regulated step in mitochondrial transport of fatty acids, and failing RVs exhibit a residual expression of CPT-1 that could be targeted (**Figure 17)** . Therefore, we reasoned that pharmacological blockade of this enzyme would further reduce FAO in failing RVs, and if indeed a reduction in fatty acid oxidation in the setting of RVF were beneficial, we would expect an improvement in RV function after etomoxir treatment. Statistical analysis revealed that after 2 weeks of treatment with etomoxir or vehicle, there was a significant deterioration of RV function over time (p=0.013) but no significant difference in TAPSE or RV systolic area between vehicle and etomoxir treated groups (**Figure 23A-B**). At the time of post-treatment echocardiogram and cardiac catheterization, etomoxir treatment did not show any improvement in RV function, nor did it modify pulmonary hypertension (**Figure 23C-H**). Importantly, etomoxir treatment did not halt the deterioration of RV function observed over time in the SuHx model (27, 162).

Figure 23.
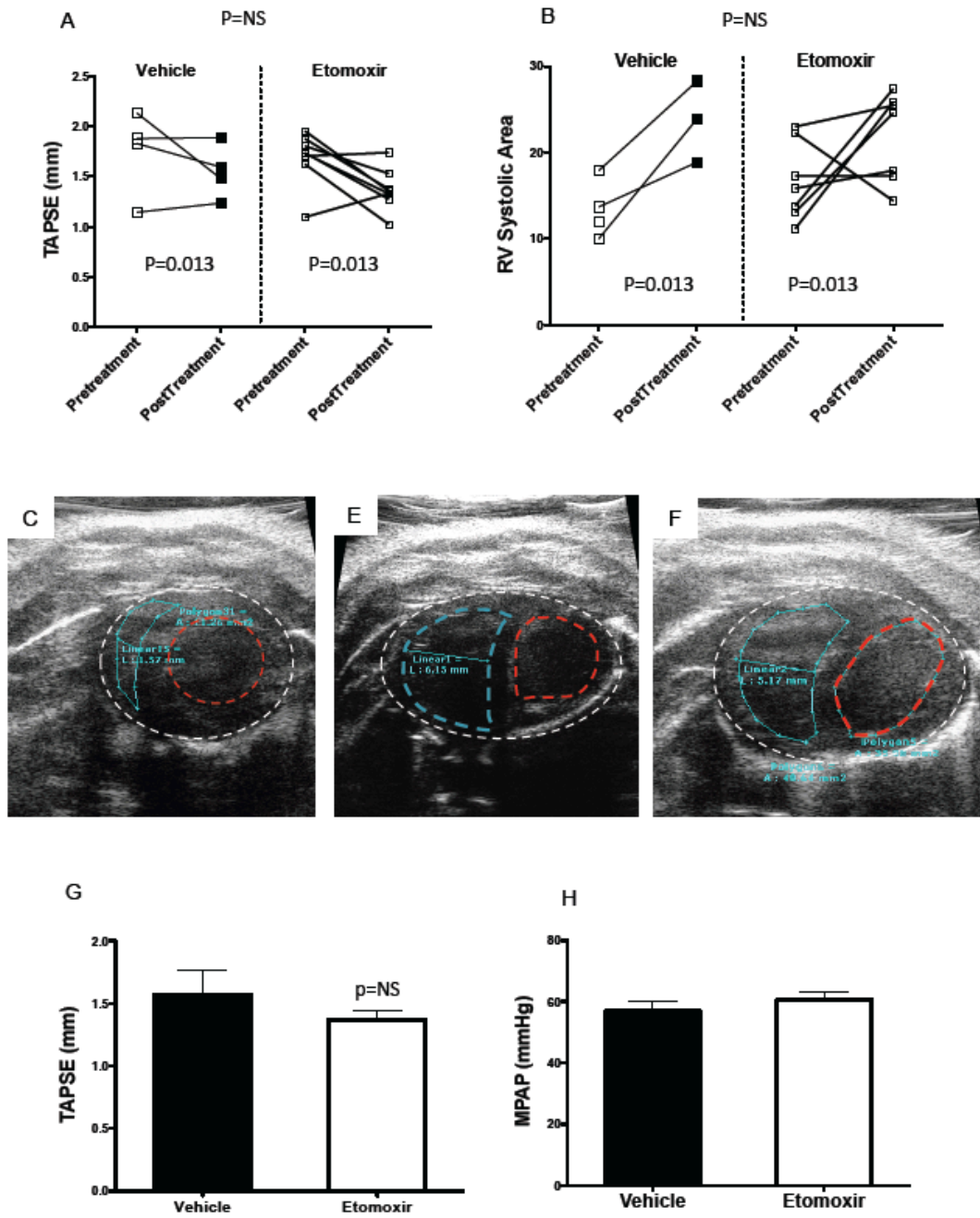
Figure 23. SuHx rats were treated with Etomoxir or Vehicle at a dose 7 mg/kg/day for 2 weeks after the animals had established RVF as assessed by echocardiogram. Paired T-test reveals an overall significant deterioration in TAPSE (A) and RV systolic area (B) in both groups. Short-axis cardiac ultrasound illustrates the RV diastolic area (blue line) from a normal rat (C), when compared with a SU5416/hypoxia rat treated with vehicle (D) or treated with etomoxir (E). There was no significant difference in the RV diastolic area between etomoxir-treated and vehicle-treated groups. Separate group analysis at the time of sacrifice did not show any significant differences in TAPSE (C) or MPAP (D) between vehicle-treated *versus* etomoxir-treated animals. N= 4-8 per group. Data are shown in mean ± SEM.

Etomoxir was first described as a metabolic modulator for the treatment of acute heart failure (133) with the rationale that during experimental myocardial infarction, an overactive 5' AMP-activated protein kinase (AMPK) would drive excessive FAO, which in turn would result in greater mitochondrial reactive oxygen species formation (133, 233). In these earlier studies, blockade of FAO by etomoxir resulted in improved functional capacity of the left ventricle, even in a model of LV chronic pressure-overload (233). Based on these findings, one would predict that chronic etomoxir treatment would have a beneficial effect in RV function. Interestingly, SuHx failing RVs treated with etomoxir did not show improved RV function, etomoxir did not lower the pulmonary artery pressure or decrease RV hypertrophy. More importantly, etomoxir treatment did not prevent the progression of RVF which is observed in this model (162). These findings suggest that inhibition of FAO might not be an effective therapeutic strategy for RVF in the setting of severe PAH.

Conversely, multiple studies have shown that the rate of fatty acid oxidation is preserved or increased in physiological/adaptive left ventricular hypertrophy, and that it decreases during the progression of heart failure (156). In a similar fashion, as shown in Chapter 6, rats with adaptive RV hypertrophy after pulmonary artery banding have increased rates of fatty acid oxidation (157). Multiple clinical trials evaluating the role of fatty acid oxidation blockers have been designed (158), however, none of these metabolic modulators have become a cornerstone in the treatment of heart failure. Moreover, no clinical trial has evaluated the role of metabolic modulators for PAH-associated RV failure. Recently, a clinical trial studying dichloroacetate, a mitochondrial modulator, has been started but it has not yet been concluded (**ClinicalTrials.gov Identifier**

NCT01083524). All together, our data would not support the use of fatty acid oxidation

blockade to treat RV failure.

7.4 Resveratrol treatment does not improve function nor prevent deterioration of

right ventricular function

Resveratrol (trans-3,5,4'-trihydroxystilbene) is a polyphenolic compound and naturally

occurring phytoalexin, has been designated the active agent. Resveratrol is a potent

inducer of sirtuins expression and it has been shown to be cardioprotective during

myocardial infarction in rats through induction of VEGF and HO-1 enhancing

neovascularization(112). Resveratrol can directly stimulate NADH dehydrogenases, and

more specifically mitochondrial complex I activity, therefore increasing mitochondrial

NAD+/NADH ratio(52). The NAD-dependent histone deacetylase sirtuin1 (SIRT1) is a

key regulator of lifespan in lower organisms and mice, and plays an important role in

cardiac energy metabolism. Several studies have shown that SIRT1 has pivotal

cardioprotective roles (153). For instance, it has been reported that upregulation of SIRT1

gene expression inhibits apoptosis, protects against oxidative stress and delays the

progression of aging in the mouse heart (6, 7). Moreover, Hsu *et al* have demonstrated

that cardiac-specific overexpression of SIRT1 protects from ischemia/reperfusion injury

(99). Furthermore, SIRT1 modulates fatty acid oxidation mainly through deacetylation of

PGC-1α (73) which increases PGC-1α activity and expression (autoregulatory

expression)(36). SIRT1 not only plays a critical role in regulating energy substrate

utilization, but also uniquely regulates angiogenesis signaling.

Activation of SIRT1 by the natural phenol resveratrol has also been shown to improve

health and survival of mice on a high-caloric diet (19). Moreover, synthetic SIRT1

activators –such as SRT1720 –have been shown to protect from diet-induced metabolic

by predominantly by enhancing FAO (66). SRT1720 another activator of SIRT1

promotes energy expenditure and enhanced expression of PGC-1α and PPAR-α (66). We

initially demonstrated that RV failure tissue is characterized by decreased expression of

SIRT1 protein in both humans and rats RVs (**Figure 24A-B**). Thus, we hypothesized that

treatment with resveratrol would increase SIRT1 protein levels and induce PGC-1α

expression and improve RV function. Interestingly, four weeks of resveratrol treatment

did not improve nor prevented the progression of RV failure (**Figure 24C**) and in

contrast, right ventricular systolic pressure was significantly increased (**mean RVSP**

105±10 mmHg).

Multiple studies have demonstrated the beneficial effects of resveratrol and a group of

investigators has even reported that resveratrol treatment ameliorates the pulmonary

hypertension caused by monocrotaline exposure(46). However, as discussed in Chapter 4,

whether the improvement in RV function in this model was attributed to partial

improvement of pulmonary hypertension (which is rather common in the monocrotaline-

injury model) or whether resveratrol has direct beneficial effects on the RV was not

investigated or discussed by the authors. Our results demonstrate that resveratrol

treatment was not sufficient to improve the function of the RV but rather worsened the

disease and increase the pulmonary artery pressure. These results are interesting because

PAH is an angiogenic disease where VEGF plays an important role. As mentioned

previously, resveratrol can induce VEGF expression and therefore contribute to

angiogenesis. However, whether this is the mechanism whereby resveratrol worsened

pulmonary hypertension in the SU5416/hypoxia remains to be investigated.

Figure 24.
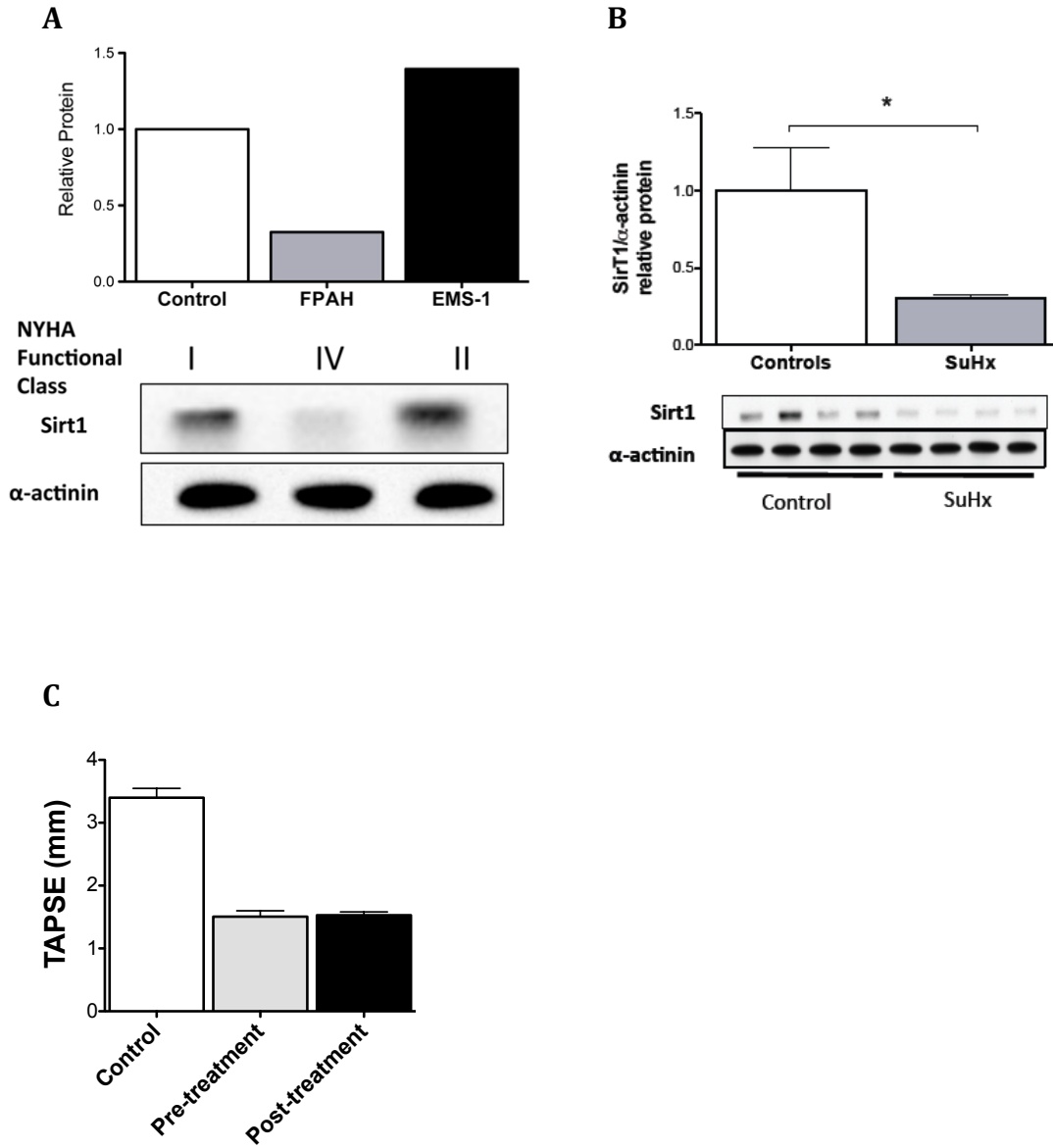
Figure 24. Protein levels of SIRT1 are decreased in SUHX rat RV tissue (A) and human

RV tissue (B). Function of the RV ventricle pre and post resveratrol treatment (C).

7.5 Treatment with rhTFAM induces significant upregulation of rat TFAm and PGC-1α transcript levels and improves RV longitudinal contractility

The mitochondrial transcription factor A, is an essential component for the maintenance and replication of mitochondrial DNA(118). Thomas, Bennett and collaborators have demonstrated that rhTFAM can stimulate mitochondrial biogenesis, and restore ATP levels in cell models of Parkinson's disease(227). Furthermore, the have demonstrated that systemic treatment of young adult mice with rhTFAM stimulates mitochondrial biogenesis, increases mitochondrial respiration in brain, heart and muscle tissues and increases brain mitochondrial ATP synthesis while reducing ROS-induced damage to proteins(227). Therefore, because maladaptive RV hypertrophy in the SU5416/hypoxia model is characterized by decreased TFAm expression, abnormal mitochondrial biogenesis and by ROS-induced damage of DNA, we hypothesized that treatment with rhTFAM would improve the abnormal changes in mitochondrial biology and therefore improve RV function in the SU5416/hypoxia model of RVF.

Although we had originally plan to treat the animals for 4 weeks, we could not continue the treatment for more than one week. However, the results were encouraging as we demonstrated that SU5416/hypoxia animals treated with rhTFAM had an improvement in TAPSE and, perhaps more importantly, exhibited a significant increase in rat TFAM and PGC-1α transcript levels (**Figure 25**). Indeed, our findings are interesting because this is perhaps the first time a genetically engineered agent specifically designed to modify mitochondrial biogenesis has been utilized to treat RV failure. However, we should still evaluate whether rhTFAM improved RVF via induction of PGC-1α, whether it modified the changes in mitochondrial ultrastructure and function

observed in maladaptive RV hypertrophy (described in Chapter 6) and, perhaps most importantly, evaluate how is rhTFAM inducing the expression of rat TFAM and PGC-1α transcript levels.
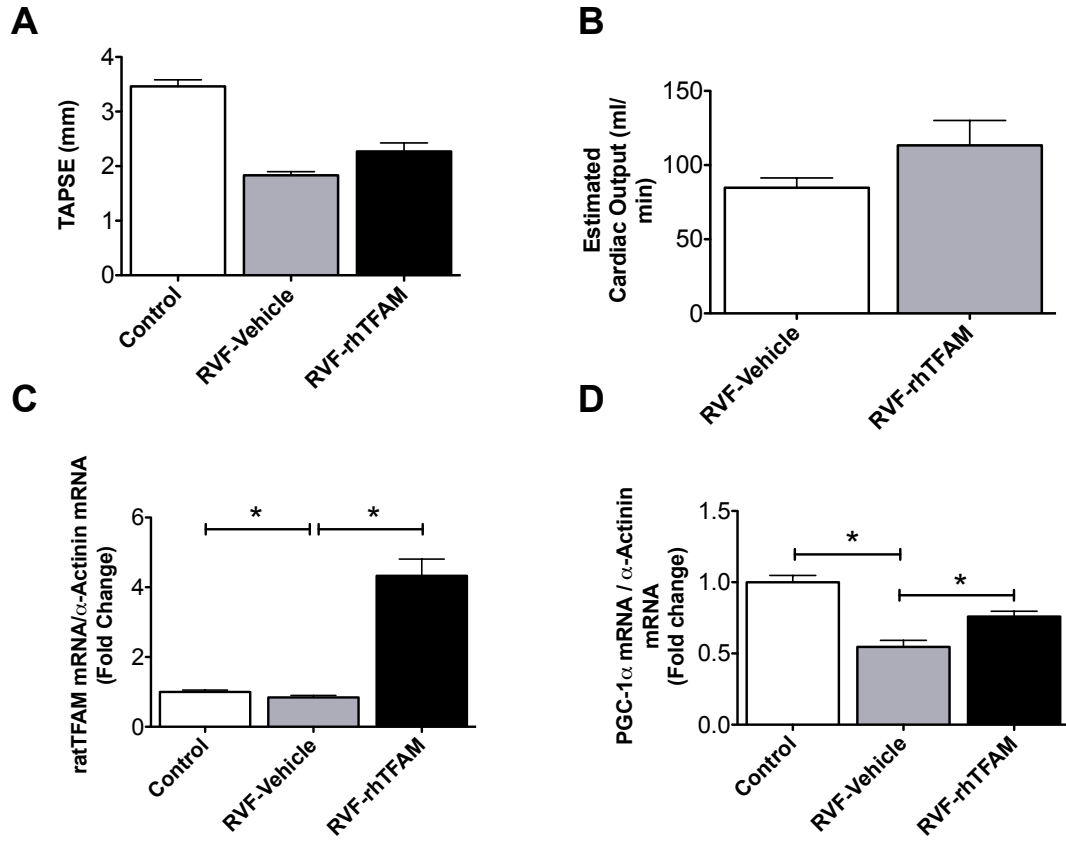
Figure 25.

Figure 25. Although not significant, treatment with rhTFAM was sufficient to improve the longitudinal contractility of the RV as assessed by tricuspid annular plane systolic excursion (TAPSE) and cardiac output (A and B). Furthermore, rhTFAM treatment significantly induced the gene expression of rat TFAM and PGC-1α, as evaluated by qPCR.

7.6 Treatment with the adrenergic receptor blocker carvedilol reverses the metabolic transcriptional profile and improves mitochondrial respiratory efficiency

We have reported that treatment with the non-selective adrenergic receptor antagonist carvedilol reverses established RVF in two different rat models of PAH (SU5416/hypoxia and monocrotaline-induced PAH), and that this improvement in RV function was associated with reduced hypertrophy and improved capillary density of the RV myocardium((26)). These changes were partially explained by an effect of carvedilol in the expression of genes that could be potentially relevant for the adaptive response of the RV to chronic pressure overload(26). However, the mechanisms by which carvedilol reverses maladaptive RV hypertrophy remain largely incomplete. Carvedilol has been shown to have pleiotrophic cardioprotective effects beyond heart-rate control. Indeed, a spectrum of anti-inflammatory, antioxidant, and anti-apoptotic actions of carvedilol have been reported in vitro and in vivo(135, 265). Based on microarray analysis, we have previously reported that RVF, in contrast to functional, compensated RV hypertrophy, is characterized by a distinct gene expression profile(55). The set of differentially expressed genes was designated "RVF-prediction set", and we speculated that these genes might play a critical role in the transition between adaptive hypertrophy and failure. Based on a similar approach, Drake and the rest of our group performed an in-depth array assessment to show that carvedilol treatment affects the expression of a number of genes from the RVF prediction set(56). An initial analysis of carvedilol-treated RVs showed that the gene expression profile mostly resembled that of the RVF tissue. However, an analysis beyond the boundaries of the prediction set revealed a small group of genes that were differentially expressed after carvedilol treatment (**Figure 26**).

137

In particular, we found a strong signal from mitochondrial dysfunction Ingenuity canonical pathway (**Figure 27A**). We examined the effect of carvedilol treatment on the expression of PGC-1α, ERR-α and PPAR-α, and their corresponding target genes and indeed found that carvedilol treatment restored PGC-1α, ERR-α, PPAR-α gene expression (**Figure 27B-C**), whereas the treatment with metoprolol had no effect on PGC-1α or PPAR-α gene expression. Furthermore, carvedilol treatment increased FAO genes expression towards control levels (**Figure 28A**).

Similar to what we did in Chapter 6, we measured respiration of mitochondria isolated from RV tissue obtained from rats treated with carvedilol. **Figure 28B** demonstrates that mitochondria obtained from SuHx-RVs had significantly reduced ADP/O ratio, which measures mitochondrial respiratory efficiency. A lower ADP/O ratio represents higher oxygen consumption per unit of ADP provided. Next, because impaired mitochondrial respiration would be reflected in decreased ATP production, we indirectly assessed decreased ATP levels by measuring the activation (phosphorylation) of the AMP-activated protein kinase (AMPK). Mammalian AMPK is sensitive to the cellular AMP/ATP ratio and is activated by metabolic stresses that inhibit ATP production (87). **Figure 28** illustrates that carvedilol treatment improved the mitochondrial ADP/O ratio and restored the protein levels of phosphorylated AMPK, which suggests that carvedilol treatment improves mitochondrial function and restores ATP levels.

Figure 26
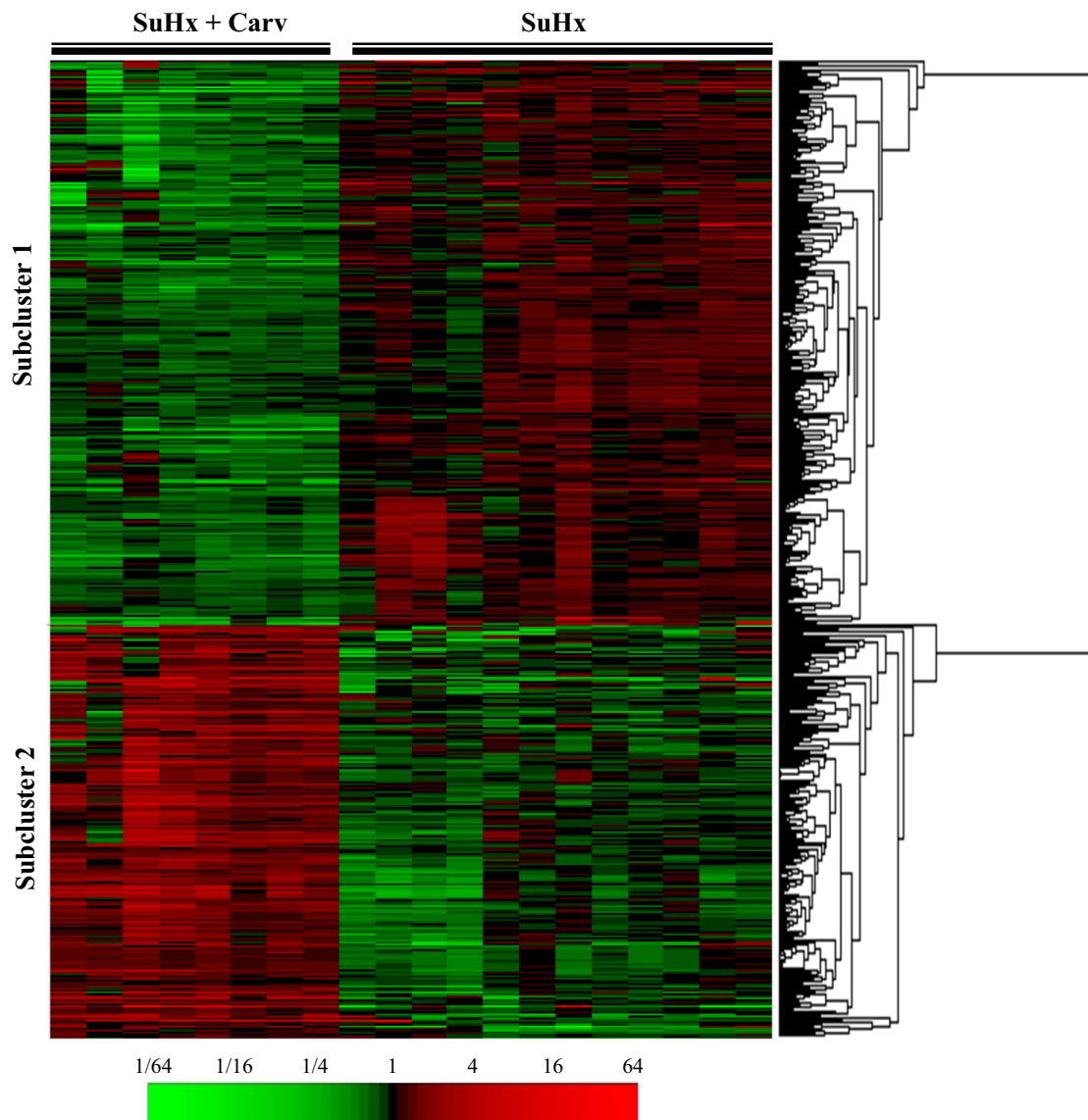
Figure 26. Cluster for class comparison analysis between SU5416/hypoxia RV (failure) and SU5416/hypoxia + carvedilol RV microarray data sets. 489 probes were called significant at an $\alpha < 0.001$ level and multivariate permutation testing gives a false discovery rate < 5%. Red represents greater relative expression than reference RNA, and green represents less relative expression than reference RNA. *Reproduced with permission from the publisher from Drake JI, Gomez-Arroyo JG, et al. Chronic carvedilol treatment partially reverses the right ventricular failure transcriptional profile in experimental pulmonary hypertension. Physiol. Genomics. 2013 Apr 30.*

Indeed, carvedilol treatment not only increased PGC-1α gene and protein expression but also the expression of PGC-1α co-activated nuclear receptors ERR-α and PPAR-α as well as their corresponding target genes and the fact that metoprolol, a selective β2 blocker, did not restore PGC-1α gene expression could suggest a β2 or perhaps an α receptor-dependent response. However, there are other pharmacological differences between metoprolol and carvedilol. As a G-coupled protein receptor, the adrenergic receptor can also bind non-classical intracellular proteins such as β-arrestins (53). The β-arrestin-dependent signaling is largely ligand dependent and, in contrast to metoprolol, carvedilol is a biased agonist that can transactivate different intracellular pathways (258). However, whether the effects of carvedilol treatment observed in this study are β-arrestin dependent remains unclear. Furthermore, it remains to be investigated whether carvedilol reversed the transcriptional profile by directly affecting PGC-1α expression or whether PGC-1α transcript levels and mitochondrial function normalized after carvedilol improved the overall cardiac function. Nevertheless, disregarding whether it is a cause or consequence, our findings are interesting, because they suggest that there are set of genes that normalize when RV failure is treated (including the mitochondrial function genes), suggesting that these genes and/or signaling pathways are indeed critical for the reversal of RV failure.

Conclusions

The first decade of the 21st century finds the community of PAH trialists and researchers in a peculiar situation: The available drugs have some impact on patient survival but do not alter the remodeled lung circulation and in contrast, effective treatments targeting the lung vessels could have detrimental effects on the failing RV. Because there are

contrasting priorities within the different cell populations of heart and lungs, the development of PAH treatments that both reduce pulmonary vascular resistance and improve RV function is not straightforward. For instance, we demonstrated that although treatment with resveratrol could have had beneficial effects on the RV, non-selective effects in other organs, such as the lung, could worsen the disease. Specific support of RV contractility can perhaps be accomplished directly with carvedilol or modulators of mitochondrial biology such as rhTFAM, but further investigations are warranted.

Figure 27
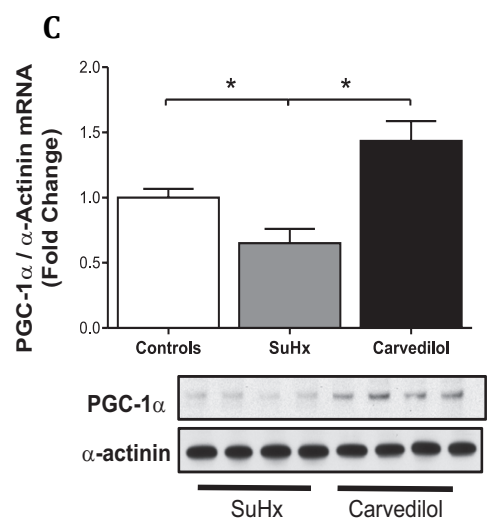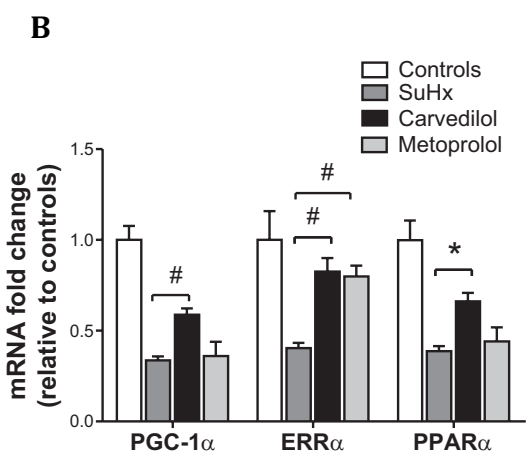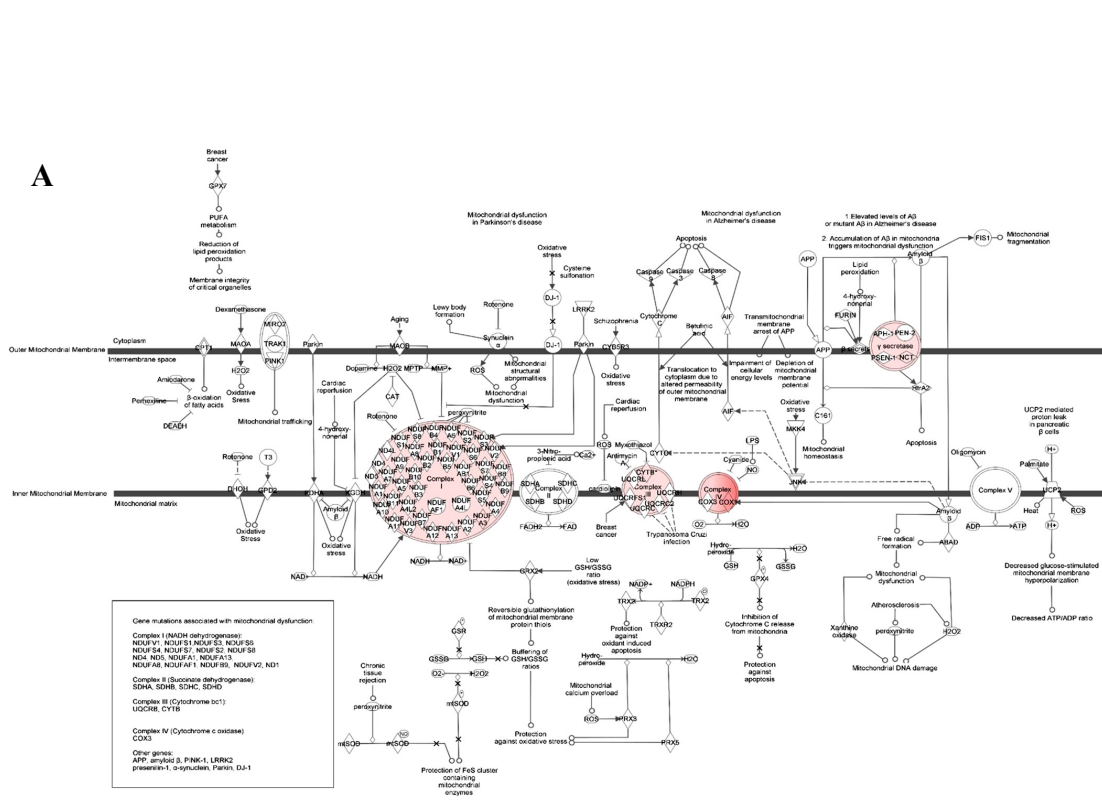
Figure 28
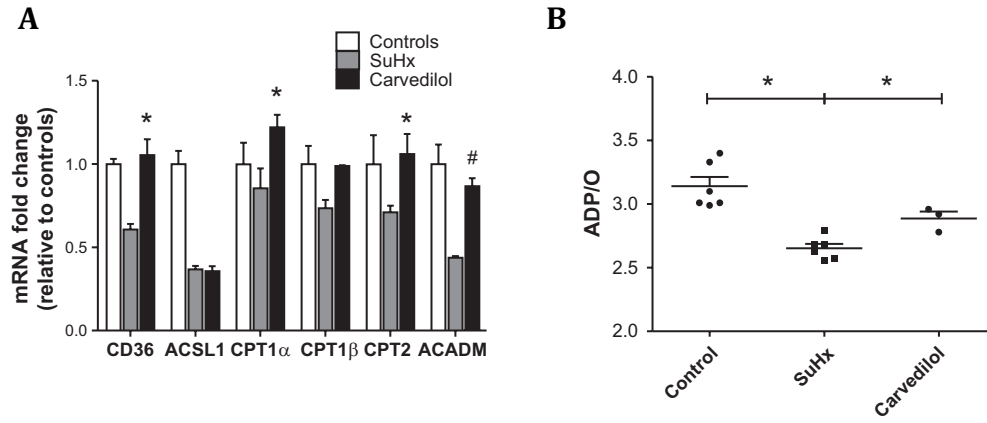
Figure 27: A) Canonical pathway analysis identified the pathways from the Ingenuity Pathway Analysis library of canonical pathways that were most significant to the dataset. Genes are colored based on fold-change comparison between the SU5416/hypoxia + carvedilol (treated) RV and the SU5416/Hypoxia (failing) RV. Red indicates a relatively higher expression in the treated RV than the failing RV, and green indicates a relatively higher expression in the failing RV than the treated. . **B)** Quantitative real-time PCR analysis of PPAR coactivator (PGC)-1α, estrogen-related receptor (ERR)-α, and peroxisome proliferator-activator receptor (PPAR)-α in control, 0.5 failing (SuHx), carvedilol-treated (carvedilol), and metoprolol-treated (metoprolol) RVs (*P <0.01, #P <0.001). *Reproduced with permission from the publisher from Drake JI, Gomez-Arroyo JG, et al. Chronic carvedilol treatment partially reverses the right ventricular failure transcriptional profile in experimental pulmonary hypertension. Physiol. Genomics. 2013 Apr 30*

Figure 28: A) Quantitative real- time PCR analysis of the PGC-1α downstream genes CD36, ACSL1, CPT1α, CPT1β, CPT2, and ACADM in control, failing (SuHx), and carvedilol-treated (carvedilol) RVs (*P <0.01, #P < 0.001). **B)** mitochondrial efficiency mea- sured as ADP/O ratio in control, failing (SuHx), and carvedilol-treated (carvedilol) RVs (*P <0.01).). *Reproduced with permission from the publisher from Drake JI, Gomez-Arroyo JG, et al. Chronic carvedilol treatment partially reverses the right ventricular failure transcriptional profile in experimental pulmonary hypertension. Physiol. Genomics. 2013 Apr 30*

8. SUMMARY OF THE DISSERTATION AND FUTURE DIRECTIONS

As mentioned throughout the dissertation, pulmonary arterial hypertension is a complex disease. However, the essence of the chapters of these thesis could be summarized in a few bullet points for any clinician or investigator interested in the study of PAH and the associated right ventricular failure:

1. Whereas the recent years have seen a dramatic increase in the number of publications regarding new pathobiological hypotheses, mechanistic studies, pre-clinical (experimental) trials and clinical studies evaluating biomarkers, mortality predictors and pharmacotherapies, PAH continues to be an incurable disease. Moreover, although multiple clinical trials and registries have demonstrated a shift in survival curves, the overall patient survival in the "modern era of targeted pharmacotherapies" remains incredibly low and the survival of "incident" PAH patients appears to be similar to that of the idiopathic PAH patients enrolled in the 1981-1991 NIH registry.

2. Patients with PAH (almost invariably) die from right ventricular failure. Therefore, characterizing and dissecting the mechanisms that underlie the transition between adaptive and maladaptive RV hypertrophy is critical for the development of new treatments. Current (and newly proposed) pharmacotherapies face a critical paradox: While the remodelled lung circulation in PAH is characterized by angiogenesis, apoptosis-resistance and cell proliferation, the failing RV suffers from ischemia, capillary rarefaction and cardiomyocyte

apoptosis, conditions that could be worsened by pharmacotherapy targeting the pulmonary vascular remodelling.

3. Current animal models of PAH are not perfect; however, far from being exclusive the animal models of chronic RV pressure-overload are complementary depending on what aspect of the disease the researcher is trying to reproduce.

4. Pressure overload might not be sufficient to drive the stressed right ventricle into failure. Although our study of patients with Eisenmenger syndrome does not provide a mechanism to explain the adaptation to pulmonary hypertension in these patients, it generates multiple hypotheses. Furthermore, the analyses of animal models of adaptive RV hypertrophy in the pulmonary artery banding rats suggest that load (pressure)-independent mechanisms contribute to the development of right ventricular failure.

5. Along with cardiomyocyte apoptosis, cardiac fibrosis, capillary rarefaction, right ventricular failure is characterized by load-independent, multilevel impairment of fatty acid oxidation and mitochondrial dysfunction. Whereas downregulation of PGC-1α could be responsible for the metabolic remodelling that we described in maladaptive right ventricular hypertrophy, further mechanistic studies are warranted. Contrary to what has been described for animal and human studies of left heart failure, we postulate that decreased fatty acid oxidation is secondary to a broader context of abnormal mitochondrial biology. Hence, metabolic modulators should focus on restoring the balance between mitochondrial biogenesis and turnover (mitophagy).

6. <u>We cannot definitely conclude whether metabolic remodelling is a cause or consequence of right ventricular failure</u>. However, the gene expression studies from rats treated with carvedilol, together with the metabolic transcriptional profile from animals with adaptive right ventricular hypertrophy after pulmonary artery banding, suggest that restoring fatty acids as the preferential substrate for the heart is indeed associated with compensated right ventricular function.

As predicted many questions remain, but perhaps the most important question that could be derived from our research work is: Can prevention of right ventricular dysfunction prolong life? The results presented in this dissertation suggests that there are indeed mechanisms of RV failure that can be targeted with the goal to preserve RV function in the setting of severe PAH.

- -

✂

List of Literature Cited

1.   **Abe K**, **Toba M**, **Alzoubi A**, **Ito M**, **Fagan KA**, **Cool CD**, **Voelkel NF**, **McMurtry IF**, **Oka M**. Formation of plexiform lesions in experimental severe pulmonary arterial hypertension. *Circulation* 121: 2747–2754, 2010.

2.   **Abe K**, **Toba M**, **Alzoubi A**, **Koubsky K**, **Ito M**, **Ota H**, **Gairhe S**, **Gerthoffer WT**, **Fagan KA**, **McMurtry IF**, **Oka M**. Tyrosine kinase inhibitors are potent acute pulmonary vasodilators in rats. *Am. J. Respir. Cell Mol. Biol.* 45: 804–808, 2011.

3.   **Abel ED**, **Doenst T**. Mitochondrial adaptations to physiological vs. pathological cardiac hypertrophy. *Cardiovasc Res* 90: 234–242, 2011.

4.   **Akhavein F**, **St-Michel EJ**, **Seifert E**, **Rohlicek CV**. Decreased left ventricular function, myocarditis, and coronary arteriolar medial thickening following monocrotaline administration in adult rats. *J Appl Physiol* 103: 287–295, 2007.

5.   **Alaynick WA**, **Kondo RP**, **Xie W**, **He W**, **Dufour CR**, **Downes M**, **Jonker JW**, **Giles W**, **Naviaux RK**, **Giguère V**, **Evans RM**. ERRgamma directs and maintains the transition to oxidative metabolism in the postnatal heart. *Cell Metab* 6: 13–24, 2007.

6. **Alcendor RR**, **Gao S**, **Zhai P**, **Zablocki D**, **Holle E**, **Yu X**, **Tian B**, **Wagner T**, **Vatner SF**, **Sadoshima J**. Sirt1 regulates aging and resistance to oxidative stress in the heart. *Circ Res* 100: 1512–1521, 2007.

7. **Alcendor RR**, **Kirshenbaum LA**, **Imai S-I**, **Vatner SF**, **Sadoshima J**. Silent information regulator 2alpha, a longevity factor and class III histone deacetylase, is an essential endogenous apoptosis inhibitor in cardiac myocytes. *Circ Res* 95: 971–980, 2004.

8. **Alvarez DF**, **Huang L**, **King JA**, **ElZarrad MK**, **Yoder MC**, **Stevens T**. Lung microvascular endothelium is enriched with progenitor cells that exhibit vasculogenic capacity. *Am J Physiol Lung Cell Mol Physiol* 294: L419–30, 2008.

9. **Ameshima S**, **Golpon H**, **Cool CD**, **Chan D**, **Vandivier RW**, **Gardai SJ**, **Wick M**, **Nemenoff RA**, **Geraci MW**, **Voelkel NF**. Peroxisome proliferator-activated receptor gamma (PPARgamma) expression is decreased in pulmonary hypertension and affects endothelial cell growth. *Circ Res* 92: 1162–1169, 2003.

10. **Arany Z**, **Foo S-Y**, **Ma Y**, **Ruas JL**, **Bommi-Reddy A**, **Girnun G**, **Cooper M**, **Laznik D**, **Chinsomboon J**, **Rangwala SM**, **Baek KH**, **Rosenzweig A**, **Spiegelman BM**. HIF-independent regulation of VEGF and angiogenesis by the transcriptional coactivator PGC-1alpha. *Nature* 451: 1008–1012, 2008.

11. **Arany Z**, **He H**, **Lin J**, **Hoyer K**, **Handschin C**, **Toka O**, **Ahmad F**, **Matsui T**, **Chin S**, **Wu P-H**, **Rybkin II**, **Shelton JM**, **Manieri M**, **Cinti S**, **Schoen FJ**, **Bassel-Duby R**, **Rosenzweig A**, **Ingwall JS**, **Spiegelman BM**. Transcriptional coactivator PGC-1

alpha controls the energy state and contractile function of cardiac muscle. *Cell Metab* 1: 259–271, 2005.

12. **Arany Z**, **Novikov M**, **Chin S**, **Ma Y**, **Rosenzweig A**, **Spiegelman BM**. Transverse aortic constriction leads to accelerated heart failure in mice lacking PPAR-gamma coactivator 1alpha. *Proc Natl Acad Sci USA* 103: 10086–10091, 2006.

13. **Archer S**, **Rich S**. Primary pulmonary hypertension: a vascular biology and translational research "Work in progress". *Circulation* 102: 2781–2791, 2000.

14. **Atkinson C**, **Stewart S**, **Upton PD**, **Machado R**, **Thomson JR**, **Trembath RC**, **Morrell NW**. Primary pulmonary hypertension is associated with reduced pulmonary vascular expression of type II bone morphogenetic protein receptor. *Circulation* 105: 1672–1678, 2002.

15. **Austin ED**, **Phillips JA**, **Cogan JD**, **Hamid R**, **Yu C**, **Stanton KC**, **Phillips CA**, **Wheeler LA**, **Robbins IM**, **Newman JH**, **Loyd JE**. Truncating and missense BMPR2 mutations differentially affect the severity of heritable pulmonary arterial hypertension. *Respir Res* 10: 87, 2009.

16. **Barger PM**, **Brandt JM**, **Leone TC**, **Weinheimer CJ**, **Kelly DP**. Deactivation of peroxisome proliferator-activated receptor-alpha during cardiac hypertrophic growth. *J Clin Invest* 105: 1723–1730, 2000.

17. **Barst RJ**, **Rubin LJ**, **Long WA**, **McGoon MD**, **Rich S**, **Badesch DB**, **Groves BM**, **Tapson VF**, **Bourge RC**, **Brundage BH**, **et al**. A comparison of continuous intravenous epoprostenol (prostacyclin) with conventional therapy for primary

pulmonary hypertension. The Primary Pulmonary Hypertension Study Group. *N Engl J Med* 334: 296–302, 1996.

18.   **Bartz RR**, **Suliman HB**, **Fu P**, **Welty-Wolf K**, **Carraway MS**, **MacGarvey NC**, **Withers CM**, **Sweeney TE**, **Piantadosi CA**. Staphylococcus aureus sepsis and mitochondrial accrual of the 8-oxoguanine DNA glycosylase DNA repair enzyme in mice. *Am J Respir Crit Care Med* 183: 226–233, 2011.

19.   **Baur JA**, **Pearson KJ**, **Price NL**, **Jamieson HA**, **Lerin C**, **Kalra A**, **Prabhu VV**, **Allard JS**, **Lopez-Lluch G**, **Lewis K**, **Pistell PJ**, **Poosala S**, **Becker KG**, **Boss O**, **Gwinn D**, **Wang M**, **Ramaswamy S**, **Fishbein KW**, **Spencer RG**, **Lakatta EG**, **Le Couteur D**, **Shaw RJ**, **Navas P**, **Puigserver P**, **Ingram DK**, **de Cabo R**, **Sinclair DA**. Resveratrol improves health and survival of mice on a high-calorie diet. *Nature* 444: 337–342, 2006.

20.   **Baybutt RC**, **Aziz SM**, **Fagerland JA**, **Olson JW**, **Gillespie MN**. Monocrotaline alters type II pneumocyte morphology and polyamine regulation. *Toxicol. Appl. Pharmacol.* 129: 188–195, 1994.

21.   **Benoist D**, **Stones R**, **Drinkhill M**, **Bernus O**, **White E**. Arrhythmogenic substrate in hearts of rats with monocrotaline-induced pulmonary hypertension and right ventricular hypertrophy. *Am J Physiol Heart Circ Physiol* 300: H2230–7, 2011.

22.   **Benza RL**, **Miller DP**, **Gomberg-Maitland M**, **Frantz RP**, **Foreman AJ**, **Coffey CS**, **Frost A**, **Barst RJ**, **Badesch DB**, **Elliott CG**, **Liou TG**, **McGoon MD**. Predicting survival in pulmonary arterial hypertension: insights from the Registry to Evaluate

Early and Long-Term Pulmonary Arterial Hypertension Disease Management (REVEAL). *Circulation* 122: 164–172, 2010.

23. **Bogaard HJ**, **Abe K**, **Vonk Noordegraaf A**, **Voelkel NF**. The right ventricle under pressure: cellular and molecular mechanisms of right-heart failure in pulmonary hypertension. *Chest* 135: 794–804, 2009.

24. **Bogaard HJ**, **Mizuno S**, **Al-Hussaini AA**, **Toldo S**, **Abbate A**, **Kraskauskas D**, **Kasper M**, **Natarajan R**, **Voelkel NF**. Suppression of histone deacetylases worsens right ventricular dysfunction after pulmonary artery banding in rats. *Am J Respir Crit Care Med* (February 4, 2011). doi: 10.1164/rccm.201007-1106OC.

25. **Bogaard HJ**, **Natarajan R**, **Henderson SC**, **Long CS**, **Kraskauskas D**, **Smithson L**, **Ockaili R**, **McCord JM**, **Voelkel NF**. Chronic pulmonary artery pressure elevation is insufficient to explain right heart failure. *Circulation* 120: 1951–1960, 2009.

26. **Bogaard HJ**, **Natarajan R**, **Mizuno S**, **Abbate A**, **Chang PJ**, **Chau VQ**, **Hoke NN**, **Kraskauskas D**, **Kasper M**, **Salloum FN**, **Voelkel NF**. Adrenergic receptor blockade reverses right heart remodeling and dysfunction in pulmonary hypertensive rats. *Am J Respir Crit Care Med* 182: 652–660, 2010.

27. **Bogaard HJ**, **Natarajan R**, **Mizuno S**, **Abbate A**, **Chang PJ**, **Chau VQ**, **Hoke NN**, **Kraskauskas D**, **Kasper M**, **Salloum FN**, **Voelkel NF**. Adrenergic receptor blockade reverses right heart remodeling and dysfunction in pulmonary hypertensive rats. *Am J Respir Crit Care Med* 182: 652–660, 2010.

28. **Bonelli M**, **Savitskaya A**, **Steiner CW**, **Rath E**, **Smolen JS**, **Scheinecker C**.

Phenotypic and functional analysis of CD4+ CD25- Foxp3+ T cells in patients with systemic lupus erythematosus. *J. Immunol.* 182: 1689–1695, 2009.

29.   **Brenner O**. PATHOLOGY OF THE VESSELS OF THE PULMONARY CIRCULATIONPART I. *Arch Intern Med*.

30.   **Bristow MR**, **Zisman LS**, **Lowes BD**, **Abraham WT**, **Badesch DB**, **Groves BM**, **Voelkel NF**, **Lynch DM**, **Quaife RA**. The pressure-overloaded right ventricle in pulmonary hypertension. *Chest* 114: 101S–106S, 1998.

31.   **Brock M**, **Trenkmann M**, **Gay RE**, **Michel BA**, **Gay S**, **Fischler M**, **Ulrich S**, **Speich R**, **Huber LC**. Interleukin-6 modulates the expression of the bone morphogenic protein receptor type II through a novel STAT3-microRNA cluster 17/92 pathway. *Circ Res* 104: 1184–1191, 2009.

32.   **Bruner LH**, **Carpenter LJ**, **Hamlow P**, **Roth RA**. Effect of a mixed function oxidase inducer and inhibitor on monocrotaline pyrrole pneumotoxicity. *Toxicol. Appl. Pharmacol.* 85: 416–427, 1986.

33.   **Buermans HPJ**, **Redout EM**, **Schiel AE**, **Musters RJP**, **Zuidwijk M**, **Eijk PP**, **van Hardeveld C**, **Kasanmoentalib S**, **Visser FC**, **Ylstra B**, **Simonides WS**. Microarray analysis reveals pivotal divergent mRNA expression profiles early in the development of either compensated ventricular hypertrophy or heart failure. *Physiol. Genomics* 21: 314–323, 2005.

34.   **Campian ME**, **Hardziyenka M**, **de Bruin K**, **van Eck-Smit BLF**, **de Bakker JMT**, **Verberne HJ**, **Tan HL**. Early inflammatory response during the development of right

ventricular heart failure in a rat model. *Eur J Heart Fail* 12: 653–658, 2010.

35. **Can MM**, **Kaymaz C**, **Tanboga IH**, **Tokgoz HC**, **Canpolat N**, **Turkyilmaz E**, **Sonmez K**, **Ozdemir N**. Increased Right Ventricular Glucose Metabolism in Patients With Pulmonary Arterial Hypertension. *Clinical Nuclear Medicine* 36: 743–748, 2011.

36. **Cantó C**, **Gerhart-Hines Z**, **Feige JN**, **Lagouge M**, **Noriega L**, **Milne JC**, **Elliott PJ**, **Puigserver P**, **Auwerx J**. AMPK regulates energy expenditure by modulating NAD+ metabolism and SIRT1 activity. *Nature* 458: 1056–1060, 2009.

37. **Casey DB**, **Badejo AM**, **Dhaliwal JS**, **Sikora JL**, **Fokin A**, **Golwala NH**, **Greco AJ**, **Murthy SN**, **Nossaman BD**, **Hyman AL**, **Kadowitz PJ**. Analysis of responses to the Rho-kinase inhibitor Y-27632 in the pulmonary and systemic vascular bed of the rat. *Am J Physiol Heart Circ Physiol* 299: H184–92, 2010.

38. **Chen Q**, **Moghaddas S**, **Hoppel CL**, **Lesnefsky EJ**. Ischemic defects in the electron transport chain increase the production of reactive oxygen species from isolated rat heart mitochondria. *Am J Physiol, Cell Physiol* 294: C460–6, 2008.

39. **Chen S**, **Rong M**, **Platteau A**, **Hehre D**, **Smith H**, **Ruiz P**, **Whitsett J**, **Bancalari E**, **Wu S**. CTGF disrupts alveolarization and induces pulmonary hypertension in neonatal mice: implication in the pathogenesis of severe bronchopulmonary dysplasia. *AJP: Lung Cellular and Molecular Physiology* 300: L330–40, 2011.

40. **Cool CD**, **Stewart JS**, **Werahera P**, **Miller GJ**, **Williams RL**, **Voelkel NF**, **Tuder RM**. Three-dimensional reconstruction of pulmonary arteries in plexiform pulmonary hypertension using cell-specific markers. Evidence for a dynamic and heterogeneous

process of pulmonary endothelial cell growth. *Am. J. Pathol.* 155: 411–419, 1999.

41. **Copple BL**, **Ganey PE**, **Roth RA**. Liver inflammation during monocrotaline hepatotoxicity. *Toxicology* 190: 155–169, 2003.

42. **Copple BL**, **Woolley B**, **Banes A**, **Ganey PE**, **Roth RA**. Anticoagulants prevent monocrotaline-induced hepatic parenchymal cell injury but not endothelial cell injury in the rat. *Toxicol. Appl. Pharmacol.* 180: 186–196, 2002.

43. **Copple BL**. Modes of Cell Death in Rat Liver after Monocrotaline Exposure. *Toxicological Sciences* 77: 172–182, 2003.

44. **Courboulin A**, **Paulin R**, **Giguère NJ**, **Saksouk N**, **Perreault T**, **Meloche J**, **Paquet ER**, **Biardel S**, **Provencher S**, **Côté J**, **Simard MJ**, **Bonnet S**. Role for miR-204 in human pulmonary arterial hypertension. *J Exp Med* 208: 535–548, 2011.

45. **Covas MI**, **Esquerda A**, **Garcia-Rico A**, **Mahy N**. Peripheral blood T-lymphocyte subsets in autoimmune thyroid disease. *J Investig Allergol Clin Immunol* 2: 131–135, 1992.

46. **Csiszar A**, **Labinskyy N**, **Olson S**, **Pinto JT**, **Gupte S**, **Wu JM**, **Hu F**, **Ballabh P**, **Podlutsky A**, **Losonczy G**, **de Cabo R**, **Mathew R**, **Wolin MS**, **Ungvari Z**. Resveratrol prevents monocrotaline-induced pulmonary hypertension in rats. *Hypertension* 54: 668–675, 2009.

47. **Culvenor CC**, **DANN AT**, **DICK AT**. Alkylation as the mechanism by which the hepatotoxic pyrrolizidine alkaloids act on cell nuclei. *Nature* 195: 570–573, 1962.

48.   **Culvenor CC**, **Edgar JA**, **Jago MV**, **Qutteridge A**, **Peterson JE**, **Smith LW**.
Hepato- and pneumotoxicity of pyrrolizidine alkaloids and derivatives in relation to
molecular structure. *Chem. Biol. Interact.* 12: 299–324, 1976.

49.   **D'Alonzo GE**, **Barst RJ**, **Ayres SM**, **Bergofsky EH**, **Brundage BH**, **Detre KM**,
Fishman AP, **Goldring RM**, **Groves BM**, **Kernis JT**. Survival in patients with
primary pulmonary hypertension. Results from a national prospective registry. *Ann
Intern Med* 115: 343–349, 1991.

50.   **Daley E**, **Emson C**, **Guignabert C**, **de Waal Malefyt R**, **Louten J**, **Kurup VP**,
Hogaboam C, **Taraseviciene-Stewart L**, **Voelkel NF**, **Rabinovitch M**, **Grunig E**,
Grunig G. Pulmonary arterial remodeling induced by a Th2 immune response. *J Exp
Med* 205: 361–372, 2008.

51.   **DeLeve LD**, **McCuskey RS**, **Wang X**, **Hu L**, **McCuskey MK**, **Epstein RB**, **Kanel
GC**. Characterization of a reproducible rat model of hepatic veno-occlusive disease.
Hepatology 29: 1779–1791, 1999.

52.   **Desquiret-Dumas V**, **Gueguen N**, **Leman G**, **Baron S**, **Nivet-Antoine V**, **Chupin S**,
Chevrollier A, **Vessieres E**, **Ayer A**, **Ferre M**, **Bonneau D**, **Henrion D**, **Reynier P**,
Procaccio V. Resveratrol Induces a Mitochondrial Complex I Dependent Increase in
NADH Oxidation Responsible for Sirtuin Activation in Liver Cells. *Journal of
Biological Chemistry* (October 31, 2013). doi: 10.1074/jbc.M113.466490.

53.   **Dewire SM**, **Violin JD**. Biased ligands for better cardiovascular drugs: dissecting g-
protein-coupled receptor pharmacology. *Circ Res* 109: 205–216, 2011.

54.   **Drake JI**, **Bogaard HJ**, **Mizuno S**, **Clifton B**, **Xie B**, **Gao Y**, **Dumur CI**, **Fawcett P**, **Voelkel NF**, **Natarajan R**. Molecular Signature of a Right Heart Failure Program in Chronic Severe Pulmonary Hypertension. *American journal of respiratory cell and molecular biology* (June 30, 2011). doi: 10.1165/rcmb.2010-0412OC.

55.   **Drake JI**, **Bogaard HJ**, **Mizuno S**, **Clifton B**, **Xie B**, **Gao Y**, **Dumur CI**, **Fawcett P**, **Voelkel NF**, **Natarajan R**. Molecular signature of a right heart failure program in chronic severe pulmonary hypertension. *Am. J. Respir. Cell Mol. Biol.* 45: 1239–1247, 2011.

56.   **Drake JI**, **Gomez-Arroyo JG**, **Dumur CI**, **Kraskauskas D**, **Natarajan R**, **Bogaard HJ**, **Fawcett P**, **Voelkel NF**. Chronic carvedilol treatment partially reverses the right ventricular failure transcriptional profile in experimental pulmonary hypertension. *Physiol. Genomics* (April 30, 2013). doi: 10.1152/physiolgenomics.00166.2012.

57.   **Drake KM**, **Zygmunt D**, **Mavrakis L**, **Harbor P**, **Wang L**, **Comhair SA**, **Erzurum SC**, **Aldred MA**. Altered MicroRNA processing in heritable pulmonary arterial hypertension: an important role for Smad-8. *Am J Respir Crit Care Med* 184: 1400–1408, 2011.

58.   **Dumitrascu R**, **Koebrich S**, **Dony E**, **Weissmann N**, **Savai R**, **Pullamsetti SS**, **Ghofrani HA**, **Samidurai A**, **Traupe H**, **Seeger W**, **Grimminger F**, **Schermuly RT**. Characterization of a murine model of monocrotaline pyrrole-induced acute lung injury. *BMC Pulm Med* 8: 25, 2008.

59.   **Elliott CG**, **Glissmeyer EW**, **Havlena GT**, **Carlquist J**, **McKinney JT**, **Rich S**,

McGoon MD, **Scholand MB**, **Kim M**, **Jensen RL**, **Schmidt JW**, **Ward K**. Relationship of BMPR2 mutations to vasoreactivity in pulmonary arterial hypertension. *Circulation* 113: 2509–2515, 2006.

60.   **Epstein RB**, **Min KW**, **Anderson SL**, **Syzek L**. A canine model for hepatic venoocclusive disease. *Transplantation* 54: 12–16, 1992.

61.   **Ergun S**, **Tilki D**, **Klein D**. Vascular wall as a reservoir for different types of stem and progenitor cells. *Antioxid. Redox Signal.* 15: 981–995, 2011.

62.   **Escribano-Subias P**, **Blanco I**, **López-Meseguer M**, **Jimenez Lopez-Guarch C**, **Roman A**, **Morales P**, **Castillo-Palma MJ**, **Segovia J**, **Gómez-Sanchez MA**, **Barberà JA**, **on behalf of the REHAP investigators**. Survival in pulmonary hypertension in spain insights from the spanish registry. *European Respiratory Journal* (February 23, 2012). doi: 10.1183/09031936.00101211.

63.   **Estep JE**, **Lamé MW**, **Morin D**, **Jones AD**, **Wilson DW**, **Segall HJ**. [14C]monocrotaline kinetics and metabolism in the rat. *Drug Metab. Dispos.* 19: 135–139, 1991.

64.   **Faber MJ**, **Dalinghaus M**, **Lankhuizen IM**, **Steendijk P**, **Hop WC**, **Schoemaker RG**, **Duncker DJ**, **Lamers JMJ**, **Helbing WA**. Right and left ventricular function after chronic pulmonary artery banding in rats assessed with biventricular pressure-volume loops. *Am J Physiol Heart Circ Physiol* 291: H1580–6, 2006.

65.   **Fang Y-H**, **Piao L**, **Hong Z**, **Toth PT**, **Marsboom G**, **Bache-Wiig P**, **Rehman J**, **Archer SL**. Therapeutic inhibition of fatty acid oxidation in right ventricular

160

hypertrophy: exploiting Randle's cycle. *J Mol Med* (August 28, 2011). doi: 10.1007/s00109-011-0804-9.

66. **Feige JN**, **Lagouge M**, **Cantó C**, **Strehle A**, **Houten SM**, **Milne JC**, **Lambert PD**, **Mataki C**, **Elliott PJ**, **Auwerx J**. Specific SIRT1 activation mimics low energy levels and protects against diet-induced metabolic disorders by enhancing fat oxidation. *Cell Metab* 8: 347–358, 2008.

67. **Finck BN**, **Kelly DP**. PGC-1 coactivators: inducible regulators of energy metabolism in health and disease. *J Clin Invest* 116: 615–622, 2006.

68. **Fong TA**, **Shawver LK**, **Sun L**, **Tang C**, **App H**, **Powell TJ**, **Kim YH**, **Schreck R**, **Wang X**, **Risau W**, **Ullrich A**, **Hirth KP**, **McMahon G**. SU5416 is a potent and selective inhibitor of the vascular endothelial growth factor receptor (Flk-1/KDR) that inhibits tyrosine kinase catalysis, tumor vascularization, and growth of multiple tumor types. *Cancer Res* 59: 99–106, 1999.

69. **Frost AE**, **Badesch DB**, **Barst RJ**, **Benza RL**, **Elliott CG**, **Farber HW**, **Krichman A**, **Liou TG**, **Raskob GE**, **Wason P**, **Feldkircher K**, **Turner M**, **McGoon MD**. The changing picture of patients with pulmonary arterial hypertension in the United States: how REVEAL differs from historic and non-US Contemporary Registries. *Chest* 139: 128–137, 2011.

70. **FULTON RM**, **HUTCHINSON EC**, **JONES AM**. Ventricular weight in cardiac hypertrophy. *British heart journal* 14: 413–420, 1952.

71. **Fuster V**, **Steele PM**, **Edwards WD**, **Gersh BJ**, **McGoon MD**, **Frye RL**. Primary

pulmonary hypertension: natural history and the importance of thrombosis. *Circulation* 70: 580–587, 1984.

72.   **Galiè N**, **Manes A**, **Negro L**, **Palazzini M**, **Bacchi-Reggiani ML**, **Branzi A**. A meta-analysis of randomized controlled trials in pulmonary arterial hypertension. *Eur Heart J* 30: 394–403, 2009.

73.   **Gerhart-Hines Z**, **Rodgers JT**, **Bare O**, **Lerin C**, **Kim S-H**, **Mostoslavsky R**, **Alt FW**, **Wu Z**, **Puigserver P**. Metabolic control of muscle mitochondrial function and fatty acid oxidation through SIRT1/PGC-1alpha. *EMBO J.* 26: 1913–1923, 2007.

74.   **Ghofrani HA**, **Morrell NW**, **Hoeper MM**, **Olschewski H**, **Peacock AJ**, **Barst RJ**, **Shapiro S**, **Golpon H**, **Toshner M**, **Grimminger F**, **Pascoe S**. Imatinib in pulmonary arterial hypertension patients with inadequate response to established therapy. *Am J Respir Crit Care Med* 182: 1171–1177, 2010.

75.   **Ghofrani HA**, **Seeger W**, **Grimminger F**. Imatinib for the treatment of pulmonary arterial hypertension. *N Engl J Med* 353: 1412–1413, 2005.

76.   **Girerd B**, **Montani D**, **Coulet F**, **Sztrymf B**, **Yaici A**, **Jais X**, **Tregouet D**, **Reis A**, **Drouin-Garraud V**, **Fraisse A**, **Sitbon O**, **O'Callaghan DS**, **Simonneau G**, **Soubrier F**, **Humbert M**. Clinical outcomes of pulmonary arterial hypertension in patients carrying an ACVRL1 (ALK1) mutation. *Am J Respir Crit Care Med* 181: 851–861, 2010.

77.   **Girerd B**, **Montani D**, **Eyries M**, **Yaici A**, **Sztrymf B**, **Coulet F**, **Sitbon O**, **Simonneau G**, **Soubrier F**, **Humbert M**. Absence of influence of gender and BMPR2

mutation type on clinical phenotypes of pulmonary arterial hypertension. *Respir Res* 11: 73, 2010.

78. **Gomberg-Maitland M**, **Maitland ML**, **Barst RJ**, **Sugeng L**, **Coslet S**, **Perrino TJ**, **Bond L**, **Lacouture ME**, **Archer SL**, **Ratain MJ**. A dosing/cross-development study of the multikinase inhibitor sorafenib in patients with pulmonary arterial hypertension. *Clin. Pharmacol. Ther.* 87: 303–310, 2010.

79. **Gomez-Arroyo J**, **Mizuno S**, **Szczepanek K**, **Van Tassell B**, **Natarajan R**, **Remedios Dos CG**, **Drake JI**, **Farkas L**, **Kraskauskas D**, **Wijesinghe DS**, **Chalfant CE**, **Bigbee J**, **Abbate A**, **Lesnefsky EJ**, **Bogaard HJ**, **Voelkel NF**. Metabolic Gene Remodeling and Mitochondrial Dysfunction in Failing Right Ventricular Hypertrophy due to Pulmonary Arterial Hypertension. *Circ Heart Fail* (November 14, 2012). doi: 10.1161/CIRCHEARTFAILURE.111.966127.

80. **Gomez-Arroyo JG**, **Farkas L**, **Alhussaini AA**, **Farkas D**, **Kraskauskas D**, **Voelkel NF**, **Bogaard HJ**. The Monocrotaline Model of Pulmonary Hypertension In Perspective. *AJP: Lung Cellular and Molecular Physiology* (September 30, 2011). doi: 10.1152/ajplung.00212.2011.

81. **Gomez-Arroyo JG**, **Farkas L**, **Alhussaini AA**, **Farkas D**, **Kraskauskas D**, **Voelkel NF**, **Bogaard HJ**. The monocrotaline model of pulmonary hypertension in perspective. *AJP: Lung Cellular and Molecular Physiology* 302: L363–9, 2012.

82. **Gomez-Arroyo JG**, **Saleem SJ**, **Mizuno S**, **Syded AA**, **Bogaard HJ**, **Abbate A**, **Taraseviciene-Stewart L**, **Sung Y**, **Kraskauskas D**, **Farkas D**, **Conrad DH**, **Nicolls**

163

MR, **Voelkel NF**. A Brief Overview of Mouse Models of Pulmonary Arterial Hypertension: Problems and Prospects. *AJP: Lung Cellular and Molecular Physiology* (February 3, 2012). doi: 10.1152/ajplung.00362.2011.

83.   **Gómez A**, **Bialostozky D**, **Zajarias A**, **Santos E**, **Palomar A**, **Martínez ML**, **Sandoval J**. Right ventricular ischemia in patients with primary pulmonary hypertension. *JAAC* 38: 1137–1142, 2001.

84.   **Gust R**, **Schuster DP**. Vascular remodeling in experimentally induced subacute canine pulmonary hypertension. *Exp. Lung Res.* 27: 1–12, 2001.

85.   **Haddad F**, **Hunt SA**, **Rosenthal DN**, **Murphy DJ**. Right ventricular function in cardiovascular disease, part I: Anatomy, physiology, aging, and functional assessment of the right ventricle. *Circulation* 117: 1436–1448, 2008.

86.   **Handoko ML**, **de Man FS**, **Happé CM**, **Schalij I**, **Musters RJP**, **Westerhof N**, **Postmus PE**, **Paulus WJ**, **van der Laarse WJ**, **Vonk-Noordegraaf A**. Opposite effects of training in rats with stable and progressive pulmonary hypertension. *Circulation* 120: 42–49, 2009.

87.   **Hardie DG**. AMP-activated/SNF1 protein kinases: conserved guardians of cellular energy. *Nat Rev Mol Cell Biol* 8: 774–785, 2007.

88.   **Hardziyenka M**, **Campian ME**, **de Bruin-Bon HACMR**, **Michel MC**, **Tan HL**. Sequence of echocardiographic changes during development of right ventricular failure in rat. *Journal of the American Society of Echocardiography : official publication of the American Society of Echocardiography* 19: 1272–1279, 2006.

89. **Hardziyenka M**, **Campian ME**, **Reesink HJ**, **Surie S**, **Bouma BJ**, **Groenink M**, **Klemens CA**, **Beekman L**, **Remme CA**, **Bresser P**, **Tan HL**. Right ventricular failure following chronic pressure overload is associated with reduction in left ventricular mass evidence for atrophic remodeling. *Journal of the American College of Cardiology* 57: 921–928, 2011.

90. **Hassoun PM**, **Mouthon L**, **Barberà JA**, **Eddahibi S**, **Flores SC**, **Grimminger F**, **Jones PL**, **Maitland ML**, **Michelakis ED**, **Morrell NW**, **Newman JH**, **Rabinovitch M**, **Schermuly R**, **Stenmark KR**, **Voelkel NF**, **Yuan JX-J**, **Humbert M**. Inflammation, growth factors, and pulmonary vascular remodeling. *Journal of the American College of Cardiology* 54: S10–9, 2009.

91. **Hayashi S**, **Mitsumori K**, **Imaida K**, **Imazawa T**, **Yasuhara K**, **Uneyama C**, **Hayashi Y**. Establishment of an animal model for pulmonary fibrosis in mice using monocrotaline. *Toxicol Pathol* 23: 63–71, 1995.

92. **Hein S**, **Arnon E**, **Kostin S**, **Schönburg M**, **Elsässer A**. Progression from compensated hypertrophy to failure in the pressure-overloaded human heart structural deterioration and compensatory mechanisms. *Circulation*.

93. **Hennigan S**, **Channick RN**, **Silverman GJ**. Rituximab treatment of pulmonary arterial hypertension associated with systemic lupus erythematosus: a case report. *Lupus* 17: 754–756, 2008.

94. **Hennigs JK**, **Keller G**, **Baumann HJ**, **Honecker F**, **Kluge S**, **Bokemeyer C**, **Brümmendorf TH**, **Klose H**. Multi tyrosine kinase inhibitor dasatinib as novel cause

of severe pre-capillary pulmonary hypertension? *BMC Pulm Med* 11: 30, 2011.

95.   **Holliday R**. Epigenetics: a historical overview. *Epigenetics* 1: 76–80, 2006.

96.   **Hopkins WE**, **Ochoa LL**, **Richardson GW**, **Trulock EP**. Comparison of the
hemodynamics and survival of adults with severe primary pulmonary hypertension or
Eisenmenger syndrome. *J Heart Lung Transplant* 15: 100–105, 1996.

97.   **Hopkins WE**. Severe pulmonary hypertension in congenital heart disease: a review of
Eisenmenger syndrome. *Curr Opin Cardiol* 10: 517–523, 1995.

98.   **Hopkins WE**. The remarkable right ventricle of patients with Eisenmenger syndrome.
Coron Artery Dis 16: 19–25, 2005.

99.   **Hsu C-P**, **Zhai P**, **Yamamoto T**, **Maejima Y**, **Matsushima S**, **Hariharan N**, **Shao D**,
Takagi H, **Oka S**, **Sadoshima J**. Silent information regulator 1 protects the heart from
ischemia/reperfusion. *Circulation* 122: 2170–2182, 2010.

100.   **Huang J**, **Wolk JH**, **Gewitz MH**, **Mathew R**. Progressive endothelial cell damage in
an inflammatory model of pulmonary hypertension. *Exp. Lung Res.* 36: 57–66, 2010.

101.   **Humbert M**, **Deng Z**, **Simonneau G**, **Barst RJ**, **Sitbon O**, **Wolf M**, **Cuervo N**,
Moore KJ, **Hodge SE**, **Knowles JA**, **Morse JH**. BMPR2 germline mutations in
pulmonary hypertension associated with fenfluramine derivatives. *Eur Respir J* 20:
518–523, 2002.

102.   **Humbert M**, **Khaltaev N**, **Bousquet J**, **Souza R**. Pulmonary hypertension: from an
orphan disease to a public health problem. *Chest* 132: 365–367, 2007.

103. **Humbert M**, **Monti G**, **Brenot F**, **Sitbon O**, **Portier A**, **Grangeot-Keros L**, **Duroux P**, **Galanaud P**, **Simonneau G**, **Emilie D**. Increased interleukin-1 and interleukin-6 serum concentrations in severe primary pulmonary hypertension. *Am J Respir Crit Care Med* 151: 1628–1631, 1995.

104. **Humbert M**, **Sitbon O**, **Chaouat A**, **Bertocchi M**, **Habib G**, **Gressin V**, **Yaici A**, **Weitzenblum E**, **Cordier J-F**, **Chabot F**, **Dromer C**, **Pison C**, **Reynaud-Gaubert M**, **Haloun A**, **Laurent M**, **Hachulla E**, **Cottin V**, **Degano B**, **Jais X**, **Montani D**, **Souza R**, **Simonneau G**. Survival in patients with idiopathic, familial, and anorexigen-associated pulmonary arterial hypertension in the modern management era. *Circulation* 122: 156–163, 2010.

105. **Humbert M**, **Sitbon O**, **Chaouat A**, **Bertocchi M**, **Habib G**, **Gressin V**, **Yaici A**, **Weitzenblum E**, **Cordier J-F**, **Chabot F**, **Dromer C**, **Pison C**, **Reynaud-Gaubert M**, **Haloun A**, **Laurent M**, **Hachulla E**, **Simonneau G**. Pulmonary arterial hypertension in France: results from a national registry. *Am J Respir Crit Care Med* 173: 1023–1030, 2006.

106. **Humbert M**, **Sitbon O**, **Simonneau G**. Treatment of pulmonary arterial hypertension. *N Engl J Med* 351: 1425–1436, 2004.

107. **Humbert M**, **Sitbon O**, **Yaici A**, **Montani D**, **O'Callaghan DS**, **Jais X**, **Parent F**, **Savale L**, **Natali D**, **Gunther S**, **Chaouat A**, **Chabot F**, **Cordier J-F**, **Habib G**, **Gressin V**, **Jing ZC**, **Souza R**, **Simonneau G**. Survival in incident and prevalent cohorts of patients with pulmonary arterial hypertension. *European Respiratory Journal* 36: 549–555, 2010.

108. **Huss JM**, **Imahashi K-I**, **Dufour CR**, **Weinheimer CJ**, **Courtois M**, **Kovacs A**, **Giguère V**, **Murphy E**, **Kelly DP**. The nuclear receptor ERRalpha is required for the bioenergetic and functional adaptation to cardiac pressure overload. *Cell Metab* 6: 25–37, 2007.

109. **Husseini Al A**, **Bagnato G**, **Farkas L**, **Gómez-Arroyo J**, **Farkas D**, **Mizuno S**, **Kraskauskas D**, **Abbate A**, **Van Tassel B**, **Voelkel NF**, **Bogaard HJ**. Thyroid hormone is highly permissive in angioproliferative pulmonary hypertension in rats. *European Respiratory Journal* 41: 104–114, 2012.

110. **Iyer S**, **Thomas RR**, **Portell FR**, **Dunham LD**, **Quigley CK**, **Bennett JP Jr**. Recombinant mitochondrial transcription factor A with N-terminal mitochondrial transduction domain increases respiration and mitochondrial gene expression. *Mitochondrion* 9: 196–203, 2009.

111. **Jais X**, **Launay D**, **Yaici A**, **Le Pavec J**, **Tchérakian C**, **Sitbon O**, **Simonneau G**, **Humbert M**. Immunosuppressive therapy in lupus- and mixed connective tissue disease-associated pulmonary arterial hypertension: a retrospective analysis of twenty-three cases. *Arthritis Rheum.* 58: 521–531, 2008.

112. **Kaga S**, **Zhan L**, **Matsumoto M**, **Maulik N**. Resveratrol enhances neovascularization in the infarcted rat myocardium through the induction of thioredoxin-1, heme oxygenase-1 and vascular endothelial growth factor. *Journal of molecular and cellular* ....

113. **Karamanlidis G**, **Nascimben L**, **Couper GS**, **Shekar PS**, **del Monte F**, **Tian R**.

Defective DNA replication impairs mitochondrial biogenesis in human failing hearts. *Circ Res* 106: 1541–1548, 2010.

114. **Kasahara Y**, **Kiyatake K**, **Tatsumi K**, **Sugito K**, **Kakusaka I**, **Yamagata S**, **Ohmori S**, **Kitada M**, **Kuriyama T**. Bioactivation of monocrotaline by P-450 3A in rat liver. *J. Cardiovasc. Pharmacol.* 30: 124–129, 1997.

115. **Kasahara Y**, **Tuder RM**, **Taraseviciene-Stewart L**, **Le Cras TD**, **Abman S**, **Hirth PK**, **Waltenberger J**, **Voelkel NF**. Inhibition of VEGF receptors causes lung cell apoptosis and emphysema. *J Clin Invest* 106: 1311–1319, 2000.

116. **Kato M**, **Kataoka H**, **Odani T**, **Fujieda Y**, **Otomo K**, **Oku K**, **Horita T**, **Yasuda S**, **Atsumi T**, **Ohira H**, **Tsujino I**, **Nishimura M**, **Koike T**. The short-term role of corticosteroid therapy for pulmonary arterial hypertension associated with connective tissue diseases: report of five cases and a literature review. *Lupus* 20: 1047–1056, 2011.

117. **Kay JM**, **Harris P**, **Heath D**. Pulmonary hypertension produced in rats by ingestion of Crotalaria spectabilis seeds. *Thorax* 22: 176–179, 1967.

118. **Kelly DP**, **Scarpulla RC**. Transcriptional regulatory circuits controlling mitochondrial biogenesis and function. *Genes Dev* 18: 357–368, 2004.

119. **Kim GH**, **Ryan JJ**, **Marsboom G**, **Archer SL**. Epigenetic mechanisms of pulmonary hypertension. *Pulm Circ* 1: 347–356, 2011.

120. **Kim JM**, **Rasmussen JP**, **Rudensky AY**. Regulatory T cells prevent catastrophic

autoimmunity throughout the lifespan of mice. *Nat Immunol* 8: 191–197, 2007.

121.   **Kim Y**, **Goto H**, **Kobayashi K**, **Sawada Y**, **Miyake Y**, **Fujiwara G**, **Chiba H**,

        Okada T, **Nishimura T**. Detection of impaired fatty acid metabolism in right

        ventricular hypertrophy: assessment by I-123 beta-methyl iodophenyl pentadecanoic

        acid (BMIPP) myocardial single-photon emission computed tomography. *Ann Nucl

        Med* 11: 207–212, 1997.

122.   **Klein M**, **Schermuly RT**, **Ellinghaus P**, **Milting H**, **Riedl B**, **Nikolova S**, **Pullamsetti

        SS**, **Weissmann N**, **Dony E**, **Savai R**, **Ghofrani HA**, **Grimminger F**, **Busch AE**,

        Schäfer S. Combined tyrosine and serine/threonine kinase inhibition by sorafenib

        prevents progression of experimental pulmonary hypertension and myocardial

        remodeling. *Circulation* 118: 2081–2090, 2008.

123.   **Kurozumi T**, **Tanaka K**, **Kido M**, **Shoyama Y**. Monocrotaline-induced renal lesions.

        Exp. Mol. Pathol. 39: 377–386, 1983.

124.   **Lai YL**, **Olson JW**, **Gillespie MN**. Ventilatory dysfunction precedes pulmonary

        vascular changes in monocrotaline-treated rats. *J Appl Physiol* 70: 561–566, 1991.

125.   **LALICH JJ**, **MERKOW L**. Pulmonary arteritis produced in rat by feeding Crotalaria

        spectabilis. *Lab. Invest.* 10: 744–750, 1961.

126.   **Lalich JL**, **Johnson WD**, **Raczniak TJ**, **Shumaker RC**. Fibrin thrombosis in

        monocrotaline pyrrole-induced cor pulmonale in rats. *Arch. Pathol. Lab. Med.* 101:

        69–73, 1977.

127.   **Lang I**, **Kneussl M**, **Frank H**, **Mlczoch J**. [Long-term follow-up of pulmonary hypertension of unknown etiology]. *Pneumologie* 44: 913–914, 1990.

128.   **Lee J**, **Reich R**, **Xu F**, **Sehgal PB**. Golgi, trafficking, and mitosis dysfunctions in pulmonary arterial endothelial cells exposed to monocrotaline pyrrole and NO scavenging. *AJP: Lung Cellular and Molecular Physiology* 297: L715–28, 2009.

129.   **Lee SD**, **Shroyer KR**, **Markham NE**, **Cool CD**, **Voelkel NF**, **Tuder RM**. Monoclonal endothelial cell proliferation is present in primary but not secondary pulmonary hypertension. *J Clin Invest* 101: 927–934, 1998.

130.   **Lehman JJ**, **Barger PM**, **Kovacs A**, **Saffitz JE**, **Medeiros DM**, **Kelly DP**. Peroxisome proliferator-activated receptor gamma coactivator-1 promotes cardiac mitochondrial biogenesis. *J Clin Invest* 106: 847–856, 2000.

131.   **Lehman JJ**, **Boudina S**, **Banke NH**, **Sambandam N**, **Han X**, **Young DM**, **Leone TC**, **Gross RW**, **Lewandowski ED**, **Abel ED**, **Kelly DP**. The transcriptional coactivator PGC-1alpha is essential for maximal and efficient cardiac mitochondrial fatty acid oxidation and lipid homeostasis. *Am J Physiol Heart Circ Physiol* 295: H185–96, 2008.

132.   **Lesnefsky EJ**, **Tandler B**, **Ye J**, **Slabe TJ**, **Turkaly J**, **Hoppel CL**. Myocardial ischemia decreases oxidative phosphorylation through cytochrome oxidase in subsarcolemmal mitochondria. *Am. J. Physiol.* 273: H1544–54, 1997.

133.   **Lopaschuk GD**, **Wall SR**, **Olley PM**, **Davies NJ**. Etomoxir, a carnitine palmitoyltransferase I inhibitor, protects hearts from fatty acid-induced ischemic injury

independent of changes in long chain acylcarnitine. *Circ Res* 63: 1036–1043, 1988.

134. **LOWRY OH**, **ROSEBROUGH NJ**, **FARR AL**, **RANDALL RJ**. Protein
measurement with the Folin phenol reagent. *J Biol Chem* 193: 265–275, 1951.

135. **Ma XL**, **Yue TL**, **Lopez BL**, **Barone FC**, **Christopher TA**, **Ruffolo RR**, **Feuerstein
GZ**. Carvedilol, a new beta adrenoreceptor blocker and free radical scavenger,
attenuates myocardial ischemia-reperfusion injury in hypercholesterolemic rabbits. *J
Pharmacol Exp Ther* 277: 128–136, 1996.

136. **Machado RD**, **Eickelberg O**, **Elliott CG**, **Geraci MW**, **Hanaoka M**, **Loyd JE**,
Newman JH, **Phillips JA**, **Soubrier F**, **Trembath RC**, **Chung WK**. Genetics and
genomics of pulmonary arterial hypertension. *Journal of the American College of
Cardiology* 54: S32–42, 2009.

137. **Machado RD**, **Pauciulo MW**, **Thomson JR**, **Lane KB**, **Morgan NV**, **Wheeler L**,
Phillips JA, **Newman J**, **Williams D**, **Galiè N**, **Manes A**, **McNeil K**, **Yacoub M**,
Mikhail G, **Rogers P**, **Corris P**, **Humbert M**, **Donnai D**, **Martensson G**,
Tranebjaerg L, **Loyd JE**, **Trembath RC**, **Nichols WC**. BMPR2 haploinsufficiency
as the inherited molecular mechanism for primary pulmonary hypertension. *Am J Hum
Genet* 68: 92–102, 2001.

138. **Maioli MA**, **Alves LC**, **Perandin D**, **Garcia AF**, **Pereira FTV**, **Mingatto FE**.
Cytotoxicity of monocrotaline in isolated rat hepatocytes: Effects of dithiothreitol and
fructose. *Toxicon* (April 21, 2011). doi: 10.1016/j.toxicon.2011.04.010.

139. **Mandl T**, **Bredberg A**, **Jacobsson LT**, **Manthorpe R**, **Henriksson G**. CD4+ T-

172

lymphocytopenia--a frequent finding in anti-SSA antibody seropositive patients with primary Sjogren's syndrome. *J. Rheumatol.* 31: 726–728, 2004.

140.   **May D**, **Gilon D**, **Djonov V**, **Itin A**, **Lazarus A**, **Gordon O**, **Rosenberger C**, **Keshet E**. Transgenic system for conditional induction and rescue of chronic myocardial hibernation provides insights into genomic programs of hibernation. *Proc Natl Acad Sci USA* 105: 282–287, 2008.

141.   **McMurtry MS**, **Archer SL**, **Altieri DC**, **Bonnet S**, **Haromy A**, **Harry G**, **Bonnet S**, **Puttagunta L**, **Michelakis ED**. Gene therapy targeting survivin selectively induces pulmonary vascular apoptosis and reverses pulmonary arterial hypertension. *J Clin Invest* 115: 1479–1491, 2005.

142.   **MINGATTO F**, **MAIOLI M**, **BRACHT A**, **ISHIIIWAMOTO E**. Effects of monocrotaline on energy metabolism in the rat liver. *Toxicology Letters* 182: 115–120, 2008.

143.   **Mitani Y**, **Maruyama K**, **Sakurai M**. Prolonged administration of L-arginine ameliorates chronic pulmonary hypertension and pulmonary vascular remodeling in rats. *Circulation* 96: 689–697, 1997.

144.   **Miura M**, **Hirose M**, **Endoh H**, **Wakayama Y**, **Sugai Y**, **Nakano M**, **Fukuda K**, **Shindoh C**, **Shirato K**, **Shimokawa H**. Acceleration of ca(2+) waves in monocrotaline-induced right ventricular hypertrophy in the rat. *Circ J* 75: 1343–1349, 2011.

145.   **Molteni A**, **Ward WF**, **Ts'ao CH**, **Solliday NH**, **Dunne M**. Monocrotaline-induced

pulmonary fibrosis in rats: amelioration by captopril and penicillamine. *Proc. Soc. Exp. Biol. Med.* 180: 112–120, 1985.

146.   **Molteni A**, **Ward WF**, **Ts'ao CH**, **Solliday NH**. Monocrotaline-induced cardiopulmonary damage in rats: amelioration by the angiotensin-converting enzyme inhibitor CL242817. *Proc. Soc. Exp. Biol. Med.* 182: 483–493, 1986.

147.   **Montani D**, **Bergot E**, **Günther S**, **Savale L**, **Bergeron A**, **Bourdin A**, **Bouvaist H**, **Canuet M**, **Pison C**, **Macro M**, **Poubeau P**, **Girerd B**, **Natali D**, **Guignabert C**, **Perros F**, **O'Callaghan DS**, **Jais X**, **Tubert-Bitter P**, **Zalcman G**, **Sitbon O**, **Simonneau G**, **Humbert M**. Pulmonary Arterial Hypertension in Patients Treated by Dasatinib. *Circulation* (March 26, 2012). doi: 10.1161/CIRCULATIONAHA.111.079921.

148.   **Montani D**, **Perros F**, **Gambaryan N**, **Girerd B**, **Dorfmuller P**, **Price LC**, **Huertas A**, **Hammad H**, **Lambrecht B**, **Simonneau G**, **Launay J-M**, **Cohen-Kaminsky S**, **Humbert M**. C-Kit-Positive Cells Accumulate in Remodeled Vessels of Idiopathic Pulmonary Arterial Hypertension. *Am J Respir Crit Care Med* 184: 116–123, 2011.

149.   **Morrell NW**, **Adnot S**, **Archer SL**, **Dupuis J**, **Jones PL**, **MacLean MR**, **McMurtry IF**, **Stenmark KR**, **Thistlethwaite PA**, **Weissmann N**, **Yuan JX-J**, **Weir EK**. [no date].

150.   **Morrell NW**. Pulmonary hypertension due to BMPR2 mutation: a new paradigm for tissue remodeling? *Proc Am Thorac Soc* 3: 680–686, 2006.

151.   **Morrow JD**, **Frei B**, **Longmire AW**, **Gaziano JM**, **Lynch SM**, **Shyr Y**, **Strauss WE**,

Oates JA, **Roberts LJ**. Increase in circulating products of lipid peroxidation (F2-isoprostanes) in smokers. Smoking as a cause of oxidative damage. *N Engl J Med* 332: 1198–1203, 1995.

152. **Nagendran J**, **Gurtu V**, **Fu DZ**, **Dyck JRB**, **Haromy A**, **Ross DB**, **Rebeyka IM**, **Michelakis ED**. A dynamic and chamber-specific mitochondrial remodeling in right ventricular hypertrophy can be therapeutically targeted. *The Journal of Thoracic and Cardiovascular Surgery* 136: 168–78– 178.e1–3, 2008.

153. **Nakagawa T**, **Guarente L**. Sirtuins at a glance. *J. Cell. Sci.* 124: 833–838, 2011.

154. **Nakayama Wong LS**, **Lamé MW**, **Jones AD**, **Wilson DW**. Differential cellular responses to protein adducts of naphthoquinone and monocrotaline pyrrole. *Chem. Res. Toxicol.* 23: 1504–1513, 2010.

155. **Nasim MT**, **Ogo T**, **Ahmed M**, **Randall R**, **Chowdhury HM**, **Snape KM**, **Bradshaw TY**, **Southgate L**, **Lee GJ**, **Jackson I**, **Lord GM**, **Gibbs JSR**, **Wilkins MR**, **Ohta-Ogo K**, **Nakamura K**, **Girerd B**, **Coulet F**, **Soubrier F**, **Humbert M**, **Morrell NW**, **Trembath RC**, **Machado RD**. Molecular genetic characterization of SMAD signaling molecules in pulmonary arterial hypertension. *Hum. Mutat.* 32: 1385–1389, 2011.

156. **Neubauer S**. The failing heart--an engine out of fuel. *N Engl J Med* 356: 1140–1151, 2007.

157. **Newman JH**, **Wheeler L**, **Lane KB**, **Loyd E**, **Gaddipati R**, **Phillips JA**, **Loyd JE**. Mutation in the gene for bone morphogenetic protein receptor II as a cause of primary pulmonary hypertension in a large kindred. *N Engl J Med* 345: 319–324, 2001.

158. **Nicolls MR**, **Taraseviciene-Stewart L**, **Rai PR**, **Badesch DB**, **Voelkel NF**.
Autoimmunity and pulmonary hypertension: a perspective. *Eur Respir J* 26: 1110–
1118, 2005.

159. **Nishimura T**, **Faul JL**, **Berry GJ**, **Vaszar LT**, **Qiu D**, **Pearl RG**, **Kao PN**.
Simvastatin attenuates smooth muscle neointimal proliferation and pulmonary
hypertension in rats. *Am J Respir Crit Care Med* 166: 1403–1408, 2002.

160. **O'Callaghan DS**, **Savale L**, **Montani D**, **Jais X**, **Sitbon O**, **Simonneau G**, **Humbert
M**. Treatment of pulmonary arterial hypertension with targeted therapies. *Nat Rev
Cardiol* 8: 526–538, 2011.

161. **Oikawa M**, **Kagaya Y**, **Otani H**, **Sakuma M**, **Demachi J**, **Suzuki J**, **Takahashi T**,
Nawata J, **Ido T**, **Watanabe J**, **Shirato K**. Increased [18F]fluorodeoxyglucose
accumulation in right ventricular free wall in patients with pulmonary hypertension and
the effect of epoprostenol. *Journal of the American College of Cardiology* 45: 1849–
1855, 2005.

162. **Oka M**, **Homma N**, **Taraseviciene-Stewart L**, **Morris KG**, **Kraskauskas D**, **Burns
N**, **Voelkel NF**, **McMurtry IF**. Rho kinase-mediated vasoconstriction is important in
severe occlusive pulmonary arterial hypertension in rats. *Circ Res* 100: 923–929, 2007.

163. **Oka T**, **Hikoso S**, **Yamaguchi O**, **Taneike M**, **Takeda T**, **Tamai T**, **Oyabu J**,
Murakawa T, **Nakayama H**, **Nishida K**, **Akira S**, **Yamamoto A**, **Komuro I**, **Otsu
K**. Mitochondrial DNA that escapes from autophagy causes inflammation and heart
failure. *Nature* 485: 251–255, 2012.

164. **Okada K**, **Tanaka Y**, **Bernstein M**, **Zhang W**, **Patterson GA**, **Botney MD**. Pulmonary hemodynamics modify the rat pulmonary artery response to injury. A neointimal model of pulmonary hypertension. *Am. J. Pathol.* 151: 1019–1025, 1997.

165. **Overbeek MJ**, **Mouchaers KTB**, **Niessen HM**, **Hadi AM**, **Kupreishvili K**, **Boonstra A**, **Voskuyl AE**, **Belien JAM**, **Smit EF**, **Dijkmans BC**, **Vonk Noordegraaf A**, **Grünberg K**. Characteristics of interstitial fibrosis and inflammatory cell infiltration in right ventricles of systemic sclerosis-associated pulmonary arterial hypertension. *International Journal of Rheumatology* 2010, 2010.

166. **Pan LC**, **Lamé MW**, **Morin D**, **Wilson DW**, **Segall HJ**. Red blood cells augment transport of reactive metabolites of monocrotaline from liver to lung in isolated and tandem liver and lung preparations. *Toxicol. Appl. Pharmacol.* 110: 336–346, 1991.

167. **Papo T**, **Piette JC**, **Legac E**, **Frances C**, **Grenot P**, **Debre P**, **Godeau P**, **Autran B**. T lymphocyte subsets in primary antiphospholipid syndrome. *J. Rheumatol.* 21: 2242–2245, 1994.

168. **Partovian C**, **Adnot S**, **Eddahibi S**, **Teiger E**, **Levame M**, **Dreyfus P**, **Raffestin B**, **Frelin C**. Heart and lung VEGF mRNA expression in rats with monocrotaline- or hypoxia-induced pulmonary hypertension. *Am. J. Physiol.* 275: H1948–56, 1998.

169. **Peacock AJ**, **Murphy NF**, **McMurray JJV**, **Caballero L**, **Stewart S**. An epidemiological study of pulmonary arterial hypertension. *Eur Respir J* 30: 104–109, 2007.

170. **Perazzo J**, **Eizayaga F**, **Romay S**, **Bengochea L**, **Pavese A**, **Lemberg A**. An

experimental model of liver damage and portal hypertension induced by a single dose of monocrotaline. *Hepatogastroenterology* 46: 432–435, 1999.

171. **Perros F**, **Dorfmuller P**, **Montani D**, **Hammad H**, **Waelput W**, **Girerd B**, **Raymond N**, **Mercier O**, **Mussot S**, **Cohen-Kaminsky S**, **Humbert M**, **Lambrecht BN**. Pulmonary Lymphoid Neogenesis in Idiopathic Pulmonary Arterial Hypertension. *Am J Respir Crit Care Med* (November 22, 2011). doi: 10.1164/rccm.201105-0927OC.

172. **Perros F**, **Dorfmuller P**, **Souza R**, **Durand-Gasselin I**, **Mussot S**, **Mazmanian M**, **Herve P**, **Emilie D**, **Simonneau G**, **Humbert M**. Dendritic cell recruitment in lesions of human and experimental pulmonary hypertension. *Eur Respir J* 29: 462–468, 2007.

173. **Perros F**, **Montani D**, **Dorfmuller P**, **Durand-Gasselin I**, **Tcherakian C**, **Le Pavec J**, **Mazmanian M**, **Fadel E**, **Mussot S**, **Mercier O**, **Herve P**, **Emilie D**, **Eddahibi S**, **Simonneau G**, **Souza R**, **Humbert M**. Platelet-derived growth factor expression and function in idiopathic pulmonary arterial hypertension. *Am J Respir Crit Care Med* 178: 81–88, 2008.

174. **Petry TW**, **Bowden GT**, **Huxtable RJ**, **Sipes IG**. Characterization of hepatic DNA damage induced in rats by the pyrrolizidine alkaloid monocrotaline. *Cancer Res* 44: 1505–1509, 1984.

175. **Pfarr N**, **Szamalek-Hoegel J**, **Fischer C**, **Hinderhofer K**, **Nagel C**, **Ehlken N**, **Tiede H**, **Olschewski H**, **Reichenberger F**, **Ghofrani AH**, **Seeger W**, **Grünig E**. Hemodynamic and clinical onset in patients with hereditary pulmonary arterial hypertension and BMPR2 mutations. *Respir Res* 12: 99, 2011.

176. **Piao L**, **Fang Y-H**, **Cadete VJJ**, **Wietholt C**, **Urboniene D**, **Toth PT**, **Marsboom G**, **Zhang HJ**, **Haber I**, **Rehman J**, **Lopaschuk GD**, **Archer SL**. The inhibition of pyruvate dehydrogenase kinase improves impaired cardiac function and electrical remodeling in two models of right ventricular hypertrophy: resuscitating the hibernating right ventricle. *J Mol Med* 88: 47–60, 2010.

177. **Piao L**, **Marsboom G**, **Archer SL**. Mitochondrial metabolic adaptation in right ventricular hypertrophy and failure. *J Mol Med* 88: 1011–1020, 2010.

178. **Pontén F**, **Gry M**, **Fagerberg L**, **Lundberg E**, **Asplund A**, **Berglund L**, **Oksvold P**, **Björling E**, **Hober S**, **Kampf C**, **Navani S**, **Nilsson P**, **Ottosson J**, **Persson A**, **Wernérus H**, **Wester K**, **Uhlén M**. A global view of protein expression in human cells, tissues, and organs. *Mol. Syst. Biol.* 5: 337, 2009.

179. **Puigserver P**, **Spiegelman BM**. Peroxisome proliferator-activated receptor-gamma coactivator 1 alpha (PGC-1 alpha): transcriptional coactivator and metabolic regulator. *Endocr Rev* 24: 78–90, 2003.

180. **Pullamsetti SS**, **Doebele C**, **Fischer A**, **Savai R**, **Kojonazarov B**, **Dahal BK**, **Ghofrani HA**, **Weissmann N**, **Grimminger F**, **Bonauer A**, **Seeger W**, **Zeiher AM**, **Dimmeler S**, **Schermuly RT**. Inhibition of microRNA-17 Improves Lung and Heart Function in Experimental Pulmonary Hypertension. *Am J Respir Crit Care Med* (December 8, 2011). doi: 10.1164/rccm.201106-1093OC.

181. **Rabinovitch M**. Molecular pathogenesis of pulmonary arterial hypertension. *J Clin Invest* 118: 2372–2379, 2008.

182. **Radstake TR**, **van Bon L**, **Broen J**, **Wenink M**, **Santegoets K**, **Deng Y**, **Hussaini A**, **Simms R**, **Cruikshank WW**, **Lafyatis R**. Increased frequency and compromised function of T regulatory cells in systemic sclerosis (SSc) is related to a diminished CD69 and TGFbeta expression. *PLoS ONE* 4: e5981, 2009.

183. **Rai PR**, **Cool CD**, **King JAC**, **Stevens T**, **Burns N**, **Winn RA**, **Kasper M**, **Voelkel NF**. The cancer paradigm of severe pulmonary arterial hypertension. *Am J Respir Crit Care Med* 178: 558–564, 2008.

184. **Ramos M**, **Lamé MW**, **Segall HJ**, **Wilson DW**. Monocrotaline pyrrole induces Smad nuclear accumulation and altered signaling expression in human pulmonary arterial endothelial cells. *Vascul. Pharmacol.* 46: 439–448, 2007.

185. **Reddy S**, **Zhao M**, **Hu DQ**, **Fajardo G**. Dynamic microRNA expression during the transition from right ventricular hypertrophy to failure. *Physiological ….*

186. **Rehman J**, **Archer SL**. A proposed mitochondrial-metabolic mechanism for initiation and maintenance of pulmonary arterial hypertension in fawn-hooded rats: the Warburg model of pulmonary arterial hypertension. *Adv. Exp. Med. Biol.* 661: 171–185, 2010.

187. **Reid MJ**, **Lamé MW**, **Morin D**, **Wilson DW**, **Segall HJ**. Involvement of cytochrome P450 3A in the metabolism and covalent binding of 14C-monocrotaline in rat liver microsomes. *J. Biochem. Mol. Toxicol.* 12: 157–166, 1998.

188. **Reindel JF**, **Ganey PE**, **Wagner JG**, **Slocombe RF**, **Roth RA**. Development of morphologic, hemodynamic, and biochemical changes in lungs of rats given monocrotaline pyrrole. *Toxicol. Appl. Pharmacol.* 106: 179–200, 1990.

189.   **Rosca MG**, **Vazquez EJ**, **Kerner J**, **Parland W**, **Chandler MP**, **Stanley W**, **Sabbah HN**, **Hoppel CL**. Cardiac mitochondria in heart failure: decrease in respirasomes and oxidative phosphorylation. *Cardiovasc Res* 80: 30–39, 2008.

190.   **Rosenberg HC**, **Rabinovitch M**. Endothelial injury and vascular reactivity in monocrotaline pulmonary hypertension. *Am. J. Physiol.* 255: H1484–91, 1988.

191.   **Sack MN**, **Disch DL**, **Rockman HA**, **Kelly DP**. A role for Sp and nuclear receptor transcription factors in a cardiac hypertrophic growth program. *Proc Natl Acad Sci USA* 94: 6438–6443, 1997.

192.   **Sakaguchi S**. Naturally arising CD4+ regulatory t cells for immunologic self-tolerance and negative control of immune responses. *Annu Rev Immunol* 22: 531–562, 2004.

193.   **Sakao S**, **Taraseviciene-Stewart L**, **Cool CD**, **Tada Y**, **Kasahara Y**, **Kurosu K**, **Tanabe N**, **Takiguchi Y**, **Tatsumi K**, **Kuriyama T**, **Voelkel NF**. VEGF-R blockade causes endothelial cell apoptosis, expansion of surviving CD34+ precursor cells and transdifferentiation to smooth muscle-like and neuronal-like cells. *The FASEB Journal* 21: 3640–3652, 2007.

194.   **Sakao S**, **Taraseviciene-Stewart L**, **Lee JD**, **Wood K**, **Cool CD**, **Voelkel NF**. Initial apoptosis is followed by increased proliferation of apoptosis-resistant endothelial cells. *The FASEB Journal* 19: 1178–1180, 2005.

195.   **Sakao S**, **Tatsumi K**. The effects of antiangiogenic compound SU5416 in a rat model of pulmonary arterial hypertension. *Respiration* 81: 253–261, 2011.

196.   **Sanchez O**, **Sitbon O**, **Jais X**, **Simonneau G**, **Humbert M**. Immunosuppressive
        therapy in connective tissue diseases-associated pulmonary arterial hypertension. *Chest*
        130: 182–189, 2006.

197.   **Sandoval J**, **Bauerle O**, **Palomar A**, **Gómez A**, **Martínez-Guerra ML**, **Beltrán M**,
        Guerrero ML. Survival in primary pulmonary hypertension. Validation of a
        prognostic equation. *Circulation* 89: 1733–1744, 1994.

198.   **Schermuly RT**, **Dony E**, **Ghofrani HA**, **Pullamsetti S**, **Savai R**, **Roth M**, **Sydykov
        A**, **Lai YJ**, **Weissmann N**, **Seeger W**, **Grimminger F**. Reversal of experimental
        pulmonary hypertension by PDGF inhibition. *J Clin Invest* 115: 2811–2821, 2005.

199.   **Schermuly RT**, **Ghofrani HA**, **Wilkins MR**, **Grimminger F**. Mechanisms of disease:
        pulmonary arterial hypertension. *Nat Rev Cardiol* 8: 443–455, 2011.

200.   **Schermuly RT**, **Kreisselmeier KP**, **Ghofrani HA**, **Yilmaz H**, **Butrous G**, **Ermert L**,
        Ermert M, **Weissmann N**, **Rose F**, **Guenther A**, **Walmrath D**, **Seeger W**,
        Grimminger F. Chronic sildenafil treatment inhibits monocrotaline-induced
        pulmonary hypertension in rats. *Am J Respir Crit Care Med* 169: 39–45, 2004.

201.   **Schwarzer M**, **Faerber G**, **Rueckauer T**, **Blum D**, **Pytel G**, **Mohr FW**, **Doenst T**.
        The metabolic modulators, Etomoxir and NVP-LAB121, fail to reverse pressure
        overload induced heart failure in vivo. *Basic Res Cardiol* 104: 547–557, 2009.

202.   **Schwenke DO**, **Pearson JT**, **Sonobe T**, **Ishibashi-Ueda H**, **Shimouchi A**, **Kangawa
        K**, **Umetani K**, **Shirai M**. Role of Rho-kinase signaling and endothelial dysfunction in
        modulating blood flow distribution in pulmonary hypertension. *J Appl Physiol* 110:

901–908, 2011.

203. **Sebastiani M**, **Giordano C**, **Nediani C**, **Travaglini C**, **Borchi E**, **Zani M**, **Feccia M**, **Mancini M**, **Petrozza V**, **Cossarizza A**, **Gallo P**, **Taylor RW**, **d'Amati G**. Induction of mitochondrial biogenesis is a maladaptive mechanism in mitochondrial cardiomyopathies. *J. Am. Coll. Cardiol.* 50: 1362–1369, 2007.

204. **Sehgal PB**, **Mukhopadhyay S**. Dysfunctional intracellular trafficking in the pathobiology of pulmonary arterial hypertension. *American journal of respiratory cell and molecular biology* 37: 31–37, 2007.

205. **Shah SJ**, **Thenappan T**, **Rich S**, **Tian L**, **Archer SL**, **Gomberg-Maitland M**. Association of serum creatinine with abnormal hemodynamics and mortality in pulmonary arterial hypertension. *Circulation* 117: 2475–2483, 2008.

206. **Shifren A**, **Durmowicz AG**, **Knutsen RH**, **Faury G**, **Mecham RP**. Elastin insufficiency predisposes to elevated pulmonary circulatory pressures through changes in elastic artery structure. *J Appl Physiol* 105: 1610–1619, 2008.

207. **Shigenaga MK**, **Hagen TM**, **Ames BN**. Oxidative damage and mitochondrial decay in aging. *Proc Natl Acad Sci USA* 91: 10771–10778, 1994.

208. **Silva-Neto JP**, **Barreto RA**, **Pitanga BPS**, **Souza CS**, **Silva VD**, **Silva AR**, **Velozo ES**, **Cunha SD**, **Batatinha MJM**, **Tardy M**, **Ribeiro CSO**, **Costa MFD**, **El-Bachá RS**, **Costa SL**. Genotoxicity and morphological changes induced by the alkaloid monocrotaline, extracted from Crotalaria retusa, in a model of glial cells. *Toxicon* 55: 105–117, 2010.

209. **Simonneau G**, **Robbins IM**, **Beghetti M**, **Channick RN**, **Delcroix M**, **Denton CP**, **Elliott CG**, **Gaine SP**, **Gladwin MT**, **Jing Z-C**, **Krowka MJ**, **Langleben D**, **Nakanishi N**, **Souza R**. Updated clinical classification of pulmonary hypertension. *Journal of the American College of Cardiology* 54: S43–54, 2009.

210. **Simonneau G**, **Robbins IM**, **Beghetti M**, **Channick RN**, **Delcroix M**, **Denton CP**, **Elliott CG**, **Gaine SP**, **Gladwin MT**, **Jing ZC**, **Krowka MJ**, **Langleben D**, **Nakanishi N**, **Souza R**. Updated clinical classification of pulmonary hypertension. *J. Am. Coll. Cardiol.* 54: S43–54, 2009.

211. **Soon E**, **Holmes AM**, **Treacy CM**, **Doughty NJ**, **Southgate L**, **Machado RD**, **Trembath RC**, **Jennings S**, **Barker L**, **Nicklin P**, **Walker C**, **Budd DC**, **Pepke-Zaba J**, **Morrell NW**. Elevated levels of inflammatory cytokines predict survival in idiopathic and familial pulmonary arterial hypertension. *Circulation* 122: 920–927, 2010.

212. **Speich R**, **Jenni R**, **Opravil M**, **Pfab M**, **Russi EW**. Primary pulmonary hypertension in HIV infection. *Chest* 100: 1268–1271, 1991.

213. **Stacher E**, **Graham BB**, **Hunt JM**, **Gandjeva A**, **Groshong SD**, **McLaughlin VV**, **Jessup M**, **Grizzle WE**, **Aldred MA**, **Cool CD**, **Tuder RM**. Modern age pathology of pulmonary arterial hypertension. *Am J Respir Crit Care Med* 186: 261–272, 2012.

214. **Steiner MK**, **Syrkina OL**, **Kolliputi N**, **Mark EJ**, **Hales CA**, **Waxman AB**. Interleukin-6 overexpression induces pulmonary hypertension. *Circ Res* 104: 236–44, 28p following 244, 2009.

215.   **Stenmark KR**, **Meyrick B**, **Galie N**, **Mooi WJ**, **McMurtry IF**. Animal models of pulmonary arterial hypertension: the hope for etiological discovery and pharmacological cure. *AJP: Lung Cellular and Molecular Physiology* 297: L1013–32, 2009.

216.   **Sugita T**, **Hyers TM**, **Dauber IM**, **Wagner WW**, **McMurtry IF**, **Reeves JT**. Lung vessel leak precedes right ventricular hypertrophy in monocrotaline-treated rats. *J Appl Physiol* 54: 371–374, 1983.

217.   **Szczepanek K**, **Chen Q**, **Derecka M**, **Salloum FN**, **Zhang Q**, **Szelag M**, **Cichy J**, **Kukreja RC**, **Dulak J**, **Lesnefsky EJ**, **Larner AC**. Mitochondrial-targeted Signal transducer and activator of transcription 3 (STAT3) protects against ischemia-induced changes in the electron transport chain and the generation of reactive oxygen species. *J Biol Chem* 286: 29610–29620, 2011.

218.   **Sztrymf B**, **Coulet F**, **Girerd B**, **Yaici A**, **Jais X**, **Sitbon O**, **Montani D**, **Souza R**, **Simonneau G**, **Soubrier F**, **Humbert M**. Clinical outcomes of pulmonary arterial hypertension in carriers of BMPR2 mutation. *Am J Respir Crit Care Med* 177: 1377–1383, 2008.

219.   **Tabima DM**, **Hacker TA**, **Chesler NC**. Measuring right ventricular function in the normal and hypertensive mouse hearts using admittance-derived pressure-volume loops. *Am J Physiol Heart Circ Physiol* 299: H2069–75, 2010.

220.   **Taegtmeyer H**. Cardiac metabolism as a target for the treatment of heart failure. *Circulation* 110: 894–896, 2004.

221. **Tamosiuniene R**, **Tian W**, **Dhillon G**, **Wang L**, **Sung YK**, **Gera L**, **Patterson AJ**, **Agrawal R**, **Rabinovitch M**, **Ambler K**, **Long CS**, **Voelkel NF**, **Nicolls MR**. Regulatory T cells limit vascular endothelial injury and prevent pulmonary hypertension. *Circ Res* 109: 867–879, 2011.

222. **Tamosiuniene R**, **Tian W**, **Dhillon G**, **Wang L**, **Sung YK**, **Gera L**, **Patterson AJ**, **Agrawal R**, **Rabinovitch M**, **Ambler K**, **Long CS**, **Voelkel NF**, **Nicolls MR**. Regulatory T cells limit vascular endothelial injury and prevent pulmonary hypertension. *Circ Res* 109: 867–879, 2011.

223. **Taraseviciene-Stewart L**, **Kasahara Y**, **Alger L**, **Hirth P**, **Mc Mahon G**, **Waltenberger J**, **Voelkel NF**, **Tuder RM**. Inhibition of the VEGF receptor 2 combined with chronic hypoxia causes cell death-dependent pulmonary endothelial cell proliferation and severe pulmonary hypertension. *FASEB J* 15: 427–438, 2001.

224. **Taraseviciene-Stewart L**, **Nicolls MR**, **Kraskauskas D**, **Scerbavicius R**, **Burns N**, **Cool C**, **Wood K**, **Parr JE**, **Boackle SA**, **Voelkel NF**. Absence of T cells confers increased pulmonary arterial hypertension and vascular remodeling. *Am J Respir Crit Care Med* 175: 1280–1289, 2007.

225. **Taraseviciene-Stewart L**, **Scerbavicius R**, **Choe K-H**, **Cool C**, **Wood K**, **Tuder RM**, **Burns N**, **Kasper M**, **Voelkel NF**. Simvastatin causes endothelial cell apoptosis and attenuates severe pulmonary hypertension. *Am J Physiol Lung Cell Mol Physiol* 291: L668–76, 2006.

226. **Teichert-Kuliszewska K**, **Kutryk MJB**, **Kuliszewski MA**, **Karoubi G**, **Courtman**

186

DW, **Zucco L**, **Granton J**, **Stewart DJ**. Bone morphogenetic protein receptor-2 signaling promotes pulmonary arterial endothelial cell survival: implications for loss-of-function mutations in the pathogenesis of pulmonary hypertension. *Circ Res* 98: 209–217, 2006.

227.   **Thomas RR**, **Khan SM**, **Smigrodzki RM**. RhTFAM treatment stimulates mitochondrial oxidative metabolism and improves memory in aged mice. *Aging (Albany ….*

228.   **Toshner M**, **Morrell NW**. Endothelial progenitor cells in pulmonary hypertension - dawn of cell-based therapy? *Int J Clin Pract Suppl* : 7–12, 2010.

229.   **Trembath RC**, **Thomson JR**, **Machado RD**, **Morgan NV**, **Atkinson C**, **Winship I**, **Simonneau G**, **Galiè N**, **Loyd JE**, **Humbert M**, **Nichols WC**, **Morrell NW**, **Berg J**, **Manes A**, **McGaughran J**, **Pauciulo M**, **Wheeler L**. Clinical and molecular genetic features of pulmonary hypertension in patients with hereditary hemorrhagic telangiectasia. *N Engl J Med* 345: 325–334, 2001.

230.   **Trompouki E**, **Bowman TV**, **Lawton LN**, **Fan ZP**, **Wu DC**, **Dibiase A**, **Martin CS**, **Cech JN**, **Sessa AK**, **Leblanc JL**, **Li P**, **Durand EM**, **Mosimann C**, **Heffner GC**, **Daley GQ**, **Paulson RF**, **Young RA**, **Zon LI**. Lineage Regulators Direct BMP and Wnt Pathways to Cell-Specific Programs during Differentiation and Regeneration. *Cell* 147: 577–589, 2011.

231.   **Tuder RM**, **Davis LA**, **Graham BB**. Targeting Energetic Metabolism: a New Frontier in the Pathogenesis and Treatment of Pulmonary Hypertension. *Am J Respir Crit Care*

Med (November 10, 2011). doi: 10.1164/rccm.201108-1536PP.

232. **Tuder RM**, **Groves B**, **Badesch DB**, **Voelkel NF**. Exuberant endothelial cell growth and elements of inflammation are present in plexiform lesions of pulmonary hypertension. *Am. J. Pathol.* 144: 275–285, 1994.

233. **Turcani M**, **Rupp H**. Etomoxir improves left ventricular performance of pressure-overloaded rat heart. *Circulation* 96: 3681–3686, 1997.

234. **Urashima T**, **Zhao M**, **Wagner R**, **Fajardo G**, **Farahani S**, **Quertermous T**, **Bernstein D**. Molecular and physiological characterization of RV remodeling in a murine model of pulmonary stenosis. *Am J Physiol Heart Circ Physiol* 295: H1351–H1368, 2008.

235. **Urboniene D**, **Haber I**, **Fang Y-H**, **Thenappan T**, **Archer SL**. Validation of high-resolution echocardiography and magnetic resonance imaging vs. high-fidelity catheterization in experimental pulmonary hypertension. *AJP: Lung Cellular and Molecular Physiology* 299: L401–12, 2010.

236. **van Bilsen M**, **van Nieuwenhoven FA**, **van der Vusse GJ**. Metabolic remodelling of the failing heart: beneficial or detrimental? *Cardiovasc Res* 81: 420–428, 2009.

237. **van de Veerdonk MC**, **Kind T**, **Marcus JT**, **Mauritz GJ**, **Heymans MW**, **Bogaard HJ**, **Boonstra A**, **Marques KM**, **Westerhof N**, **Vonk-Noordegraaf A**. Progressive right ventricular dysfunction in patients with pulmonary arterial hypertension responding to therapy. *J. Am. Coll. Cardiol.* 58: 2511–2519, 2011.

238. **van Rooij E**, **Marshall WS**, **Olson EN**. Toward microRNA-based therapeutics for heart disease: the sense in antisense. *Circ Res* 103: 919–928, 2008.

239. **van Wolferen SA**, **Marcus JT**, **Westerhof N**, **Spreeuwenberg MD**, **Marques KMJ**, **Bronzwaer JGF**, **Henkens IR**, **Gan CT-J**, **Boonstra A**, **Postmus PE**, **Vonk Noordegraaf A**. Right coronary artery flow impairment in patients with pulmonary hypertension. *Eur Heart J* 29: 120–127, 2008.

240. **Virbasius JV**, **Scarpulla RC**. Activation of the human mitochondrial transcription factor A gene by nuclear respiratory factors: a potential regulatory link between nuclear and mitochondrial gene expression in organelle biogenesis. *Proc Natl Acad Sci USA* 91: 1309–1313, 1994.

241. **Voelkel N**, **Reeves JT**. Chapter 10: Primary Pulmonary Hypertension. In: *Pulmonary Vascular Diseases*, edited by Moser KM. New York: Marcel Dekker, Inc, 1979.

242. **Voelkel NF**, **Gerber JG**, **McMurtry IF**, **Nies AS**, **Reeves JT**. Release of vasodilator prostaglandin, PGI2, from isolated rat lung during vasoconstriction. *Circ Res* 48: 207–213, 1981.

243. **Voelkel NF**, **Gomez-Arroyo J**, **Abbate A**, **Bogaard HJ**, **Nicolls MR**. Pathobiology of pulmonary arterial hypertension and right ventricular failure. *European Respiratory Journal* 40: 1555–1565, 2012.

244. **Voelkel NF**, **Gomez-Arroyo J**, **Bogaard HJ**, **Abbate A**, **Nicolls MR**. Pathobiology Of Pulmonary Arterial Hypertension and Right Ventricular Failure. *European Respiratory Journal* Inpress, 2012.

245. **Voelkel NF**, **Gómez-Arroyo J**. The harmonics of rodent pulmonary hypertension models. *Int. J. Clin. Pract.* 65 Suppl 172: 1–2, 2011.

246. **Voelkel NF**, **Quaife RA**, **Leinwand LA**, **Barst RJ**, **McGoon MD**, **Meldrum DR**, **Dupuis J**, **Long CS**, **Rubin LJ**, **Smart FW**, **Suzuki YJ**, **Gladwin M**, **Denholm EM**, **Gail DB**, **National Heart Lung and Blood Institute Working Group on Cellular and Molecular Mechanisms of Right Heart Failure**. Right Ventricular Function and Failure: Report of a National Heart, Lung, and Blood Institute Working Group on Cellular and Molecular Mechanisms of Right Heart Failure. *Circulation* 114: 1883–1891, 2006.

247. **Voelkel NF**, **Reeves JT**. *Pulmonary Vascular Diseases*. New York: Marcel Dekker, Inc, 1979.

248. **Voelkel NF**, **Tuder RM**. Hypoxia-induced pulmonary vascular remodeling: a model for what human disease? *J Clin Invest* 106: 733–738, 2000.

249. **Vonk-Noordegraaf A**, **Galiè N**. The role of the right ventricle in pulmonary arterial hypertension. *European Respiratory Review* 20: 243–253, 2011.

250. **Wagenvoort CA**. Pathology of Lung-Tissue and Lung Vessels in Valvular Heart-Disease. *B Eur Physiopath Res* 13: P9–P10, 1977.

251. **Wang L**, **Tamosiuniene R**, **Voelkel N**, **Gera L**, **Nicolls M**. Restoration of Regulatory T Cells (Tregs) Prevents Autoimmune Inflammation (AI) and Pulmonary Hypertension (PH) in Rats. *Am J Respir Crit Care Med* 179: A2355, 2009.

252.	**Wang X-X**, **Zhang F-R**, **Shang Y-P**, **Zhu J-H**, **Xie X-D**, **Tao Q-M**, **Zhu J-H**, **Chen J-Z**. Transplantation of autologous endothelial progenitor cells may be beneficial in patients with idiopathic pulmonary arterial hypertension: a pilot randomized controlled trial. *J. Am. Coll. Cardiol.* 49: 1566–1571, 2007.

253.	**Wang Y-P**, **Yan J**, **Beger RD**, **Fu PP**, **Chou MW**. Metabolic activation of the tumorigenic pyrrolizidine alkaloid, monocrotaline, leading to DNA adduct formation in vivo. *Cancer Lett.* 226: 27–35, 2005.

254.	**Weir EK**, **Will DH**, **Alexander AF**, **McMurtry IF**, **Looga R**, **Reeves JT**, **Grover RF**. Vascular hypertrophy in cattle susceptible to hypoxic pulmonary hypertension. *J Appl Physiol* 46: 517–521, 1979.

255.	**White RJ**, **Meoli DF**, **Swarthout RF**, **Kallop DY**, **Galaria II**, **Harvey JL**, **Miller CM**, **Blaxall BC**, **Hall CM**, **Pierce RA**, **Cool CD**, **Taubman MB**. Plexiform-like lesions and increased tissue factor expression in a rat model of severe pulmonary arterial hypertension. *Am J Physiol Lung Cell Mol Physiol* 293: L583–90, 2007.

256.	**Wilson DW**, **Lamé MW**, **Dunston SK**, **Segall HJ**. DNA damage cell checkpoint activities are altered in monocrotaline pyrrole-induced cell cycle arrest in human pulmonary artery endothelial cells. *Toxicol. Appl. Pharmacol.* 166: 69–80, 2000.

257.	**Wilson DW**, **Segall HJ**, **Pan LC**, **Lamé MW**, **Estep JE**, **Morin D**. Mechanisms and Pathology of Monocrotaline Pulmonary Toxicity. *Critical Reviews in Toxicology* 22: 307–325, 1992.

258.	**Wisler JW**, **Dewire SM**, **Whalen EJ**, **Violin JD**, **Drake MT**, **Ahn S**, **Shenoy SK**,

Lefkowitz RJ. A unique mechanism of beta-blocker action: carvedilol stimulates beta-arrestin signaling. *Proc Natl Acad Sci USA* 104: 16657–16662, 2007.

259.   **Wong YY**, **Ruiter G**, **Lubberink M**, **Raijmakers PG**, **Knaapen P**, **Marcus JT**, **Boonstra A**, **Lammertsma AA**, **Westerhof N**, **van der Laarse WJ**, **Vonk Noordegraaf A**. Right ventricular failure in idiopathic pulmonary arterial hypertension is associated with inefficient myocardial oxygen utilization. *Circ Heart Fail* 4: 700–706, 2011.

260.   **Woods LW**, **Wilson DW**, **Segall HJ**. Manipulation of injury and repair of the alveolar epithelium using two pneumotoxicants: 3-methylindole and monocrotaline. *Exp. Lung Res.* 25: 165–181, 1999.

261.   **Xu MH**, **Gong YS**, **Su MS**, **Dai ZY**, **Dai SS**, **Bao SZ**, **Li N**, **Zheng RY**, **He JC**, **Chen JF**, **Wang XT**. Absence of the adenosine A2A receptor confers pulmonary arterial hypertension and increased pulmonary vascular remodeling in mice. *J. Vasc. Res.* 48: 171–183, 2011.

262.   **Xu W**, **Koeck T**, **Lara AR**, **Neumann D**, **DiFilippo FP**, **Koo M**, **Janocha AJ**, **Masri FA**, **Arroliga AC**, **Jennings C**, **Dweik RA**, **Tuder RM**, **Stuehr DJ**, **Erzurum SC**. Alterations of cellular bioenergetics in pulmonary artery endothelial cells. *Proc Natl Acad Sci USA* 104: 1342–1347, 2007.

263.   **Yeager ME**, **Frid MG**, **Stenmark KR**. Progenitor cells in pulmonary vascular remodeling. *Pulm Circ* 1: 3–16, 2011.

264.   **Yet SF**, **Perrella MA**, **Layne MD**, **Hsieh CM**, **Maemura K**, **Kobzik L**, **Wiesel P**,

Christou H, **Kourembanas S**, **Lee ME**. Hypoxia induces severe right ventricular dilatation and infarction in heme oxygenase-1 null mice. *J Clin Invest* 103: R23–9, 1999.

265. **Yue TL**, **Cheng HY**, **Lysko PG**, **McKenna PJ**, **Feuerstein R**, **Gu JL**, **Lysko KA**, **Davis LL**, **Feuerstein G**. Carvedilol, a new vasodilator and beta adrenoceptor antagonist, is an antioxidant and free radical scavenger. *J Pharmacol Exp Ther* 263: 92–98, 1992.

266. **Yuki H**, **Sato S**, **Arisaka Y**, **Kato S**, **Tomoike H**. Orally administered beraprost sodium inhibits pulmonary hypertension induced by monocrotaline in rats. *Tohoku J. Exp. Med.* 173: 371–375, 1994.

267. **Yuyama H**, **Fujimori A**, **Sanagi M**, **Koakutsu A**, **Sudoh K**, **Sasamata M**, **Miyata K**. The orally active nonpeptide selective endothelin ETA receptor antagonist YM598 prevents and reverses the development of pulmonary hypertension in monocrotaline-treated rats. *Eur J Pharmacol* 496: 129–139, 2004.

268. **Zeisberg EM**, **Tarnavski O**, **Zeisberg M**, **Dorfman AL**, **McMullen JR**, **Gustafsson E**, **Chandraker A**, **Yuan X**, **Pu WT**, **Roberts AB**, **Neilson EG**, **Sayegh MH**, **Izumo S**, **Kalluri R**. Endothelial-to-mesenchymal transition contributes to cardiac fibrosis. *Nat Med* 13: 952–961, 2007.

Vita

Jose Guadalupe Gomez Arroyo was born on December 26th 1984 in Mexico City, Mexico, where he lived until the age of 19. He began medical school at the Monterrey Institute of Technology and Higher Education in the year of 2003 and moved to the northern city of Monterrey, Mexico in 2005 where he continued his medical education. Jose did his medical internship in multiple hospitals in Monterrey and Mexico City, including the San Jose Tec de Monterrey Hospital and the prestigious Instituto Nacional de Ciencias Medicas y Nutricion "Salvador Zubiran" in Mexico City. In 2008, he rotated at the University of Missouri Kansas City – Truman Medical Center and at Harvard Medical School – Beth Israel Deaconess and Boston Children's Hospital for clinical clerkships in Internal Medicine, Critical Care and Pediatric Cardiology, respectively. After his graduation from medical school in 2009, he started his social service year at the Instituto Nacional de Cardiologia "Ignacio Chavez". Under the supervision of Professor Julio Sandoval Zarate, Jose began studying the lung circulation and the right ventricle and tried to further his training by joining Professor Norbert F. Voelkel's laboratory in the year of 2010. In the year of 2012 he was admitted as a degree seeking student at the Virginia Commonwealth University Graduate School in the Molecular Biology and Genetics program.